Adaptive Regenerative Braking in Electric Vehicles

Zur Erlangung des akademischen Grades eines

DOKTORS DER INGENIEURWISSENSCHAFTEN (Dr.-Ing.)

von der KIT -Fakultät für Maschinenbau des
Karlsruher Institut für Technologie (KIT)
genehmigte

DISSERTATION

von

M. Sc. Rayad Kubaisi

Tag der mündlichen Prüfung :	12.01.2018
Hauptreferent:	Prof. Dr. rer. nat. Frank Gauterin
Korreferent:	Prof. Dr.-Ing. Martin Doppelbauer

Vorwort des Herausgebers

Die Fahrzeugtechnik ist kontinuierlich großen Veränderungen unterworfen. Klimawandel, die Verknappung einiger für Fahrzeugbau und -betrieb benötigter Rohstoffe, Digitalisierung, globaler Wettbewerb, gesellschaftlicher Wandel und das rapide Wachstum großer Städte erfordern neue Mobilitätslösungen, die vielfach eine Neudefinition des Fahrzeugs erforderlich machen. Die Forderungen nach Steigerung der Energieeffizienz, Emissionsvermeidung, erhöhter Fahr-, Arbeits- und Datensicherheit, Benutzerfreundlichkeit, gemeinsamer Nutzbarkeit und angemessenen Kosten finden ihre Antworten nicht aus der singulären Verbesserung einzelner technischer Elemente, sondern benötigen Systemverständnis und eine domänenübergreifende Optimierung der Lösungen.

Hierzu will die Karlsruher Schriftenreihe für Fahrzeugsystemtechnik einen Beitrag leisten. Für die Fahrzeuggattungen Pkw, Nfz, Mobile Arbeitsmaschinen und Bahnfahrzeuge werden Forschungsarbeiten vorgestellt, die Fahrzeugsystemtechnik auf vier Ebenen beleuchten: das Fahrzeug als komplexes mechatronisches System, die Mensch-Fahrzeug-Interaktion, das Fahrzeug in Verkehr und Infrastruktur sowie das Fahrzeug in Gesellschaft und Umwelt.

Elektrofahrzeuge erlauben beim Verzögern des Fahrzeugs die Rückwandlung kinetischer und potentieller Energie in elektrische Energie, was zu dem guten Wirkungsgrad dieser Fahrzeuge beiträgt. Neben Systemen, die eine generatorische Bremsung nur bei Betätigung des Bremspedals aktivieren, gibt es zunehmend Systeme, die eine weitgehende Steuerung der Längsdynamik des Fahrzeugs allein mit dem Fahrpedal erlauben. Dabei wird bei vollständiger Freigabe des Fahrpedals oder bei kleinen Betätigungswinkeln ein generatorisches Bremsmoment gestellt. Dies kann als ein bestimmtes Bremsmoment oder eine bestimmte Fahrzeugverzögerung im Fahrzeug fest

vorgegeben oder vom Fahrer in Stufen einstellbar sein. Oftmals wird auch das durch die Motorbremse eines verbrennungskraftmotorisch angetriebenen Fahrzeugs gegebene Verzögerungsverhalten simuliert. Die Betätigung des Bremspedals ist so nur selten erforderlich, nämlich wenn das Rekuperationsmoment nicht die aufgrund der Fahrsituation erforderliche Verzögerung des Fahrzeugs darstellen kann. Diese von vielen Fahrern als angenehm empfundene „Ein-Pedal-Bedienung“ hat jedoch den Nachteil, dass es in der Praxis auch dann zur Rekuperation und damit zu Wandlungsverlusten kommt, wenn es die Fahrsituation nicht erfordert. Auch finden sich in der Literatur Hinweise, dass verschiedentlich, vor allem in Stop & Go-Situationen, vorgegebene Fahrzeugverzögerungen als zu abrupt und stark empfunden werden.

Hier setzt die Arbeit von Herrn Kubaisi an, in der er ein adaptives regeneratives Bremssystem vorschlägt. Dies passt die Stärke der Rekuperation unter Berücksichtigung der Fahrzeugcharakteristik und der Leistungsfähigkeit der Komponenten des Antriebsstrangs an den Fahrstil des Fahrers, an die Fahrsituation und an die aktuelle Fahrerintention an, um so eine gute Balance zwischen Fahrkomfort und Energieeffizienz zu erzielen.

Frank Gauterin

Karlsruhe, 16.1.2018

Abstract

Driving an electric vehicle is considered to be locally emission-free and contributes to the reduction of transportation emissions in cities. Additionally, electric vehicles excel in terms of dynamic driving. However, the short driving range of most electric vehicles is one of the main reasons for their slow spread.

One of the measures used to increase the driving range of electric vehicles is regenerative braking, where the kinetic energy of the vehicle is recovered as electric energy. This recuperated energy increases the driving range of the vehicle.

In this dissertation, an adaptive regenerative braking system is presented. Depending on the driver's type and on the current traffic situation, this system selects an appropriate regenerative braking level.

To realize such a system, methods that determine the driver's type and the driver's intention have been developed by analyzing the driving operation. The inference of the driver's intention while driving was done by the means of a Multi-Dimensional Hidden Markov Model (MDHMM).

By knowing the driver's type and his intention, an appropriate braking level can be selected that takes into account the physical limitations of the vehicle components.

By integrating the developed system, it can be shown that an increase in driving range can be achieved without affecting the comfort of the driver.

Kurzfassung

Elektrofahrzeuge fahren lokal emissionsfrei und tragen damit dazu bei, die Emissionen in Städten zu reduzieren. Zusätzlich, zeichnen sich Elektrofahrzeuge durch ein dynamisches Fahrverhalten aus. Nachteilig wirkt sich bei den meisten Elektrofahrzeugen, die geringe Reichweite auf die Akzeptanz bei Neuwagenkäufern aus.

Eine der Maßnahmen zur Erhöhung der Reichweite von Elektrofahrzeuge ist das regenerative Bremsen. Hierbei wird die kinetische Energie des Fahrzeugs durch generatorisches Bremsen als elektrische Energie zurückgewonnen. Diese zurückgewonnene Energie erhöht die Reichweite des Autos.

In dieser Dissertation, wird ein adaptives regeneratives Bremssystem vorgestellt. Dieses System wählt abhängig vom Fahrertyp und der aktuellen Verkehrssituation ein geeignetes regeneratives Bremsniveau aus.

Um ein solches System zu realisieren, wurden Verfahren entwickelt, welche einerseits den Fahrertyp und andererseits die Fahrerintention durch Analyse des Fahrbetriebs ermitteln. Dazu wurde u.a. ein mehrdimensionales verstecktes Markov-Modell (MDHMM) entwickelt.

Bei Verwendung des Fahrertyps und der Intention des Fahrers, kann so eine geeignete Bremsstufe ausgewählt werden, die die physikalische Begrenzung der Fahrzeugkomponenten berücksichtigt.

Durch den Einsatz des entwickelten Systems, kann gezeigt werden, dass eine Erhöhung der Reichweite erreicht werden kann, ohne den Komfort des Fahrers zu beeinträchtigen.

Table of Contents

List of Figures

List of Tables

List of Abbreviations

AARP	Akustik-Allrad-Rollenprüfstand (German)
ACP	Adaptive Cruising Point
ABS	Anti-Lock Braking System
ARB	Adaptive Regenerative Braking
ARTEMIS	Assessment and Reliability of Transport Emission Models and Inventory Systems
ASM	Asynchronous Motor
ASR	Antriebsschlupfregelung (German), See TCS
AWD	All-Wheel Drive
BBW	Brake-By-Wire
BEV	Battery Electric Vehicle
BMS	Battery Management System
CAN	Controller Area Network
CPS	Combined Pedal Solution
CRBS	Cooperative Regenerative Braking System
EBA	Emergency Brake Assist

EBS	Engine Brake Simulation
EDLC	Electric Double Layer Capacitor
EHB	Electro-hydraulic Brake
EMB	Electro Mechanical Brake
ESP	Electronic Stability Program
FAST	Fahrzeugsystemtechnik (German)
FCEV	Fuel Cell Electric Vehicle
FOC	Field Orientation Control
FTP	Federal Test Procedure
FWD	Front Wheel Drive
GM	Gipps' Model
GUI	Graphical User Interface
GPS	Global Positioning System
HEV	Hybrid Electric Vehicle
HMM	Hidden Markov Model
HSA	Hill-Start Assist
ICE	Internal Combustion Engine
IDM	Intelligent Driver Model
KIT	Karlsruhe Institute of Technology

LIC	Lithium Ion Capacitor
MCU	Motor Control Unit
MDHMM	Multi-Dimensional Hidden Markov Model
NEDC	New European Driving Cycle
PCC	Predictive Cruise Control
PEV	Pure Electric Vehicle
PHEV	Plug-in Hybrid Electric Vehicle
RMSE	Root Mean Square Error
RWD	Rear Wheel Drive
SLDS	Switching Linear Dynamic System
SOC	State of Charge
SPS	Standard Pedal Solution
SRBS	Serial Regenerative Braking System
SSE	Sum of Square Error
StVO	Straßenverkehrsordnung (German)
TCS	Traction Control System
TSECC	TÜV Süd Electric Car Cycle
VCU	Vehicle Control Unit
WLTP	Worldwide Harmonized Light Duty Test Procedure

Nomenclature

Symbol	Unit	Description
F_{Bf}	[N]	Braking force on the front axle
F_{Br}	[N]	Braking force on the rear axle
F_{Gf}	[N]	Static axle load on the front axle
F_{Gr}	[N]	Static axle load on the rear axle
N_{f}	[N]	Dynamic axle load on the front axle during braking
N_r	[N]	Dynamic axle load on the rear axle during braking
μ	[-]	Friction utilization
μ_{ad}	[-]	Adhesion coefficient
μ_{sl}	[-]	Sliding friction coefficient
μ_{f}	[-]	Required adhesion on the front axle
μ_{r}	[-]	Required adhesion on the rear axle
z	[-]	Braking rate
z_{limit}	[-]	Braking rate upper limit
m_{vhcl}	[kg]	Vehicle mass
h	[m]	Center of mass height
lw	[m]	Wheelbase
s	[-]	Slip
η_G	[-]	Quality grade of braking
a_{ij}	[-]	Transition probability

π	[-]	Initial Probability
b_j	[-]	Emissions probability
$\overline{x}$	$[m/s^2]$	Average lateral acceleration
σ	[-]	Standard deviation of lateral acceleration
I_{max}	[A]	Maximum regenerated current
a_{ver}	$[m/s^2]$	Regenerative deceleration rate
t_{max}	[s]	Maximal charging duration
v	[m/s]	Speed
s_0	[m]	Minimum safe distance to lead vehicle
Δx_{lead}	[m]	Braking distance of the lead vehicle
v_l	[m/s]	Speed of the lead vehicle
b_{lead}	$[m/s^2]$	Deceleration of the lead vehicle
Δx_{ego}	[m]	Braking distance of the ego vehicle
b_{ego}	$[m/s^2]$	Deceleration of the ego vehicle
s^*	[m]	Desired distance to lead vehicle
b_{kin}	$[m/s^2]$	Kinematic deceleration
t_r	[s]	Reaction time
v_{safe}	[m/s]	Safe speed

Acknowledgement

This work was done during my time as a research assistant at the Institute of Vehicle System Technology (FAST) at the Karlsruhe Institute of Technology (KIT).

This work is dedicated to:

Mom & Dad. I really miss you. Thank you for your guidance and support throughout my whole life. Without you, I wouldn't have been who I am now.

Thawab. My wife and friend. Sorry for the all-nighters at the office and for not being there on weekends during the writing of this Dissertation.

Redwan & Auwab. You guys are the treasure of my life. Sorry for sometimes not being there for you guys to tuck you in bed and kiss you good night.

Prof. Dr. rer. nat. Frank Gauterin. Thank you for offering me a place at your institute and accepting to be my supervisor.

Dr. Ing. Martin Giessler. Thank you for your continuous support and help during my time at the Institute.

German Academic Exchange Service (DAAD). Thanks for offering me this great opportunity to do my Ph.D. in Germany.

Karlsruhe, November 2017

Rayad Kubaisi

1 Introduction

1.1 Motivation

One of the measures used to increase the driving range of electric vehicles is regenerative braking, where the kinetic energy of the vehicle is converted into electric energy which is then recuperated into the vehicle's battery.

The amount of recuperated energy varies depending on the selected regenerative braking strategy and on the braking torque applied by the motor.

The implemented strategies can be part of the braking system actuated by the braking pedal and can be also actuated by the accelerator pedal independent from the braking system [1].

In a conventional Internal Combustion Engine (ICE) vehicle, engine drag torque is produced when releasing the accelerator pedal. However, this is not necessarily the case in a Battery Electric Vehicle (BEV).

Several strategies exist for the regenerative braking actuated by the accelerator pedal in BEVs.

In some strategies, engine compression braking is emulated in order to retain the similar driving feeling to that of a conventional vehicle in coasting mode [2].

In other cases, a constant braking torque [3] or a constant deceleration value is selected that complies with the limits of the vehicle components [4].

In [5], a field study for regenerative braking actuated by the release of the accelerator pedal in electric vehicles from a user perspective was made.

They found that “drivers quickly learn to use and accept a system, which is triggered via accelerator”. However, there were also reports of difficulty in the interaction. In some cases, the deceleration of the system was described as being “too strong”. In other cases, the deceleration was too abrupt, especially in ‘stop & go’ situations. In some situations, the drivers “simply wanted to coast”. As a conclusion, “it appears reasonable to integrate options to customize or switch off the system”.

Some vehicles offer the driver the opportunity to select the intensity of regenerative braking according to their preference. The settings range from high deceleration to low deceleration as well as no active deceleration at all [6].

This helps the driver select the appropriate setting for his preference. From an energetic point of view, it is always better to use the kinetic energy of the vehicle to propel the vehicle forward instead of recuperating it which is connected to losses when converting it into another form [7]. Therefore, if the intention of the driver would be to cruise or roll, the setting for turning off regenerative braking could be selected. However, if a deceleration is intended, i.e. because of approaching a vehicle, the level of deceleration can be flexibly adjusted by selecting a comfortable deceleration setting for the drivers preference and partially recuperating energy [6].

In this dissertation, the concept of Adaptive Regenerative Braking (ARB) is introduced. This concept automatically tailors the setting of regenerative braking when releasing the accelerator pedal to the driver and the driving situation. This can be achieved by learning and inferring how the driver normally drives and automatically adapting the strategy of the regenerative braking system according to:

- Driving style of the driver
- Driving situation and the driver’s intention

- Vehicle's characteristics and components limits.

The proposed layout of such a system can be seen in Figure 1.

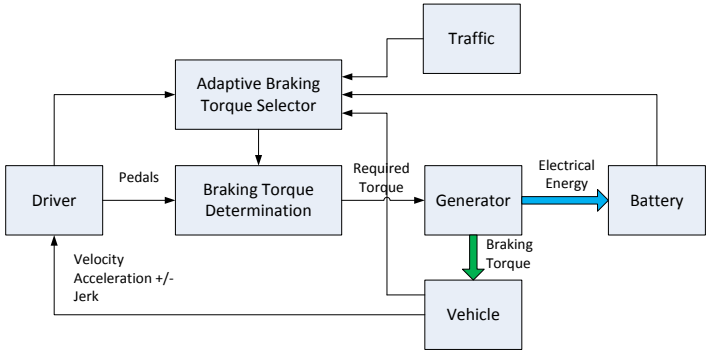

Figure 1: Adaptive regenerative braking concept

The driver's type and driving style can be inferred by analysis of the driver's interaction with the vehicle. The driving situation and the driver's intention can be inferred by analyzing the reaction of the driver to the vehicle's situation in the environment and traffic. For that, the system has to be able to monitor the driver's input commands while at the same time being able to perceive the environment. This is achieved in the **Adaptive Braking Torque Selector** function block.

According to the driver type and driving situation, an efficient and comfortable deceleration corresponding to a given electric braking torque can be selected in the **Braking Torque Determination** function block, taking into consideration the vehicle limitations.

This is then sent as a **Required Torque** signal to the **Generator** which in turn generates the **Braking Torque** decelerating the vehicle and **Electrical Energy** being recuperated into the battery

1.2 Work Outline

The presented work is structured as follows:

In **chapter 2**, the state of the art of the electric vehicle and its components is shown. This is followed by an introduction into regenerative braking and the common strategies used to control it.

In **chapter 3**, the concept of adaptive regenerative braking is proposed and the necessary steps to realize it are explained.

Chapter 4 covers the driver as an integral part of any advanced assistance system. Two main aspects are then investigated in detail: **Driver type** and **Driver intention recognition**. The methods used for both aspects are examined. A new distance-based method to detect the driver's type during braking is introduced and an appropriate model for the recognition of the driver's intention is introduced and modeled.

Chapter 5 explores the limitations different components and aspects of the vehicle can have on the selection of an appropriate braking torque.

Finally, in **chapter 6,** the methods used to test and compare different regenerative braking strategies are explained. After that, a comparison of the driving range increase potential of the different strategies is made.

2 State of the Art

2.1 The Electric Vehicle

In the face of finite petroleum reserves and imminent threats from climate change in many areas, concepts for a resource-conserving life are sought out.

Individual mobility, with its high visibility in everyday life, stands out in this endeavor and is the focus of politics and society nowadays.

One of the possible solutions to the given challenges is electric vehicles which are characterized by the local emission-free operation. However, the global emission-free of an electric vehicle (EV) can only be guaranteed when used electric energy is provided by regenerative energy sources.

In addition to the high purchase costs, the short driving range is a major disadvantage of electric vehicles. This is mainly due to the low energy density of traction batteries, and the batteries weight, which in turn limit the range of the vehicles [8]. As a comparison, to reach the same driving range of 1 liter of diesel, the electric accumulator has to be for example 10 times as big and 20 times heavier [9].

Even though incentives for the spread of electric vehicles exist in different parts of the world, their spread is still limited.

According to the International Energy Agency, just over two million electric vehicles were registered worldwide as of 2016, with 60% of them being BEVs [10].

The International Council on Clean Transportation (ICCT) in one of its recent publications, made a global comparison on incentive policies used globally to drive the electrification of the vehicles on the streets in different parts of the world [11].

Depending on the level of electrification, different concepts and types of electric vehicles currently exist. Two main categorizations of electric vehicles exist in terms of propulsion energy source.

Hybrid Electric Vehicles (HEVs) are vehicles with two or more energy storage systems, both of which must provide propulsion power either together or independently [12]. These vehicles are also categorized based on the degree of hybridization. One special type is the **Plug-in Hybrid Electric Vehicle (PHEV)** that can be charged and can drive electrically for a longer distance [13].

A **Pure Electric Vehicle (PEV)** on the other hand uses only electricity to provide the propulsion power. The source of this electric energy could either be from a fuel-cell in **Fuel Cell Electric Vehicles (FCEV)** or from a battery in **Battery Electric Vehicles (BEV)**.

Figure 2 shows the maximum driving range of currently available electric drive concepts compared to the conventional Internal Combustion Engine (ICE) drive [9]. These values were based on figures given by the vehicles' manufacturers. The figure also shows the electrically operated phases in green and the conventionally operated phases with the combustion engine in red.

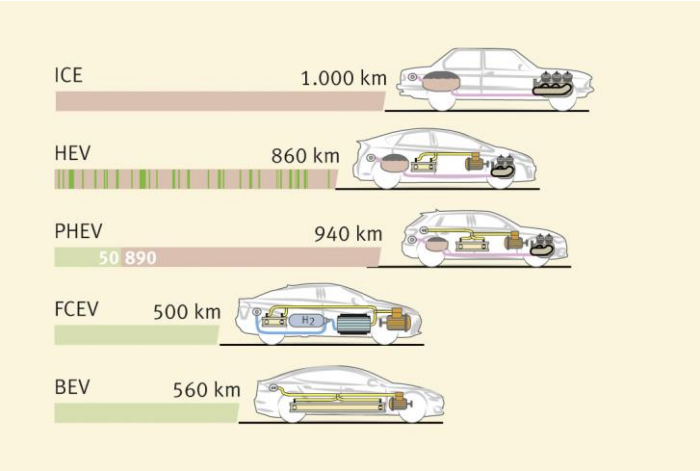

Figure 2: Electrification and driving range © WWU/MEET [9]

In [14], the powertrain architectures of electrified vehicles are reviewed, and the important technologies used in these vehicles are explained in [15]. A comparison of energy consumption and cost of ownership of these different electric vehicle types was made in [16].

Some studies look at the EV as an opportunity to be Integrated into the network [17] and to use it as short-term energy storage on city scales.

Due to the fact that the batteries have a limited amount of energy, and charging them takes a relatively long time (measured in hours), which isn't as convenient as going into a tank station and refilling the tank in a matter of minutes, acceptance of the battery electric vehicle isn't that high.

Acceptance of EVs has a lot of barriers as studied by [18]. In a long-term field study, they studied if EV experience was related to EV acceptance. Participants reported a wide range of advantages, but also barriers to acceptance. The characteristic of the electric drives which allows the maxi-

mum torque to be available at low speeds is praised. The study also found out that "Experience had a significant positive effect on the general perception of EVs and the intention to recommend EVs to others, but not on attitudes and purchase intentions".

One of the major issues related to the limited drive range of electric vehicles is range anxiety. Range anxiety is the worry of a person driving an electric vehicle that the battery will run out of power before the destination or a suitable charging point is reached [19]. If a potential buyer cannot be assured of having constantly-available and compatible charging stations for their vehicle, they will not purchase an EV. Some measures that can be taken against range anxiety, such as parking configurations, charger design, convenient 'EV- only' parking, free charging, and legislation are examined in [20].

2.1.1 The Battery Electric Vehicle (BEV)

Even though vehicle manufacturers of BEVs promise long driving ranges the 'real world' values tend to differ. Next Green Car Ltd.[1] conducts its own independent tests on electric vehicles and shows that the actual values differ from what is promised [21].
Figure 3 shows a comparison between officially marketed range (NEDC cycle) and a real-world range of the current electric vehicles on the market.

Depending on the environmental conditions where the vehicle is used, these figures can become even worse especially in very hot or very cold climates.

[1] Next Green Car Ltd is an independent company developing data and digital solutions in the automotive sector.

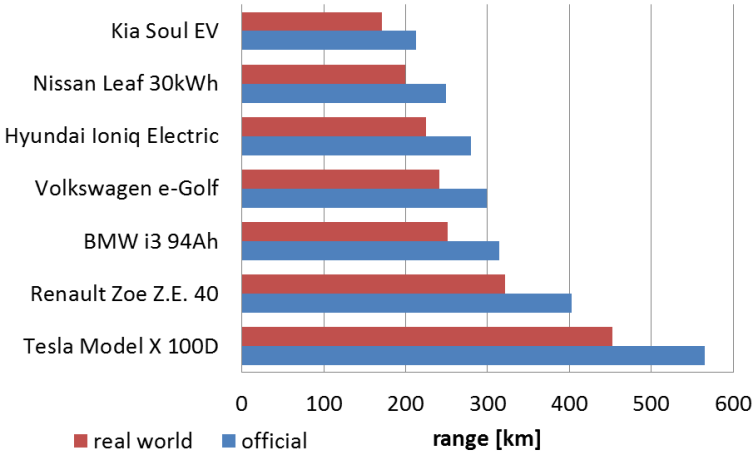

Figure 3: Ranges of current BEVs. Data source [21]

The measures that can be used to increase the efficiency of electric vehicles and the effectiveness of these measures are summarized in [22].

Some of these measures that are related to the technologies of the BEV are:

- Reducing of electric losses of the converters
- Increasing the energy efficiency of the motor
- Improvement in battery technology
- Reducing the losses in the conductors and connectors
- Improving lighting and heating of the vehicle
- Reducing mechanical losses in tires and improving aerodynamics
- Using energy recovering systems

Lightweight construction can also help reduce energy consumption and thus increase the range, as a lighter vehicle has lower driving resistances to overcome.

Another method for increasing the efficiency is optimizing the driving strategy by using intelligent control. This makes more sense in HEVs since the possibilities of different driving strategies and combinations exist. The application of this approach must take into consideration the comfort and even security of the vehicles and people [22].

Route optimization is also a field being investigated [23]. The goal is to find optimized paths between any source and a destination node in the road network. This is done by using the topography and traffic conditions of the road network. An advantage of having such a system is that the optimization goal can be set (i.e. efficiency, dynamics, comfort) and isn't only limited to efficiency.

A routing system that could extend the driving range of EVs through calculating the minimum energy route to a destination was developed in [24].

In [25], a system was designed to optimize the velocity trajectory of the vehicle and concluded that it "can result in 5% fuel saving compared to a Cruise Controller with constant velocity set point". In [26], it was shown that by using a system optimized for energy management "fuel consumption along the commuter route(s) can be reduced by 4%-9% and battery usage by 10%-15%". Several commercially available systems already exist on the market such as the Porsche-InnoDrive that was co-developed at our institute [27].

An important approach to increasing the range is energy recuperation by means of regenerative braking. The electric motor operates as a generator and converts the kinetic energy of the vehicle during deceleration into

electrical energy. Contrary to conventional braking, energy is thus obtained for the movement, instead of generating frictional heat.

The focus of this work is on Battery Electric Vehicles (BEVs). Therefore, aspects related to Hybrid Electric Vehicles (HEV) or Plug-in Hybrid Electric Vehicles (PHEV) are not taken into consideration. Other than the braking system, components that are normally available in conventional vehicles won't be discussed.

2.1.2 The Electric Drive Train

In the following chapters, the focus will be on the two main components in an electric drive; the electric motor and energy storage. Then, the braking mechanics with a focus on stability and safety will be discussed. After that, regenerative braking is introduced and the state of research and strategies used in the field of regenerative braking will be discussed.

One of the advantages of using electric motors and their unique torque characteristics in battery electric vehicles is that it removes the need for any complicated transmission or clutch. The vast majority of current BEV vehicles exploit this advantage and the motor is usually connected to the drive wheels via a single reduction ratio often incorporated in the differential unit [28].

2.1.3 Energy Storage

The energy storage device, from the viewpoint of regenerative braking, should be capable of accepting and storing the energy that is recuperated during braking.

The energy storage should have a high charge rate cable of charging intense peaks of energy during the braking phase and a good efficiency rate with losses as low as possible.

The energy storage should also have a high capacity while at the same time having as little weight as possible [29].

Temperature relevant requirements are also very important as vehicles work in conditions from -30 up to 100 degrees depending on its location within the vehicle.

A lot of possibilities and devices exist for energy regeneration and storage in electric vehicles starting with hydraulic accumulators and flywheels and ending with supercapacitors. In a review of regenerative braking systems, these possibilities were discussed in detail in [30].

According to [31] some of the most important requirements of an energy storage device in an electric vehicle include:

- High specific energy; i.e. the range potential of the vehicle is high.
- High specific power; i.e. the acceleration potential of the vehicle is high.
- High cycle stability; i.e. the characteristics of the storage don't change with repeated charging.

Other factors such as low manufacturing costs and safety issues are to be considered as well. These and other requirements have been discussed and investigated in [8].

A Ragone plot [32], which describes the relationship between specific energy and specific power of an energy storage technology can be used to compare different technologies. An example comparing current technologies is shown in Figure 4.

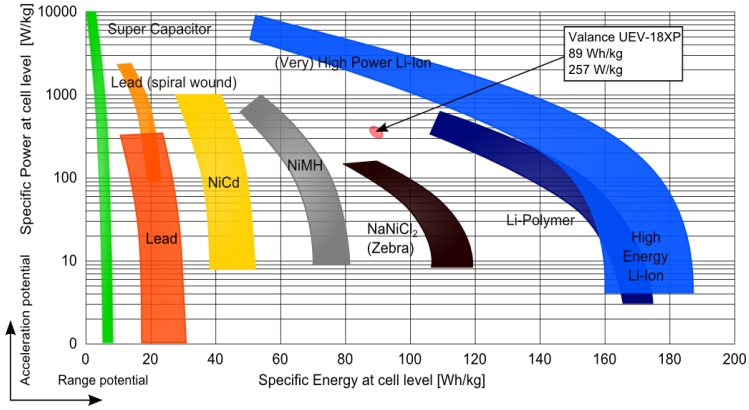

Figure 4: Comparison of different electric energy storage devices. Data source [8]

The figure shows that Li-ion batteries have relatively high specific power and specific energy and are therefore great candidates for BEVs. However, lithium accumulators can only be used in a narrow temperature window and have the risk of destruction when overcharged or deeply discharged. Therefore, a Battery Management System (BMS) is required. Another special feature of lithium-ion accumulators is that they allow higher discharge currents than charging currents.

At a high State Of Charge (SOC), the BMS drops the allowable charging current of lithium-ion accumulators, since the maximum cell voltage should not be exceeded during charging [31].

Even though the Li-ion batteries excel in both specific energy and specific power characteristics, they can't compete in terms of cycle stability with an electric double-layer capacitor (EDLC) or supercapacitor. In comparison to chemical energy storage devices, EDLCs show a lot lower specific energy but a very high specific power, as well as a very high cycle stability and, are

therefore an optimal solution for short-term energy storage since EDLC's can be charged and discharged in seconds.

Table 1 shows a comparison of different characteristics of Li-ion batteries and supercapacitors.

Table 1: Performance comparison of Li-ion batteries and supercapacitors according to [33]

	Li-ion Batteries	supercapacitor
Specific Energy [Wh/kg]	100-200	5 (typical)
Specific Power [W/kg]	1000-3000	Up to 10000
Cycle Life	500 and higher	1 million or 30000 h
Cost per Wh	0.5 – 1 $	20 $ (typical)

The difficulty in achieving high values for all these requirements has led to the suggestion that electric vehicles may best be powered by a pair of batteries. The main unit would be optimized for range (specific energy) and another for power (specific power). The second unit would be recharged from the range unit during stops or less demanding driving [34].

New devices have appeared that combine the advantages of both, such as lithium-ion capacitors (LIC) which are hybrid electrochemical energy storage devices that combine the intercalation mechanism of a lithium-ion battery with the cathode of an electric double-layer capacitor (EDLC). These have higher power density as compared to batteries, and are safer in use than lithium-ion batteries (LIBs), in which thermal runaway reactions may occur [35].

2.1.4 Electrical Motors and Power Electronics

One of the greatest advantages of electric motors is that they can almost provide their maximum torque from a standstill. The motor is capable of

producing practically the same maximum torque at all speeds from zero up to a specific speed called the base speed. This region of characteristics is known as the “constant torque” region. In this region, the available power increases as the rotational speed increases. The next region is called “constant power” region where the available torque drops as the rotational speed increases [36].

These characteristics make electric motors very good vehicle drives; there is no clutch and no switchable gear necessary to operate. Due to the high dynamics of electric motors, different torques can be set within a very short time.

An electric motor is made of a fixed part, the stator, and a rotating part, the rotor. Torque is generated by the means of a magnetic field. The motors differentiate by the source of this magnetic field.

In [37], an extensive study on the selection of electric motor drives for electric vehicles was made and the different types of electric motors and their working principles are explained.

Nowadays, induction motors are often used in automotive applications due to “simple construction, reliability, ruggedness, low maintenance, low cost, and ability to operate in hostile environments. The absence of brush friction permits the motors to raise the limit for maximum speed, and the higher rating of speed, enable these motors to develop high output” [37].

The most common type of rotor is the squirrel-cage where aluminum bars are cast into slots in the outer periphery of the rotor and are then short-circuited together at both ends by rings. The induced currents flow through the aluminum better than the rotors body [38]. A 3 phase AC current passing through the 120^{o} shifted stator windings producing a rotating magnetic field. A current will be induced in the bars of the squirrel cage and it will start to rotate, hence the name induction motors where electricity is in-

duced in the rotor by magnetic induction rather than direct electrical connection. The induced current in squirrel cage bars variate due to the rate of change of magnetic flux in one squirrel bar pair which is different from another, due to its different orientation. This variation of current in the bar will change over time. Figure 5 shows a cross-section of an induction motor.

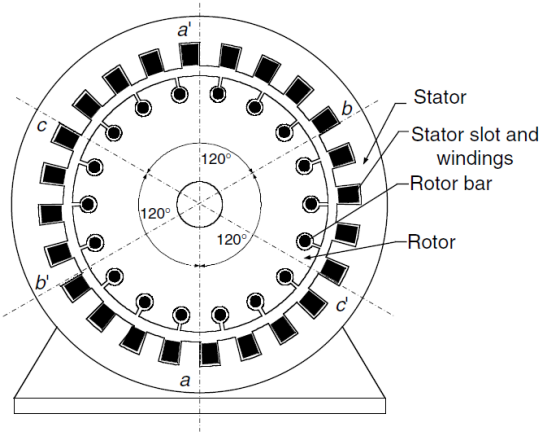

Figure 5: Cross section of an induction motor [38]

The speed difference between the stator field and rotor field is referred to as slip. Up to a certain amount of slip, the generated torque increases. From the overturning moment (sometimes called the pull-out torque) which is the highest torque, the available torque decreases due to the rotor inductance. Examples of vehicles with ASM are the Tesla Roadster and the Mercedes-Benz A-Class F-Cell (V168) which was used as the base for the test vehicle used in the scope of this work and described in Appendix 9.2.

The speed variation in induction motors is achieved by changing the frequency of the voltage. This is sometimes called constant volt/hertz control which is done by the means of the inverter in the power electronics.

Figure 6 shows the basic topology of the electric drivetrain in regards to the power electronics.

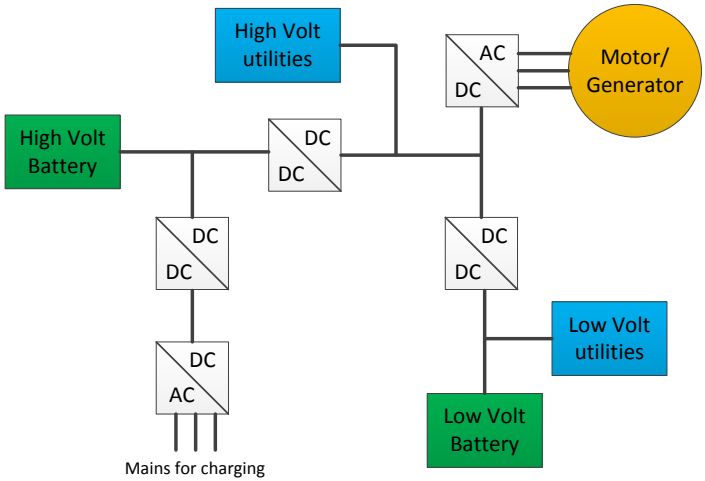

Figure 6: Simplified topology of the power electronics according to [13]

The DC voltage of the batteries is converted into an appropriate AC voltage fed into the phases of the stator generating the magnetic field. This varies the torque-speed characteristics of the motor by simultaneously controlling the voltage and frequency. This approach is more suitably applied to motors that operate with relatively low-speed regulation. However, this approach shows poor response to frequent and fast speed varying, which is a requirement in modern vehicles, and also shows poor operation efficiency due to the poor power factor. Field Orientation Control (FOC) overcomes the disadvantages of the constant volt/hertz control. The aim of FOC is to maintain the stator field perpendicular to the rotor field in order to produce the maximum torque [38].

In the ‘constant torque’ region, continuous operation at peak torque will not be allowable because the motor will overheat, so an upper limit will be imposed by the controller [36].

In the ‘constant power’ region, extended speed range operation beyond base speed is accomplished by flux weakening, once the motor has reached its rated power capability [37]. That is why this region is also called the ’field weakening’ region. A properly designed induction motor, with field orientation control, can achieve field weakened range of 3-5 times the base speed [39].

Electric motors can be also used as a generator, which allows recuperation of the kinetic braking energy. A normalized characteristics curve of an electric motor in all 4 quadrants of operation is depicted in Figure 7.

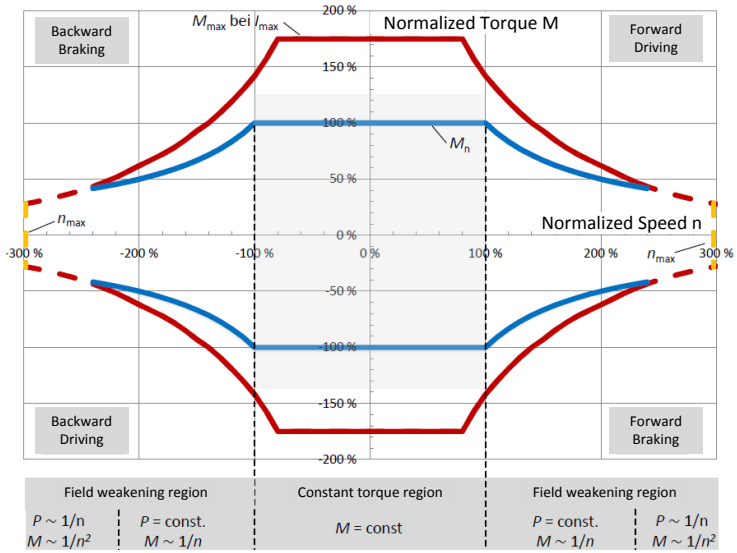

Figure 7: Normalized characteristic curves of an electric motor according to [13]

The x-axis represents the rotational speed of the motor shaft and the y-axis represents the deliverable torque by the motor. The motor works as a generator in both quadrants 2 (braking while driving in reverse) and 4 (braking while driving forward).

The characteristics of the used electric motor are important for defining the possible regenerative braking (2^{nd} and 4^{th} Quadrant) because it defines the maximum possible braking torque. Especially at higher speeds, such as on highways, it becomes critical because the maximum available torque drops with the increase of speed and is relatively small.

2.1.4.1 Limitations Imposed by the Motor and Inverter

The currents flowing through the switching devices and the motor should be limited due to the thermal limit imposed by the motor design. This current limit should at least be equal to the rated current of the motor. The power electronics has to ensure that whatever the user does, the output current does not exceed a safe value, other than for clearly defined overload (e.g. 120% for 60 seconds) which the motor and inverter will have been specified and rated for. This imposes an upper limit on the permissible torque. In the constant torque region, this limit normally corresponds to half the pull-out torque [36] as seen in Figure 8.

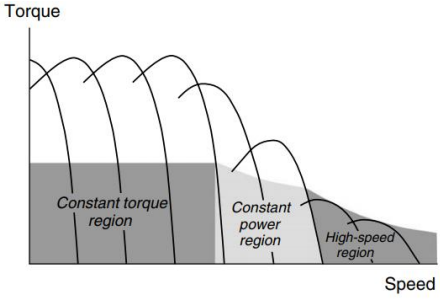

Figure 8: Different regions of induction motor operation [36]

In the constant power region, it is not possible to increase the voltage anymore and the flux, therefore, reduces inversely with the frequency. Since the stator and rotor currents are also thermally limited, the maximum permissible torque is also reduced as the speed increases [36].

2.1.4.2 The Motor as a Generator

For negative slips, i.e. when the rotor is turning in the same direction but at a higher speed than the traveling field, the motor' torque is negative. This means that the motor develops a torque that opposes the rotation. In this region the machine acts as an induction generator, converting mechanical power from the shaft into electrical power into the supply system [36] as can be seen in Figure 9.

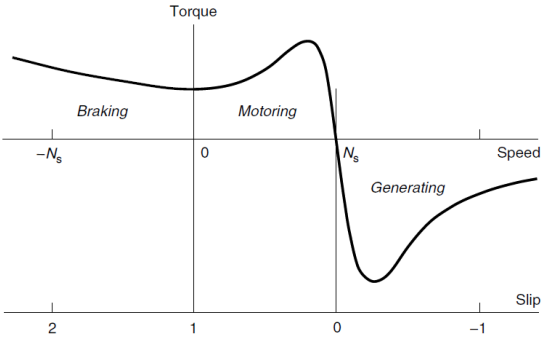

Figure 9: Torque-speed curve of an induction motor [36]

No changes need to be made to an induction motor to turn it into an induction generator. All that is needed is a source of mechanical power to turn the rotor faster than the synchronous speed. It is also important to mention that Induction machines can only generate when they are connected to the

power supply because the excitation flux is not present until the motor is supplied with magnetizing current [36].

2.1.5 BEV Architectures

Whereas ICE driven vehicles are typically powered by one engine only, electric vehicles can integrate several motors and are from the architecture perspective more flexible [14].

Figure 10 shows some of the architectures of current electric vehicles.

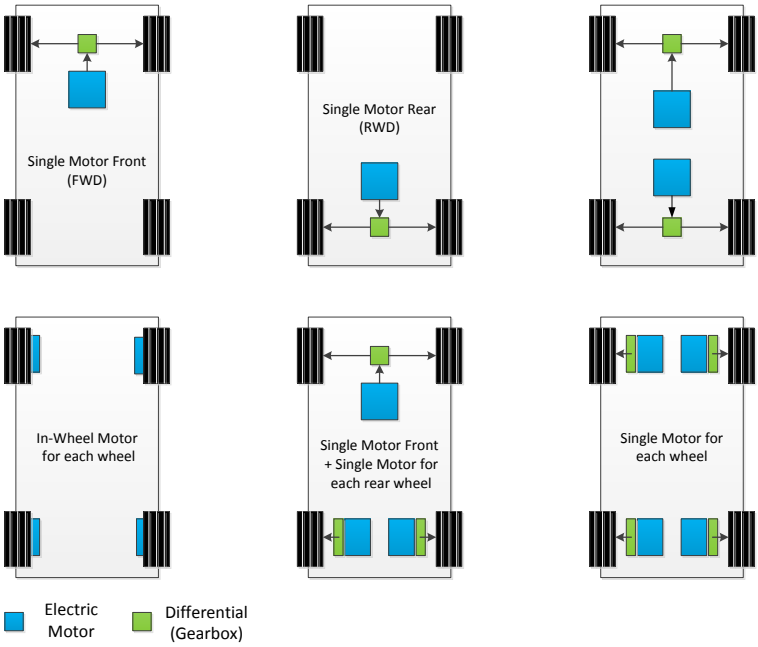

Figure 10: Different BEV architectures according to [14], [38] & [40]

Each concept has its own advantages and disadvantages.

By having a single motor propelling one axle, the costs are reduced and the controlling complexity as well. However, it is not possible to control the torque delivered to each individual wheel independently.

Having an independent motor for each wheel allows for torque-vectoring capabilities such as yaw moment control, anti-lock braking and traction control [41].

One other alternative is using In-wheel motors or so-called wheel hub drives; where the motor is located directly in the wheel. This can “free up packaging space and spare more space for battery package, cargo, and passengers” [14]. However, this configuration has its own caveats; the motors are in an exposed position where they can be easily damaged and also the unsprung mass of the motor with the wheel is very high which affects the driving comfort and safety negatively.

Which architecture is the best cannot be answered simply and is dependent on the type of vehicle and its use. For example, the author of [42] explored the design space of multicriteria optimization of an electric sports vehicle drivetrain.

However, what is very important to consider is the combination of architecture and regenerative braking strategy especially when studying stability as will be discussed in 5.1.3.

[40] studied the different requirements of having different architectures on the design of the regenerative braking system. An extensive comparison between a Front Wheel Drive (FWD) electric vehicle and an All-Wheel Drive (AWD) vehicle was made.

2.1.6 The Braking System

Figure 11 shows a schematic representation of a vehicle braking system [43]. This type of system is a power-assisted braking system. The pressure on the master cylinder (5) is applied by the driver through the brake booster (7). This booster works with a vacuum that is supplied from the throttle of a conventional ICE. In electric vehicles, this vacuum has to be supplied by a dedicated vacuum pump since no adequate vacuum is available elsewhere.

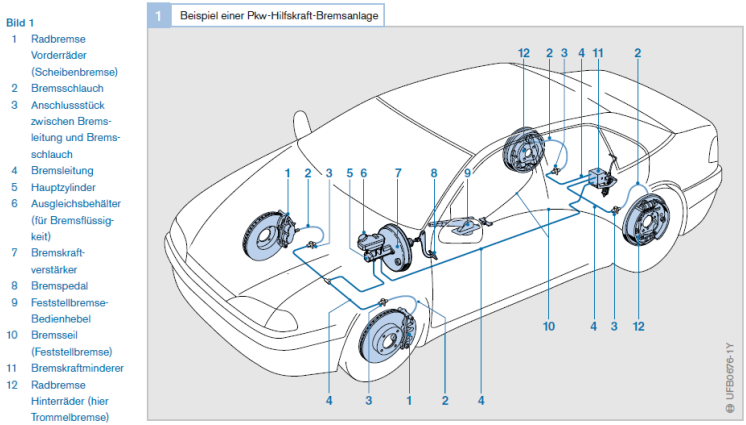

Figure 11: Schematic representation of a vehicle brake system [43]

Standard [1] demands that with a defective braking system an assisted braking of a medium deceleration of 2,44 m/s^2 is still possible. Therefore, vehicles are built with two separate brake circuits. The master cylinder feeds both circuits. When the brake is applied the piston closes the holes of the expansion tank (6) and pressure can build up in the system. This pressure is then transferred to the wheel brakes via the brake lines and hoses.

The wheel brakes can be either drum or disk brakes. In modern vehicles, disk brakes are installed since they can dissipate more heat and are also more stable [43].

The brake circuits can be designed in several ways, whereby in practice two designs are mainly used. In the II arrangement, the front and rear axle each have a separate brake circuit. In the X arrangement, each front wheel and the diagonally opposite wheel on the rear axle are in one circuit. The X arrangement is installed mainly in front loaded vehicles, to ensure a sufficiently high adhesion potential in the event of a brake circuit failure [43].

Figure 12 shows the forces acting on a vehicle during braking.

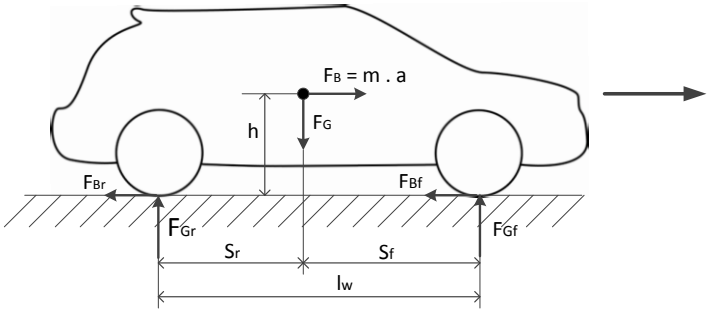

Figure 12: Forces acting on the vehicle during braking according to [44]

The friction utilization during braking for the whole vehicle is defined as the quotient of braking force to axle load:

$$\mu = \frac{F_B}{F_G} = \frac{F_{Bf} + F_{Br}}{F_G} = \frac{\mu_f \cdot F_{Gf} + \mu_r \cdot F_{Gr}}{F_G} \qquad (2.1)$$

Figure 13 shows the relationship between friction utilization and slip. At zero slip, there is no deformation of the tire tread in the circumferential direc-

tion. Consequently, no braking force is transmitted and no braking can occur.

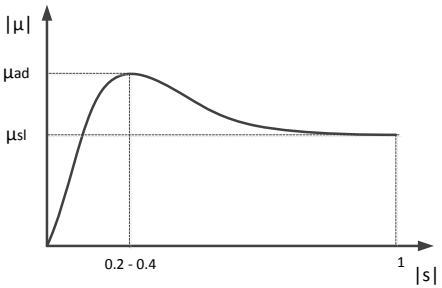

Figure 13: Friction utilization vs. slip [44]

The maximum friction utilization (adhesion coefficient) $\mu_{max} = \mu_{ad}$ is achieved at a slip ratio between 0.2 and 0.4. With a fully slipping wheel (s =1), the adhesion coefficient represents the sliding friction coefficient μ_{sl}.

The braking rate of the vehicle (z) is defined as follows:

$$z = \frac{b}{g} = \frac{m \cdot b}{m \cdot g} = \frac{\mu_f \cdot F_{Gf} + \mu_r \cdot F_{Gr}}{F_G} \qquad (2.2)$$

The physical limit of the braking rate happens at the maximum friction utilization at the rear and front wheels which is dependent on the road type and conditions and therefore:

$$z_{limit} = \frac{\mu_{ad} \cdot F_{Gf} + \mu_{ad} \cdot F_{Gr}}{F_G} = \mu_{ad} \qquad (2.3)$$

In reality z_{max} is smaller than z_{limit} , because the front axle reaches the skidding limit first [44].

The quality grade is defined for the entire vehicle at maximum deceleration as:

$$\eta_G = \frac{z_{max}}{z_{limit}} = \frac{z_{max}}{\mu_{ad}} \leq 1 \qquad (2.4)$$

The higher the quality grade the shorter the braking distance is.

The braking system has to ensure the stability and steerability of the vehicle. When a tire blocks, it slides over the road and no lateral side forces can be transmitted to the road. In the case that the rear wheels lock, the rear wheels ability to support lateral forces is reduced to zero. If some slight lateral force acts on the body of the vehicle; by side wind or centrifugal force, a yaw moment develops which can be only compensated for by the front axle. This moment turns the vehicle out of the line of action of the resulting tractive force and results in the loss of directional stability. In the case that the front wheels block, the front wheels ability to support lateral forces is reduced to zero. This results in the loss of directional control. However, If a lateral force acts on the body of the vehicle, a yaw moment develops which turns the vehicle into the line of action of the resulting tractive force, meaning that directional stability is still available [44].

From what has been discussed, it can be summarized that braking systems have two main criteria that should be fulfilled: From the perspective of braking stability, the rear axle is not allowed to block before the front axle in order to ensure the vehicle's stability. From the perspective of braking distance, the shortest braking (stopping) distance has to be ensured.

According to [1] the required friction utilization during braking in order for the axle not to block is :

$$\mu_f = \frac{F_{Bf}}{N_f} = \frac{F_{Bf}}{F_{Gf} + z \cdot \frac{h}{l_w} \cdot m_{vhcl} \cdot g} \qquad (2.5)$$

$$\mu_r = \frac{F_{Br}}{N_r} = \frac{F_{Br}}{F_{Gr} - z \cdot \frac{h}{l_w} \cdot m_{vhcl} \cdot g} \qquad (2.6)$$

The ideal braking force distribution is achieved when the adhesion potential of both axles are used up at the same time ($\mu_f = \mu_r$).

By knowing the parameters of the vehicle and by using equations ((2.5) and (2.6) the ideal braking ratio for each braking rate can be calculated and depicted by the “I curve” in Figure 14.

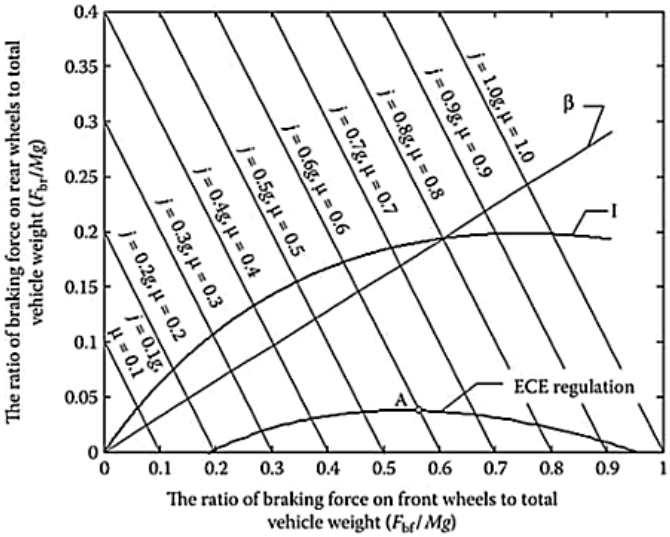

Figure 14: Ideal braking force distribution [38]

The x-axis depicts the ratio of the front axle braking force to the weight of the vehicle and the y-axis depicts the ratio of the rear axle braking force to the weight of the vehicle. Due to the fact that the dynamic weight of the

vehicle shifts on to the front axle during braking the “I curve” has this distinct progressive curve. To ensure a stable braking process as mentioned, the front axis needs to block before the rear axle, therefore, the braking ratio has to be selected under the “I curve” [44].

This is complex to achieve in the vehicle using hydraulic braking, and therefore a fixed rear-front ratio that fulfills the ECE regulations [1] that require that the vehicle has to be stable up to z = 0.8 is designed and is depicted in Figure 14 by the “ß line”.

The standard [1] also states that the friction utilization curve of the rear axle shall not be situated above that for the front axle for all braking rates between 0.2 and 0.8:

$$z \geq 0.1 + 0.85(\mu - 0.2) \quad \forall \quad 0.2 \leq \mu \leq 0.8 \tag{2.7}$$

This can also be plotted as a curve and can also be seen at the bottom of Figure 14 (ECE regulations). In other words, this represents the minimum braking force on the rear axle when the front axle locks in order to utilize the rear axle when the front axle is locked.

Some vehicles use pressure relief valves to limit the pressure increase in the brakes of the rear axle from reaching a certain value to stay near the brake force distribution of the ideal brake force distribution [43].

Modern anti-lock braking systems (ABS) close the intake valves of the rear Brakes, as long as a greater slip than the front is measured. As a result, the braking force distribution of the ideal curve can be further approximated [43].

Integrating Regenerative Braking (RB) into the existing braking system can have effects on the braking system.

Depending on the type of regenerative braking, the system software, the modulation hardware, and the pedal feel might be greatly influenced and need to be designed again [4].

The authors of [45] see the challenge in “the way of distributing the required braking force between the regenerative braking system and the mechanical friction braking system so as to recover the kinetic energy of the vehicle as much as possible without losing the necessary braking performance”. Using different strategies, the effect on the optimal braking feel and on the optimal energy recovery were analyzed.

In terms of performance, introducing RB into the vehicle can have some significant effects, both positive and negative, on the brake system performance. “On the positive side, the reduction in friction brake usage can substantially decrease operating temperatures and increase the life of the friction materials. On the negative side, the reduction in friction brake usage can increase the risk of damage due to poor cleaning of corrosion of the friction surface” [46]. The same study also proposed how a brake system configuration for a regenerative braking equipped vehicle may be balanced differently than a system for a vehicle with conventional braking.

2.2 Regenerative Braking

According to the European regulations [1], "*Electric regenerative braking* means a braking system which, during deceleration, provides for the conversion of vehicle kinetic energy into electrical energy". This is done in BEVs by the means of using the electric motor as a generator during braking [38] as shown in Figure 15.

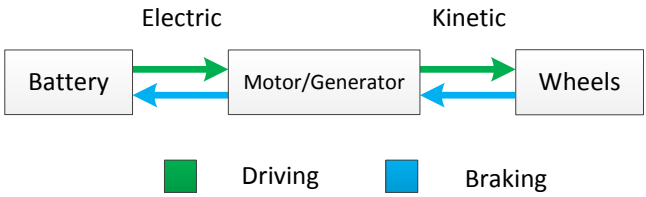

Figure 15: Flow of energy in a BEV according to [38]

In contrast to conventional braking, energy is thus generated for the movement (increase in driving range) rather than being dissipated as heat due to friction.

In the rest of this work, the focus would not be on how this is realized in the motor and the dynamics that hide behind since it is not the focus of this work. A simple negative torque signal is sent to the Motor Control Unit (MCU) and it takes care of the rest.

The regenerative braking potential is determined as mentioned before by the available braking torque from the motor which, in turn, is dependent on the rotational speed of the motor. This potential is also limited by the charging state of the energy storage and also by specific driving situations. These limitations will be discussed in detail in chapter 5.1.

The author of [47] did a benchmark of regenerative braking for fully electric vehicles. He described the various control systems used and also described what a simulation model of such a vehicle would look like.

2.2.1 RB Categories

According to the regulations [1], regenerative braking systems are categorized into two categories:

Category A: an electric regenerative braking system which is not part of the service braking system; and shall only be activated by the accelerator control and/or the gear neutral position

Category B: an electric regenerative braking system which is part of the service braking system, and shall have only one actuating unit which in our case is the brake pedal.

The pedal/torque characteristics of a system implementing both strategies are shown in Figure 16.

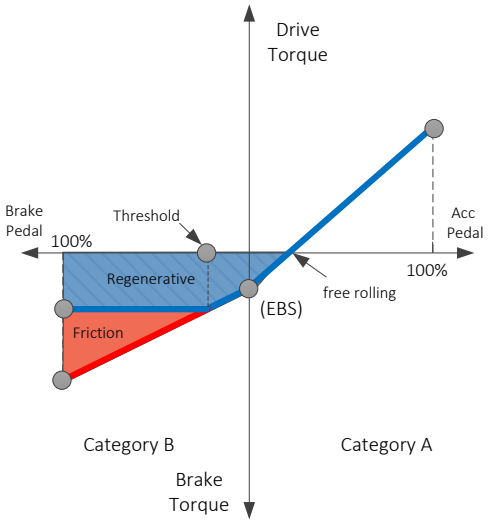

Figure 16: Combined Serial Regenerative Braking Strategy (SBRS) according to [1] & [48]

As shown, when the accelerator pedal is fully released the motor generates a negative braking torque causing the vehicle to decelerate. This braking torque upon release of the accelerator can be set as Engine Brake Simula-

tion (EBS). It is also shown that in order to achieve rolling (zero torque applied), the gas pedal should be pressed to a certain position, called the free rolling or sailing point [49].

The EBS could also be set to 0 and in this case, the line will go through the origin meaning that no negative or positive torque will be applied when no pedal is applied and the vehicle is simply let to roll.

2.2.2 Category B Strategies

The easiest way to realize a regenerative braking system is by simply adding up the deceleration caused by the motor and the braking system as done in serial regenerative braking systems.

2.2.2.1 Serial Regenerative Braking System (SRBS)

This type of system is easy to implement and very economical and is used when no big changes to the original braking system are to be made and no blending of electric and hydraulic braking is wanted [4].

In such systems, the braking is purely electric at the beginning and after a given threshold (a defined pedal movement before the master cylinder is pressed), the friction braking comes into action [4] as seen in Figure 16.

The amount of hydraulic braking torque that is applied is equal in magnitude to that not delivered electrically.

This strategy is very good with low decelerations as in regular road driving where a large portion of the kinetic energy can be recovered. The biggest disadvantage is that the braking torque is speed dependent [4] and is therefore set either to a comfortable level or to a level that can be ensured at all rotational speeds.

2.2.2.2 Cooperative Regenerative Braking System (CRBS)

This type of system is also called parallel regenerative braking because it is capable of applying electric and hydraulic braking at the same time while being able to control the proportion of each separately and thus ensuring a total amount of needed braking torque independent of the motor rotational speed [4]. Figure 17 shows the relationship between the brake pedal and the generated braking torque.

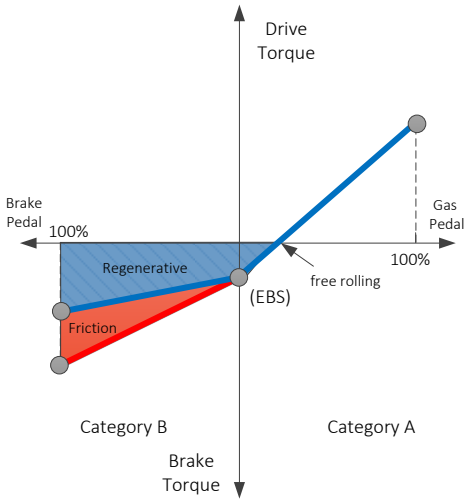

Figure 17: Combined Cooperative Regenerative Braking Strategy (CRBS) according to [1] & [48]

The main advantage of a CRBS system is that it is speed-independent and can utilize the full potential of the electric brake maximizing the recuperated energy [4] as shown in Figure 18.

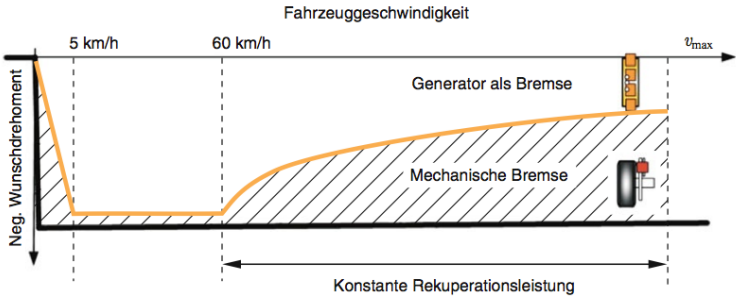

Figure 18: CRBS [50]

It can be noted that RB is reduced to zero at low speeds. This will be discussed in chapter 2.2.4.

However, CRBS implies additional costs for hydraulic blending and completely or partially decoupling the brake pedal from the brake circuit [4]. This decoupling can be achieved by installing a brake by wire system in the vehicle.

2.2.2.3 Brake-By-Wire

With the introduction of Anti-Lock Braking Systems (ABS) and the Electronic Stability Program (ESP), the addition of a hydraulic aggregate that can independently build up brake pressure is necessary. By having such braking systems in a vehicle, other safety and comfort functions such as Hill-Start Assist (HSA) or Emergency Brake Assist (EBA) can be realized [43].

A Brake-By-Wire system (BBW) completely decouples the brake pedal from the brake force. These systems provide all the assistance functions previously mentioned. The decoupling of the brake pedal and the braking force makes it possible to build up higher or lower braking forces at a given brake pedal position than with a comparable conventional system.

With BBW, a comfort stop can be realized, in which the braking force is lowered shortly before the vehicle stops. This prevents a jerky stop [43].

For recuperation, a BBW system is of high relevance, as it can be used to divide the deceleration request of the driver between different brake actuators without changing the pedal feel. For example, the maximum recuperation torque of the motor can be retrieved and the remaining torque request of the driver, which cannot be covered by the electric motors, is delivered by the mechanical brakes.

Since the available recuperation torque depends on several factors as will be discussed in chapter 5.1, the split between mechanical and recuperative braking torque can be variably controlled by the controller and the driver does not notice the changing composition of the braking force.

A BBW system is implemented in several ways. One implementation is the electro-hydraulic brake (EHB), in which a hydraulic braking system is electrically controlled [51]. This has the advantage that the hydraulic braking is available if the electronics fail. Another possibility is the electromechanical brake (EMB), in which the complete power and signal transmission are done by electrical means. An EMB has higher demands on the safety concept and reliability of the actuators [52].

Selecting the strategy for category B depends on the typology of the EV and on the extent to which the braking system needs to be modified. [53] made a comparison between serial and parallel braking strategies using various driving cycles.

2.2.3 Category A Strategies

In modern electric vehicles, the accelerator pedal could be used for three functions: acceleration, coasting and brake energy recuperation as was shown in Figure 16. A ‘one pedal driving experience’ is considered to be an

asset in congested stop-and-go traffic situations where it can provide a smoother and more relaxed way of driving in heavy traffic.

Nissan includes in its 2018 leaf a new one-pedal driving system which is activated by a button. This “e-Pedal” can start, accelerate, brake and totally stop the vehicle with no need for the braking pedal [54].

By integrating deceleration by means of regenerative braking into the accelerator pedal, drivers are expected to use the electric brake more often than the hydraulic brake [49]. However, the pedal system of a car is a crucial connection between driver and car and any modification of this part can lead to decreasing acceptance [49].

In [5], a one-year field study (n=80) on regenerative braking using the accelerator pedal from the users perspective was made irrespective of which particular regeneration strategy is implemented in the vehicle. They found that most drivers quickly learned to interact with the system, which was triggered via accelerator. Furthermore, conventional braking maneuvers decreased significantly as the majority of deceleration actions could be executed through regenerative braking alone. However, some drivers reported difficulties when adapting to the system. In some cases, the deceleration of the system was described as being “too strong”. In other cases, the deceleration was too abrupt, especially in stop-&go situations. In some situations, the drivers “simply wanted to coast”. As a solution, they suggested offering different levels of regeneration so the intensity of the deceleration could be individually modified to overcome these difficulties.

In [55], an evaluation of the interaction concepts for the longitudinal dynamics of electric vehicles was made. They found that test drivers evaluated an EV with a stronger deceleration in the regeneration phase as more directly controllable than EV concepts with less deceleration.

In [49], a study on the impact of a Combined Pedal Solution (CPS) used for acceleration and braking on acceptance and energy consumption was made. The results showed that the drivers preferred stronger electric braking and the combined pedal solution more than a conventional pedal solution. They also found that points of criticism of the CPS were that “the area of sailing was more difficult to find (i.e. neither stepping on the brake nor on the accelerator pedal) and when driving with the CPS many glances to the gauge were needed in order to obtain information whether the car is sailing, accelerating or regenerating energy”.

Whatever the selected strategy for this category, some regulations apply according to [1]:

- Electric regenerative braking systems which produce a retarding force upon release of the accelerator shall generate a braking light signal according to the following provisions:

Table 2: Activation values of the braking lights according to [1]

Vehicle deceleration	Signal generation
≤ 0.7 m/s²	The signal shall not be generated
> 0.7 m/s² and ≤ 1.3 m/s²	The signal may be generated
> 1.3 m/s²	The signal shall be generated

  In all cases, the signal shall be de-activated at the latest when the deceleration has fallen below 0.7 m/s².

- The action on the service braking control (braking pedal) must not reduce the braking effect generated by the release of the accelerator control. Therefore the continuity of the graphs between category A and category B should be guaranteed as shown in Figure 16 and Figure 17.

2.2.3.1 Engine Brake Simulation (EBS)

Most motorists are used to driving a conventional vehicle with an internal combustion engine. If the accelerator pedal is released while driving and no more torque is requested from the engine, a design-related drag torque occurs. Depending on the number of cylinders, the compression ratio, the friction losses, the closed-throttle partial vacuum in petrol (gasoline) engines and other factors, this torque is different.

An electric motor, however, has almost no losses in idle compared to the combustion engine due to the small inertia of the driving motor [2].

To retain the similar driving feeling to that of conventional vehicles in coasting mode, emulated engine compression braking (EECB) is implemented. The electric motor (EM) provides negative torque to emulate the engine drag torque for charging the battery, thus making use of the kinetic coasting energy [2].

If energy recovery is initiated in this case, the driver is given a familiar driving experience and the vehicle's efficiency is increased. In order to simulate the deceleration characteristics of an internal combustion engine-powered vehicle, the electric motor must specify a suitable braking torque depending on the driving situation. Within the scope of this work, this was modeled to simulate a diesel engine and the appropriate gear selection depending on vehicle speed and can be seen in Figure 19.

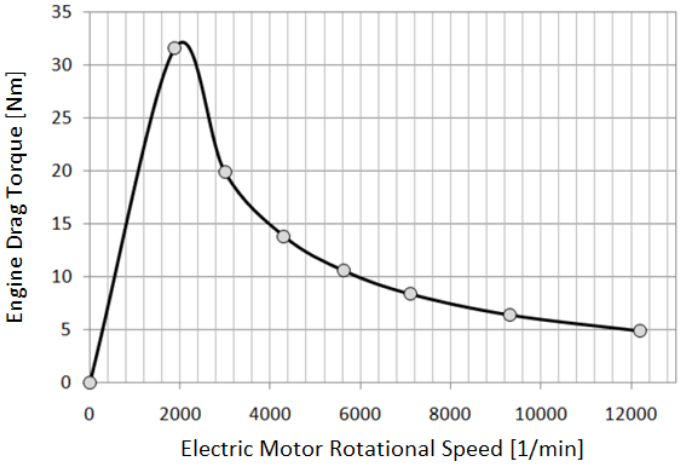

Figure 19: Example of EBS using a diesel engine according to [56]

The drag torque of traditional combustion vehicles yields typical deceleration values of 0.5 m/s² for routine driving situations [57]. However, the average deceleration values reported for normal driving in urban environments are about 1.0 m/s² [58] which means that there is potential for more deceleration than EBS.

2.2.3.2 Constant Torque

According to [3], the “throttle-off” torque characteristics are suggested to be as seen in Figure 20.
This approach is also used by some vehicle manufacturers. Some vehicles allow the driver to choose from multiple levels of regeneration due to their preference such as the current Volkswagen e-up [6].

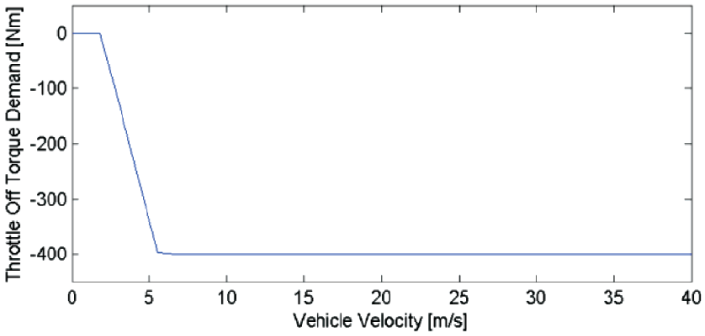

Figure 20: Throttle-off torque characteristic according to [3]

By selecting an appropriate constant torque, it can be ensured that this torque is always available at all rotational speeds. This torque can also be selected so that it correlates to a specific deceleration. Some deceleration values by current manufacturers are listed in Table 3.

Table 3: Sample of deceleration rates by different manufacturers

manufacturer	Deceleration rate
Nissan Leaf e-Pedal	2 m/s^2 [54]
BMW i3	1.6 m/s^2 [59]

[60] mentions that the use of the electric motor as a generator in today's electric vehicles is mostly limited to decelerations smaller than 0.3 g.

One can also notice that the torque at very low speeds does not exist. Afterwards, a linear increase in braking torque takes place up to a constant value. This is common in electric vehicle drives and will be discussed.

2.2.4 Regenerative braking at low speeds

According to [48], regenerative braking at low speeds is limited in order to prevent a reversing process and thus a backward rolling of the vehicle.

“At low speeds, no regeneration is possible because the process is less efficient at low power because of the substantial fixed mechanical losses, thus regeneration is not possible at low speeds and must be supplemented by mechanical brakes” [30].

In the study of safety aspects of regenerative braking [3], it was also stated that regenerative braking at low speeds “is especially dangerous for low-velocity brake applications such as up/downhill braking situations. For this consideration, the regenerative braking switch-off threshold should be set up. The level of the threshold is a trade-off between the recaptured energy via regenerative braking and the safety considerations, which is determined by the control system and the E-Motor properties. It may also be dependent upon the E-Motor and wheels connection, e.g. the fixed driveline ratio will require higher regenerative braking switch off velocity level in comparison to the driveline equipped with a multi-speed or Continuously Variable Transmission (CVT) gearbox.”

In a study about energy balance in regenerative braking strategies [47], it was mentioned that “at lower speeds, relatively little current is being produced by the generator to ensure desirable battery recharge efficiencies. Therefore, at these speeds, the frictional brakes are applied to decrease electrical cycling through the generator and batteries”. This micro-cycling (short-term charge and discharge cycles) reduces the life and efficiency of the battery pack.

[61] studied the effect of motor efficiency on regenerative braking at low-speed stages and presented a revised control strategy that can help increase the efficiency of energy recovery.

3 Adaptive Regenerative Braking

3.1 Advanced Driver Assistant Systems (ADAS)

According to [62], the driving task is viewed as a hierarchical task with three levels: navigation, guidance, and control as shown in Figure 21.

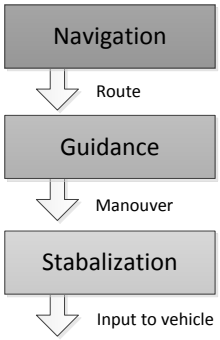

Figure 21: The three-level driving task model according to [62]

Advanced Driver Assistance Systems (ADAS) are provided to assist at different levels with each level having its own time frame where decisions need to be made [63].

Navigation refers to the high-level task of route-planning and the correlation of driving directions to signs and landmarks on the road. This happens on a time scale > 10 sec.

Guidance refers to the selection of the speed and path in response to the road geometry, hazards, traffic and the physical environment. This happens on a time scale of 1-10 sec.

Control or stabilization refers to the exchange of information and control inputs between the driver and the vehicle. Most control activities are skill-based and performed with little conscious effort. This happens on a time scale of < 1 sec.

Furthermore, the support that can be provided at each task level is also split into three layers: perception, decision and action layer.

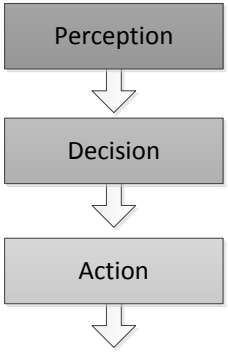

Figure 22: ADAS support levels according to [63]

For an ADAS to function well, it should be able to perceive the environment, the driver and his decisions, and the vehicle to be able to decide if the action is achievable.

3.2 Proposed Concept

An Adaptive Regenerative Braking concept is proposed as mentioned in the motivation of this work.

If the system is able to infer the deceleration decision made by the driver in the guidance layer, it will be able to help him execute it in the control layer in a manner that is comfortable for him.

By doing that the braking comfort is achieved while ensuring that the most possible energy for this maneuver is recovered.

The focus of this work will be on category (A) regenerative braking which is activated by the release of the accelerator pedal and is not part of the braking system. In principle, the system adapts the level of regenerative braking when releasing the accelerator pedal to the driver's type and driver's intention. So for example, if the intention of the driver is to roll then no regenerative braking is initiated. If the driver's intention is to decelerate, then an appropriate regenerative braking level is selected that ensures that it is comfortable and at the same time as efficient as possible.

Three core tasks are to be executed In order to realize this concept as seen in Figure 23 :

1. Driver type recognition
2. Driver intention recognition
3. Braking torque selection

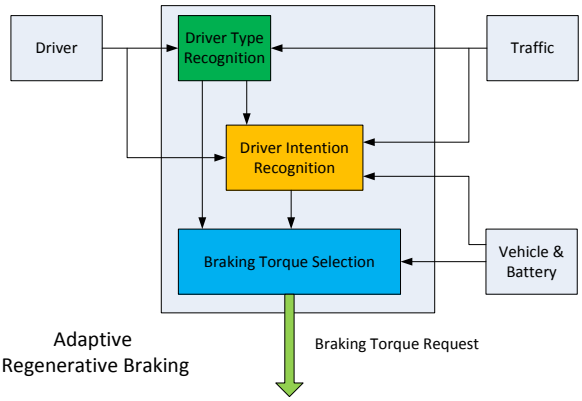

Figure 23: Adaptive Regenerative Braking concept

In the upcoming chapters, each sub-component will be separately explained, developed and validated.

3.3 Perception

To realize the proposed system, it is important to be able to perceive the environment in which the vehicle is moving and to which the driver reacts.

Since the system will be assisting in longitudinal braking, the environment in front of the vehicle is of utmost importance. The most important values needed for the proposed concept are the distance to the lead vehicle and the relative speed of the lead vehicle as well. These are key values the driver of the ego vehicle uses to decide on how to react to the change of behavior of the lead vehicle for a safe longitudinal control [64].

Figure 24: Perception of lead vehicle

The most common sensors and technologies used for distance measurements are Radio Detection and Ranging (RADAR), Light Detection and Ranging (LIDAR), Cameras and Ultrasonic Sensors.

The author of [65] investigated the influence of the horizontal field of view of these sensors on system performance.

The requirements of the sensors for the proposed system were investigated within the scope of this work and it was concluded that both Radar and Lidar are good candidates for the proposed system [66]. However, Radars are more economical and are less sensitive to snow, rain, and fog than Lidar [67] which made it the sensor of choice for the proposed system.

The study made in [68] states that the driver reacts to the change in relative speed between his car and the lead vehicle only when the distance to the lead vehicle is less than 150 m. Therefore, from the drivers perspective, [69] came to a conclusion that a sensor range of 150 m is sufficient since a reliable course prediction at larger distances is hardly possible.

3.4 Case Study

To develop and evaluate the proposed concept a case study is needed.

For the proposed concept, the best option would be to use a vehicle driving in normal traffic since the objective is to study the interaction of driver with the traffic environment. A BEV is available at the Institute of Vehicle System Technology where this work was done and can be used for this purpose [70]. However, the available vehicle is under development and doesn't have the required permits to drive on the street with normal traffic, and can be driven only on private test tracks. Therefore this option can't be used to test the effectiveness of the system in normal traffic conditions, but it can be used to validate the driver type classification and driver intention recognition subsystems

If tests are to be conducted on a test track, the traffic has to be planned carefully and isn't as real as one would have on a normal street. However, the results would be more reproducible since it is being controlled by the designer of the experiment.

Using a test bench produces accurate energy consumption. However, it isn't beneficial for this kind of testing because the influence of traffic is not testable. Several concepts for test benches that can simulate traffic already exist, but the interaction of the driver with this traffic isn't realistic.

A vehicle in the loop system tries to integrate a real vehicle with traffic in a virtual environment. Examples of such a system are presented in [71] and [72].

Driving Simulators are also an option where traffic can be modeled, but the dynamics of braking and the effectiveness on comfort can't be considered since the achievable decelerations are limited.

Using a simulation model in a simulation environment can be used to develop the concept and test it. The possibility of modeling traffic in a simulation environment is explained in chapter 6.2.4.

Within the scope of this work, two case studies will be used; a simulation model and a real BEV.

Details about the used simulation model and test vehicle can be seen in Appendix 9.1 and 9.2 respectively.

4 The Driver

In order for an advanced driver assistant system (ADAS) to properly assist the driver, it is necessary for the system to have information about the driver. For example, adaptive transmission control uses the interaction of the driver with the vehicle to select an appropriate transmission ratio for the current driving situation [73]. Modern systems even monitor the driver inside the cockpit such as fatigue and distraction warning systems [74]. With the increase of autonomous vehicles, this becomes even more important [75]. For the proposed system, the driver's type of deceleration and his intention are of utmost importance and will be studied in detail in this chapter.

4.1 Driver Type Classification Methods

In the literature, there is no standard definition of driver type. It is also not differentiated between driver type and driving style and both are used as synonyms. In general, the dynamic driving style of the driver on the road is of interest since the driver's type can be evaluated based on the actions he performs.

The methods used to quantify this can be either subjective or objective.

A psychological project called (S.A.N.T.O.S) was conducted as a cooperation between several automotive companies and several German universities and studied this in detail in [76].

They first suggested categorizing into 5 different driver types:

- Sporty – reckless

- Dynamic – progressive
- Routined – clarified
- Unobtrusive – conservative
- Anxious – reserved

The classification was made using the following measurements:

- Maximum longitudinal acceleration
- Maximum longitudinal deceleration
- Maximum lateral acceleration
- Maximum combined acceleration (vector addition of longitudinal and lateral acceleration)
- Accumulated speed difference in the test segment.

In [77], 6 types ranging from calm to dynamic were defined subjectively and were obtained by asking the individual probands using a questionnaire with no quantitative measurements.

The S.A.N.T.O.S. study found out that there is a correlation between these driver types and the longitudinal and lateral accelerations but that they were also dependent on the characteristics of the driven segment [78]. Figure 25 shows the distribution function of the maximum lateral acceleration for two different driving segments.

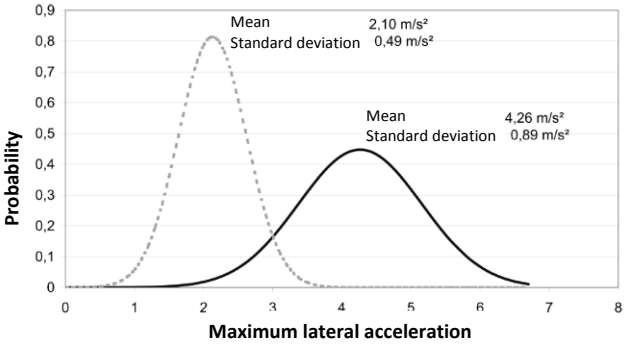

Figure 25: Lateral acceleration on different segments according to [79]

However, The classification into five or six driver types is according to [76] afflicted with shortcomings. Therefore, a distinction in the driver types sporty, normal and relaxed is sufficient to influence the properties of driver assistance systems [79].

In [80], some of the most important methods used nowadays were gathered. Table 4 gives an overview of some of the recent methods used to categorize the driver type.

According to [79], the driver is categorized as sporty, normal and relaxed while driving in curves. This approach isn't suitable for the proposed system as the main value that is exerted on the driver during braking is the longitudinal deceleration, not the lateral.

In [81], the driver type is categorized according to the longitudinal acceleration during acceleration and the lateral acceleration when driving in a curve on the highway exits and during lane changing. In this approach, the driver is categorized as sporty, middle, and comfortable. The tests made proved that the sporty driver had the highest longitudinal and lateral acceleration in all mentioned maneuvers. A significant difference can be seen in the startup

and curve driving maneuver. However, because of the acceleration values being low during highway exit and lane change, the difference isn't very significant. This approach proved that acceleration (both longitudinal and lateral) can be used for the categorization, but is hard in situations where the acceleration values aren't high. Additionally, the proposed system relies on a navigation device for localization.

Table 4: Some of the methods used for classifying the driver

Source	Values used	Categories
[79]	Lat. & long. acc.	sporty, normal, relaxed
[81]	Lat. & long. acc. + GPS	sporty, middle, comfortable
[82]	Jerk	aggressive, normal, calm
[83]	safety limit of the normal driver, utilization of the friction circle and acc. & dec. potential	sporty, average, gentle
[84]	acc. & brake pedal + change time	sporty, defensive, routined
[85]	acc. pedal and acc. pedal gradient, brake pressure, lateral acc.& steering angle gradient	dynamic, normal, relaxed
[86]	acc. & dec. pedal, speed and acceleration	sporty, eco and a gradient in between

In [82], the driver type is categorized according to the standard deviation of jerk (the differential of acceleration) during acceleration and braking maneuvers. This approach also took into account that the driver type isn't constant during the whole driving sequence but can change between different maneuvers. The standard deviation of jerk is calculated in a predefined time window. However, the selection of the time window proved to be a critical parameter that influenced the results. Smaller time windows give

good classification results but show a frequent change in the driver type that isn't very useful. Bigger time windows are more useful but don't detect all changes and include a lot of noise and unnecessary information that influence the accuracy of the classification. This approach categorized the driver as calm, normal and aggressive.

As discussed, even when the different methods use similar terms to describe the driver, the underlying meaning is different. Different types of sensors and equipment are also used and some of the methods are applied after measurements are finished. Some allow real-time measurement and classification using complex calculations and algorithms. Some focus on using easily accessible values from the CAN-Bus of the vehicle with no additional sensors to be installed [84].

Often, only indirectly, one can conclude what is meant by the term driving style and its characteristics. An objective description of the driving behavior is hardly possible, different names are subjectively understood [81].

In [87] a limit is defined for normal drivers, i.e. at a speed of 50 km/h lateral acceleration over 4 m/s^2 is described as unpleasant. That means that the measured maximum values of acceleration and deceleration of different drivers can be used as a comfort limit when designing the system later on.

In [86] fuzzy logic is used to classify the driver into sporty and eco using mainly pedal values and speed and acceleration after the drive and not in real time.

One of the advantages of using a simulation tool such as CarMaker from IPG is that it has a built-in driver simulation which is an intelligent driver based on a lot of studies and experience. This tool allows us to modify the behavior of the driver in the simulation. It categorizes the driver into defensive, normal and aggressive. Details of this driver and the quantities used to model its behavior are explained in Appendix 9.4. These three types of

drivers will be used when developing the system and will be later on validated with tests with real drivers.

One can notice the distinction between acceleration and deceleration values, but the same driver always has the same tendency in both. It will also later be shown after our proband tests that the default values are a little bit high and don't describe the drivers well.

The different parameters of the simulation environment driver allowed us to do initial tests on the simulation vehicle and also design the proposed system later on.

The authors of [83] clearly state that it should be fundamentally differentiated between the braking and acceleration behavior. While the acceleration behavior is significantly dependent on the power of the vehicle as [88] mentions, the braking behavior remains almost unaffected as seen in Figure 26.

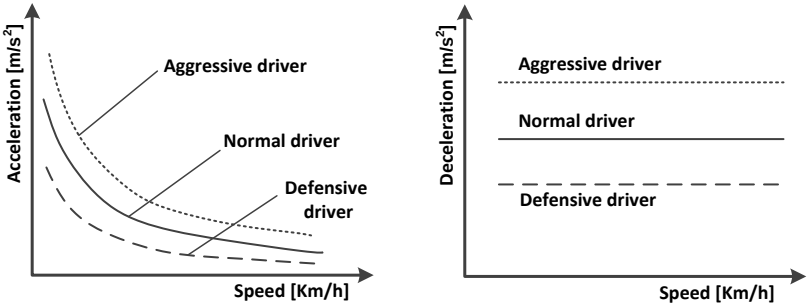

Figure 26: Profiles of different drivers: longitudinal acc. vs. speed (left) & longitudinal dec. vs speed (right) [83]

This means that same driver could behave differently during accelerating and decelerating. By using this definition, it could be that the driver is rather

aggressive during acceleration to enjoy the dynamic performance of electric vehicles and a defensive during deceleration in order to regenerate as much energy as possible. Therefore another measure that is more reliable for determining the driver's type during deceleration has been proposed and developed.

4.1.1 Distance-Based Classification

4.1.1.1 Concept

Figure 27 shows the accelerator pedal value, distance to lead vehicle, and speed of a driver approaching a vehicle in front of him. It can be noticed that at a certain distance to the lead vehicle the driver releases the accelerator pedal completely[2] before applying the brakes later on.

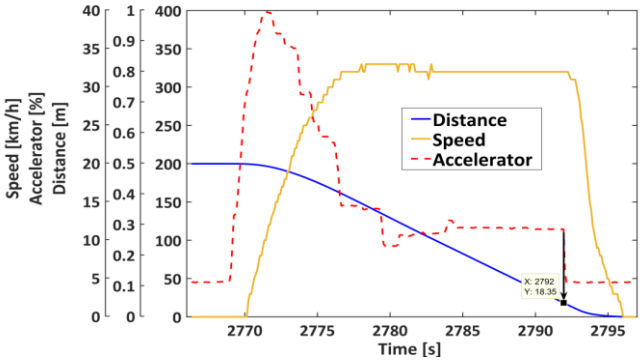

Figure 27: Distance-based driver type classification concept

[2] It can be noticed that even with a fully released accelerator pedal a positive value is still registered. This is an offset added in the VCU software to realize a creeping function.

Due to the fact that the drivers brake differently, the distance to the obstacle (being a vehicle or traffic light) at which the driver releases the accelerator pedal in order to brake differs. This distance is a function of the driver type and the speed of his vehicle as well as the relative speed to the lead vehicle defined by the difference in speed between the ego and lead vehicle.

This release distance can be used to infer the driver type during deceleration.

To obtain these release distances, tests were designed that can give us this release distance for different driver types at different speeds of the ego vehicle and the lead vehicle. This was done using the simulation model that enabled the selection of different driver types. These tests were then recorded and an empirical function for each driver was derived. These functions can now be used to classify the type of the driver by knowing the release distance and speeds at which this event happened (ego vehicle speed and relative speed to lead vehicle). By measuring which function is closer to the registered release point, the driver type can be categorized. The release point can be determined during driving when the pedal is released and the intention of the driver changes from cruising or rolling into braking as it will be shown in chapter 4.2.

Figure 28 shows an example of the functions of the defensive and aggressive drivers with the lead vehicle having a speed of 0 km/h.

Plotted on this figure is also a point that represents a test driver releasing the pedal at 50 km/h at a distance of 100 m from the lead vehicle. By comparing the position of this point in relation to the two plotted graphs it can be concluded that this driver can be categorized as defensive when braking.

The previous profiles are based on the measurements made in the simulation software with the default value for the drivers according to Table 19.

However, as will be shown later, these values were a bit high in comparison to the real test drives made later and will be discussed in chapter 4.1.4.

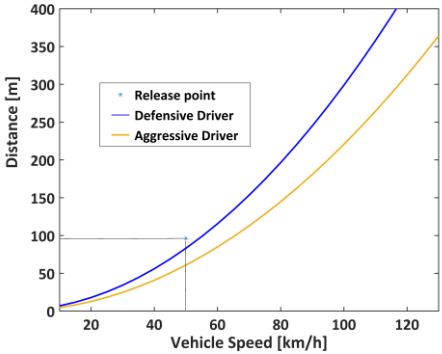

Figure 28: Distance-based driver type classification example with the velocity of the leading vehicle being 0 km/h

4.1.1.2 Properties of the Proposed Method

In all of the previously mentioned approaches, the driver type is determined after the driver has initiated or started the braking maneuver. This approach, on the other hand, has the advantage of being predictive. Since the release distance of the accelerator pedal is measured and used for categorization, this means that the driver type is predicted before he starts to decelerate with the brake pedal.

This approach also focuses on the driver type when decelerating independently from his acceleration style.

It is also important to mention that by using the accelerator pedal not only is the type prediction faster but if it relied on the brake pedal a bigger devia-

tion in distance will be seen because the driver's time to change from the accelerator to the brake pedal also differs according to Table 19.

However not all accelerator pedal releases correspond to an intention in braking and therefore this method also needs to benefit from the driver intention recognition task explained later.

Secondly, these tests in the simulation software used a virtual radar sensor. However, the available test vehicle isn't equipped with a radar sensor. A solution for doing the tests with the real vehicle is described in Appendix 9.2.

4.1.1.3 Parameterization

The tests were done using the simulation vehicle and repeated at 10 km/h Intervals with different types of drivers.

For the cases where the lead vehicle was faster than the ego vehicle weren't taken into consideration because they won't lead to a braking maneuver as the vehicle will never be able to approach the lead vehicle.

The release distances of each test were recorded and analyzed [89]. By varying the values at a constant speed of the lead vehicle, the data collected for each speed of the lead vehicle can be plotted. Some examples are shown in Figure 29.

A regression polynomial fitting was made after that in order to get an equation that represents each type of driver.

All four plots were made on the same scale of the y-axis representing the release distance for comparison at different lead vehicle speeds. It can be seen how the shape of the functions change as the lead vehicles speed increases and the relative speed decreases as well.

These results were obtained using the different types of drivers available in the simulation environment. The accuracy of this method will be validated against real test drives.

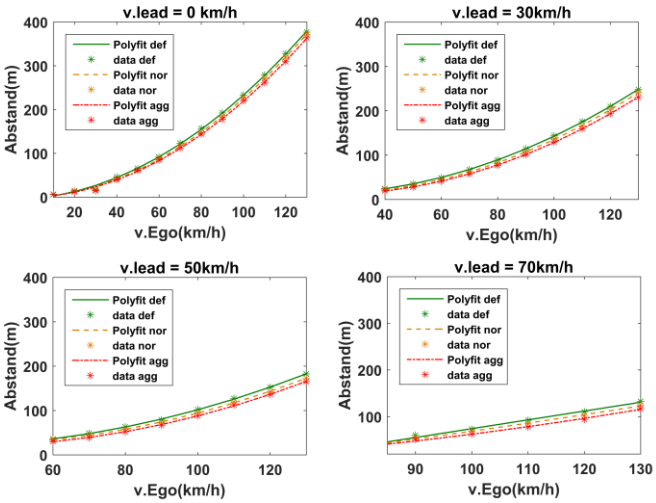

Figure 29: Simulation results for different driver release profiles at different lead vehicle speeds [89]

4.1.2 Validation

4.1.2.1 Experimental Construction

In order to have a good idea of how real drivers react when braking, real test drives had to be made.

The complete test track that was available at Campus North of KIT was a straight track of almost 800 m. A 600 m piece was equipped with traffic

pylons and stop signs to divide the test track into several segments as shown in Figure 30.

Depending on the speed that is to be reached during an experiment an appropriate number of segments is assigned to each experiment.

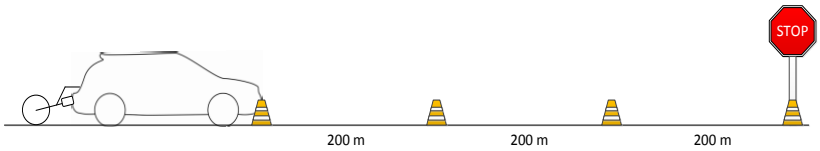

Figure 30: Experiment Setup

4.1.3 Test Drivers

Eight probands[3] took part in these tests and each proband was asked to drive several tests emulating all three types of drivers at different speeds. In total 111 different tests were made.

The probands were given a brief overview of what the experiments will be and what they are supposed to do. The purpose of the test was kept hidden in order to keep the drivers from having any bias.

During the tests, the regenerative braking of the vehicle was turned off in order to see how the drivers would interact with the vehicle with no regenerative braking. At the beginning, each driver was given the time he needed to get comfortable with driving the vehicle.

For the goal of knowing the driver type, the following experiments were made.

[3] The probands were male between 25 and 36 with more than 5 years of experience driving a vehicle and have driven electric vehicles before.

4.1.4 Cruising Experiments

In this experiment, the driver was asked to accelerate to a given speed and then try to cruise at that speed. At the end, the driver is supposed to brake defensively, normally and aggressively so that the vehicle comes to a stop at the end of the segment. What each term meant and which definition was used was kept undisclosed. It was desired to know what each interpretation of the term meant to each individual proband. Additionally, it was preferred to know how the drivers will react when there is no engine braking from the vehicle and the cruising deceleration is only due to the air and rolling resistances. Therefore the RB was set to zero in these tests.

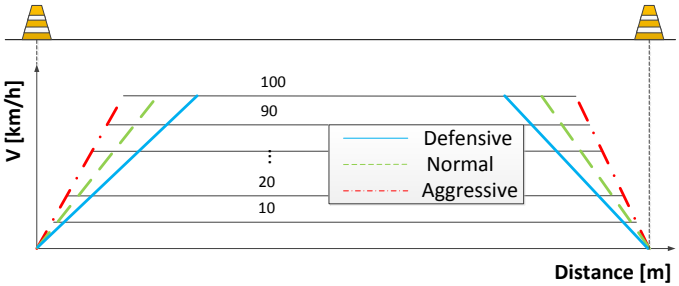

Figure 31: Cruising experiments setup

Figure 32 shows the measured decelerations during braking for all three types of drivers.

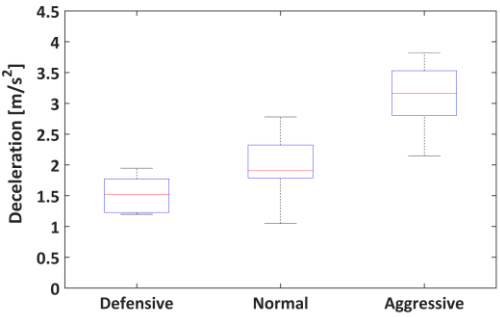

Figure 32: Detected decelerations during the experiments

When a driver is told to brake normally, the driver would brake how he tends to normally brake which could be defensive or aggressive but not as a normal driver according to the defined classification. It can be seen that the deceleration rates that occurred when the drivers were told to brake normally cover the whole range of the deceleration rates that occurred when they were asked to brake defensively as well as a portion of the aggressive braking. For this reason, the focus will be on defensive and aggressive braking since the probands all have a feeling for what those two terms mean. It can be concluded that normal braking has a different meaning for each person, whereas defensive and aggressive definitely correlate with lower and higher deceleration rates respectively. Therefore, the results of the normal braking experiments won't be taken into consideration when measuring the accuracy of the classification.

By analyzing the test measurements of the real test drives in Figure 32, the comfort limit of different driver types will be newly defined.

At a first glance one is tended to take the median value of each category as a representation of the group; however, since the limits are being

considered, the value that corresponds with the majority of the group was taken and that is at the 75% level of the boxplots:

Table 5: New comfort limits of driver types

	defensive	aggressive
acceptable deceleration rate [m/s^2]	-1.8	-3.5

It can be seen that these values are lower than the default values used before and the following accuracy analysis was made using the new limits.

The accuracy of the method was defined as follows:

$$Accuracy = \frac{\#\ correct\ classifications}{\#\ all\ experiments} \qquad (4.1)$$

A correct classification means that the method categorized the driver type to be the same as the driver type intended according to the design of the individual experiment.

At the beginning, 66 cruising experiments were conducted. After excluding the results of the normal driver tests, 48 were left. Using the rest of the data, cross-validation on the measured experiments was made and came to the following results:

Table 6: Accuracy of proposed method

		Accuracy
# of all experiments	48	85%
# of correct classifications	41	

# of experiments under 60km/h	30	97%
# of correct classifications under 60km/h	29	
# of experiments over 60 km/h	18	67%
# of correct classifications over 60km/h	12	

The results were split into two ranges: under and over 60 km/h or urban speeds and highway speeds. The results at the lower speeds were significantly better. These are the speeds that represent urban driving.

The false classifications at speeds over 60 km/h can be connected to several reasons:

For safety reasons when conducting the experiments, there wasn't really a vehicle in the front, but rather a stop sign. Estimating the distance to a stop sign on the sign of the road at high speeds and far distances is a challenge. According to [68], the person is only able to react correctly if the distance to the object is 150 m or less which is not the case for speeds over 60 km/h.

The experiment was designed to accelerate to a given speed and then stay at that speed for a while and then decelerate. This caused problems that were given as feedback from the probands: first of all, the driver was constantly concentrating on the dashboard to cruise at a specific speed. At higher speeds, that made it difficult to concentrate on the distance to the stop sign as well. Secondly, the test track wasn't long enough to allow the acceleration to higher speeds with low accelerations rates and then also manage to brake in the desired manner, leading to the driver braking too late and falsely being classified as an aggressive driver.

Most of the false classifications are of defensive drivers being classified as aggressive. When the driver is told to brake defensively and releases the

pedal at a distance greater than 150 m while braking defensively and when the vehicle comes nearer to the stop sign the driver notices that this level of braking wouldn't make it and stop at the stop sign and therefore increases the braking intensity beyond the defensive limit.

4.2 Driver Intention Recognition

For an ADAS System to assist the driver in the task being performed, it is necessary for the system to be able to infer the situation and the trajectory of the vehicle planned by the driver in order to be able to assist him in a proper way. Evidence about the driver's control input to the vehicle offers a means of inference of the probable maneuver being executed [90]. Conclusions about the probable maneuver can be drawn from direct driver monitoring or from observing both vehicle and surrounding object data [91]. Several approaches exist that use a combination of several observations to make these conclusions.

4.2.1 Intention Recognition Methods

The methods used for driver intention recognition come from a wide spectrum of applications, the most popular one being speech recognition.

The aim of a driver behavior prediction system is to forecast the trajectory of the vehicle, which could allow a driver assistance system to compensate for dangerous or uncomfortable circumstances.

Intention maneuvers may be planned on operational, tactical, or strategic timescales. These timescales have been proposed by [92] and [93].

"The operational, or critical, timescale, on the order of hundreds of milliseconds, is the shortest possible timescale for human interaction. Tactical, or short-term, timescales are on the order of seconds and encompass many

successive critical operations. Finally, the strategic, or long-term, group is associated with minutes or hours of prior planning" [94].

The method selected should be appropriate to the intentions that are needed to be inferred depending on the application of the ADAS. For the proposed method in this work, inferring the driver's intention on a tactical level is of great importance.

[94] reviewed the field of driver behavior and intent recognition with the focus on tactical maneuvers.

Table 7 shows a list of methods used in the literature on this level, for which intention they were used, and what quantities were used to achieve that.

Table 7: Some methods used for driver intention recognition

Source	Intention to be recognized	Method used	Quantities used
[95]	Stop at an intersection	SLDS & HMM	Speed & pedal stroke
[96]	Stop at an intersection	AR-HMM	Speed, pedal stroke, and past movements
[97]	Lane change	CHMM	Steering angle, steering rate, and lateral acceleration
[98]	Lane change	SVM & HMM	Speed, steering angle, gas pedal, distance to lead vehicle
[99]	Overtaking	Fuzzy Logic	Distance to lead vehicle, relative speed, brake pressure, accelerator pedal value and change rate
[100]	Driving intention	Fuzzy Logic	Pedal travel, pedal travel change rate, and speed

[95] compared Switching Linear Dynamic Systems (SLDS) and Hidden Markov Models (HMM) in order to predict the probability of the future stop at an intersection. The quantities used were the speed of the vehicle and the pedal stroke which is defined as “the subtraction of the stroke of the brake pedal from the stroke of the accelerator pedal”.

[96] improved upon [95] by using Auto-Regressive Hidden Markov Model (AR-HMM) which uses information from past movements. This allowed a more “accurate prediction since human’s behavior is strongly related to past actions”.

[97] used continuous Hidden Markov Models (CHMM) to predict a left or right lane change or if the driver intended to stay in the current lane.

[98] compared state vector machines (SVM) and Hidden Markov Models (HMM). He concluded that “HMM is good at mapping temporal variations and SVM offer a powerful sample by sample prediction accuracy. A combined recognition system that can inherit the merits of these two frameworks may prove useful.”

[99] relied on Fuzzy Logic in order to predict overtaking maneuvers. The relevant indicators used for this prediction were acquired from the CAN Bus of the vehicle and include distance between ego and lead vehicle, the relative speed between the vehicles, brake pressure, accelerator pedal, and accelerator pedal change rate.

[100] used Fuzzy Logic to infer the driving intention of being accelerating or decelerating and the level of this intention to intelligently control an HEV using the pedals travel, pedals travel change rate and speed of the vehicle.

The mentioned methods were analyzed in detail. Within the scope of this work, several approaches to the task at hand were tested and compared in [101]. In the end, HMM was chosen as the method to be used for the detec-

tion of deceleration intentions. In the following chapter, hidden markov models will be described in detail as well as the modeling procedure.

Several motivations exist for using HMM for the proposed system.

HMMs support recognition of temporal data patterns. This is particularly useful because humans perform different actions on a variable time-scale. Even within a lane change, the internal states may vary in time. HMM provide an excellent framework for such temporal mappings.

The general idea behind the use of HMM is that a driver can be "modeled as having a (possibly large) number of internal mental states. Progressing through those internal mental states during driving, the driver develops the intention to start a maneuver" [102]. However, this sequence of mental states is hidden. An HMM can be trained to recognize this hidden sequence of states. In turn, the maneuver can be broken up into a chain of consecutive actions, which can be modeled and analyzed as an HMM [103].

4.2.2 Hidden Markov Models (HMM)

Previous studies have shown that human behavior can be observed as a sequence of internal 'mental' states each with its own particular behavior and transition probabilities [104]. Given sufficient training sequences, 'estimation' can be used to train model parameters adequately. Trained models can then use 'decoding' to determine the hidden sequence of states that correspond to a particular driver behavior.

HMM is used in a lot of fields of information technology and robotics i.e. in automatic voice recognition.

"A hidden Markov model is a collection of finite states connected by transitions. Each state is characterized by two sets of probabilities: a transition probability, and a discrete output probability distribution or continuous

output probability density function which, given the state, defines the conditional probability of emitting each output symbol from a finite alphabet or continuous random vector" [105].

According to [103], the elements of an HMM are as follows:

1. N, the number of states in the model.

2. M, the number of distinct observation symbols per state, i.e., the discrete alphabet size which corresponds to the physical output of the system being modeled.

3. The state transition probability distribution, $= \{a_{ij}\}$, where a_{ij} is the transition probability of taking the transition from state i to state j.

$$a_{ij} = P[q_{t+1} = S_j | q_t = S_i], \ 1 \leq i, j \leq N \tag{4.2}$$

4. The observation symbol probability distribution in state j, $B = \{b_j(k)\}$, where

$$b_j(k) = P[v_k \, at \, t \mid q_t = S_j], \ 1 \leq j \leq N, \ 1 \leq k \leq M \tag{4.3}$$

5. The initial state distribution $\pi = \{\pi_i\}$ where

$$\pi_i = P[q_1 = S_i], \ 1 \leq i \leq N \tag{4.4}$$

For convenience, the compact notation is used to indicate the parameter set of the model.

$$\lambda = (A, B, \pi) \tag{4.5}$$

Given this definition of HMM, there are three basic problems of interest that must be solved for the model to be used in real-world applications [103]: the evaluation problem, the decoding problem, and the learning problem.

Intention recognition can be formulated as the **Evaluation** problem for HMM's: Given an observation sequence O and a set of parameterized models (one for each discrete maneuver that is to be distinguished), what is the probability that this sequence has been generated by the respective model? This can be solved using the forward-backward algorithm described in [103].

The **Decoding** problem explains how, given a model, a state sequence can be generated that best "explains" the observations in some meaningful sense.

The **Learning** problem covers how to adjust the model parameters of $\lambda = (A, B, \pi)$ to maximize $P(O|\lambda)$ in order to be able to do the evaluation. This is solved using the Baum-Welch algorithm described in [103] as well.

Several Types of HMMs exist: **Ergodic** HMMs are fully connected meaning that every state of the model could be reached (in a single step) from every other state of the model. A **Left-right** model has the property that as time increases the state index increases (or stays the same), i.e., the states proceed from left to right [103]. Figure 33 shows an illustration of a 4-state ergodic HMM and a 4-state left-right HMM.

The selection of an appropriate type depends on the intentions to be determined and how they interact with each other. For the proposed system an ergodic HMM is suitable to describe the interaction between different driving maneuvers.

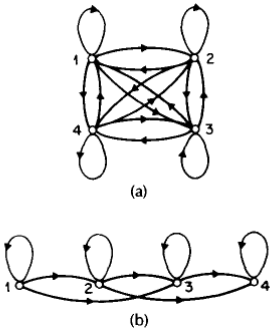

Figure 33: (a) ergodic HMM, (b) left-right HMM [103]

For the purpose of the proposed system, an ergodic Multi-dimensional Discrete Hidden Markov Model (MDHMM) was used as the base for each intention developed.

4.2.3 Model Development

In [106] the concept of a double layer model for intention recognition was established. Within this hierarchical model, the primitive driving patterns are abstracted in a lower layer, and the long-term driving patterns are extracted in another layer as can be seen in Figure 34.

[107] used this concept where a lower layer and upper layer HMM is used. The lower layer is responsible for detecting the short-term driving behavior and the upper layer is responsible for detecting the long-term driving behavior or maneuvers which represent the intentions of the driver during navigation.

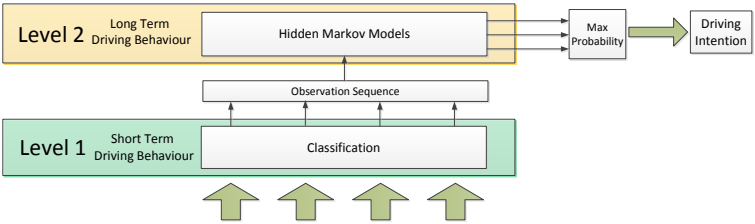

Figure 34: Concept of a double layer intention recognition according to [107]

However, in the scope of this work, it was proven that using an HMM in the lower layer is more calculating intensive and can be reduced by using a fuzzy logic model or by even using a simple categorization logic [101].

Several studies were made in the scope of this work to analyze the design of the lower layer (number of submodules and signals and levels in each one) which in term defined the alphabet of the HMM in [108], [101], and [109]. The end results are shown in Table 8 where the lower layer was divided into 6 sub-blocks. Each sub-block is responsible for the categorization of a single signal resulting in a drastically increased accuracy of the model.

Table 8: Signals of the lower layer

Signal	# of levels
Acc. pedal value	6
Acc. pedal change rate	8
Brake pedal value	2
Vehicle speed	4
Distance value	7
Distance change value	7

This information is then sent to the upper layer. In this layer, a separate MDHMM is modeled and trained for each intention. The following intentions were selected to be modeled which will be needed for the brake torque selection later.

Table 9: List of selected intentions to model

Model	Intention
M1	Acceleration
M2	Cruising
M3	Rolling
M4	Normal Braking
M5	Emergency Braking
M6	Brake Pedal Braking

The intention of normal braking is defined as the driver releasing the accelerator pedal with the intention of braking but before applying the brakes with the brake pedal. Emergency braking is the same but with the intention of braking hardly because of approaching the lead vehicle in an emergency situation.

Within the scope of this work, the intention of releasing the accelerator pedal because of approaching a curve was also modeled and investigated in the simulation environment In [101]. However due to the lack of steering wheel signal in the test vehicle this intention wasn't pursued further.

The four relevant intentions for the ARB are cruising, rolling, normal braking and emergency braking and the designated braking strategy to each intention will be explained in chapter 5.2. The results of the upper layer are several probabilities and the model with the highest probability is selected as the actual intention as seen in

Figure 35.

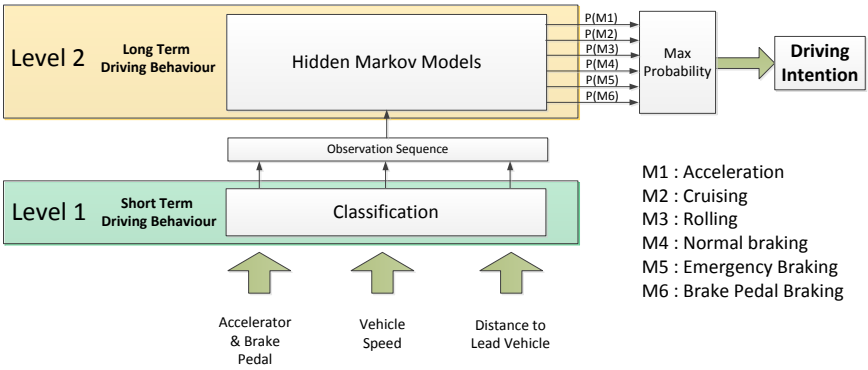

Double Layer Intention Recognition

Figure 35: Application of double layer intention recognition

During the development phase, the models were designed and trained using data gathered from driving the simulation vehicle in the simulation environment. After making sure the models worked reliably the next step was to train the models using data from real test drives in order to get a more accurate model with more realistic results.

4.2.4 Parameterization (Training)

As mentioned before, in order to be able to solve the evaluation problem of an HMM $\lambda = (A, B, \pi)$, it is necessary to know the parameters $A, B \; and \; \pi$ of the HMM. This is done by solving the learning problem where an initial model is taken and using the Baum-Welch algorithm the probability state

transition probability distribution A and the observation symbol probability distribution B can be defined.

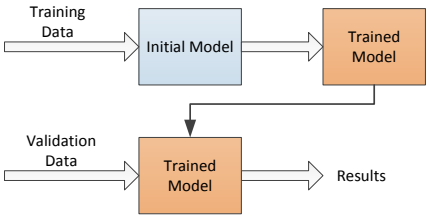

Figure 36: Normal training and validation

To optimize the driving intention recognition, the previous cruising measurements as well additional test drives with the same probands were planned and executed. The measurements were used to parameterize and optimize the models of the recognition algorithms. In addition to the coasting experiments made in 4.1.2.1, the probands were asked to conduct the following experiments as well.

4.2.4.1 Emergency Braking Experiments

In this experiment, the driver was asked to accelerate to a given speed and then emergency brake when a sound signal is heard. The sound signal was always triggered at the same location without the drivers knowing that. This was conducted in this manner to know where the intention of the driver changed on the track to improve the accuracy of labeling.

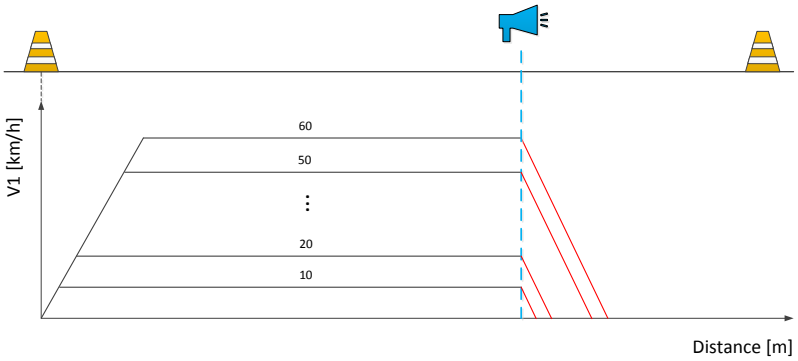

Figure 37: Emergency braking experiments setup

4.2.4.2 Rolling Experiments

In this experiment, the driver was asked to accelerate to a given speed and then release the accelerator pedal at a distance from the end of the segment so that the vehicle will come to a stop at the end of the segment by rolling alone.

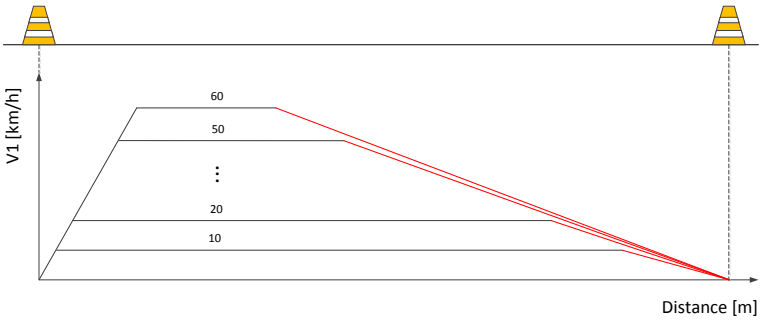

Figure 38: Rolling experiments setup

4.2.4.3 Data Labeling

In order for the training algorithm to be able to work, the training data has to be labeled accordingly. A GUI (Graphical User Interface) using Matlab was developed in [108] that allows labeling in an efficient and accurate way. It was then further developed to automatically label certain events and event triggers that can automatically be detected such as acceleration start and braking with the braking pedal to improve the labeling accuracy. The tool is explained in Appendix 9.5.

After labeling the measured data, it could be used to train the corresponding models.

These models are then used to detect the driver's intention. In order to do so, the probability of the current maneuver being generated by this driving model is calculated.

The model with the highest logarithmic likelihood probability is the most likely model to represent the driver's intention and is then selected as the intention.

4.2.5 Validation

Cross-validation is used when it is desired to estimate how accurately a predictive model will perform in practice. The dataset is split into two parts: training and validating datasets. The training dataset is used to parameterize the model and the validating data set is used to determine how good the model is. One of the most commonly used methods is the k-fold cross-validation. Using this approach the complete data set is divided into k parts. These k parts are then split into training and validating datasets [110].

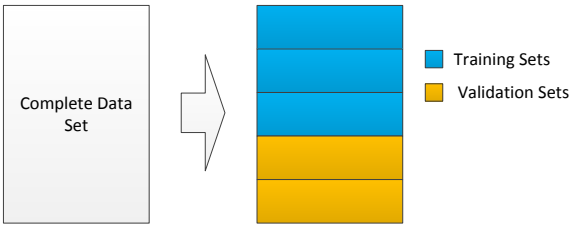

Figure 39: K-fold cross-validation according to [110]

How to select k is the tricky part. The dilemma comes from trying to maximize both datasets in order to get the best training and validation results. One simple approach is called Leave One Out Cross Validation (LOOCV) where (k-1) parts are used for training and only one set is left for validation [110]. In our case, each set represents an experiment and the validation will be made using also one experiment as seen in Figure 40.

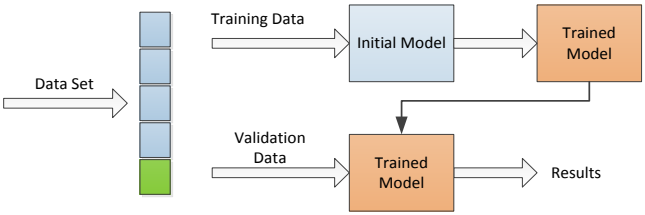

Figure 40: Cross-validation according to [110]

An example with good results of comparing the labeled intentions with the resulting predicted intentions of the MDHMM can be seen in Figure 41.

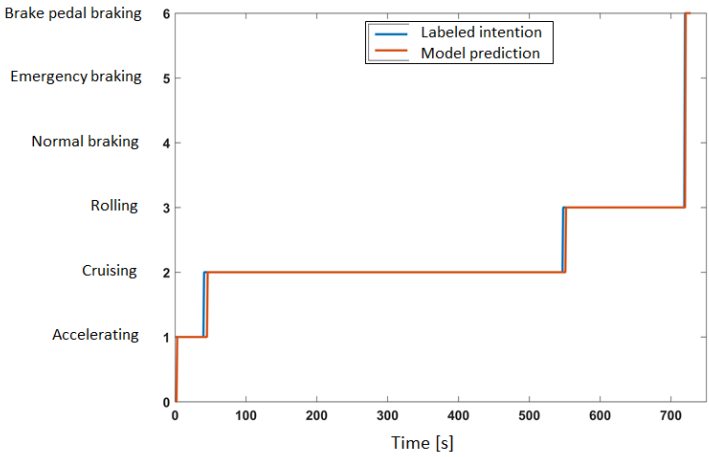

Figure 41: Comparing labeled and predicted intentions

In this experiment, the driver was at first accelerating, and then he cruised for a great period. After that, he rolled for a while before braking with the braking pedal.

It can be seen that for the most part of the experiment, really good accuracy is achieved and the predicted intention matches the labeled intention very well.

However, it can also be seen that the problems of mismatch occur when there is a change in intention. This is due to the fact that while labeling, the time stamp when the change happened from one intention to the other can't be coined accurately as this is a mental decision that happens in the head of the driver and "the maneuver start timestamp is not clearly defined" [102]. Therefore, the accuracy of these transition phases depends on the experience of the labeling person.

Figure 42 shows the accuracy results for each individual intention covering all the experiments made for one labeling attempt. The person who labeled the data didn't understand what emergency braking was and has therefore labeled it falsely. It can be seen that the accuracy results of the intention of emergency braking are really bad.

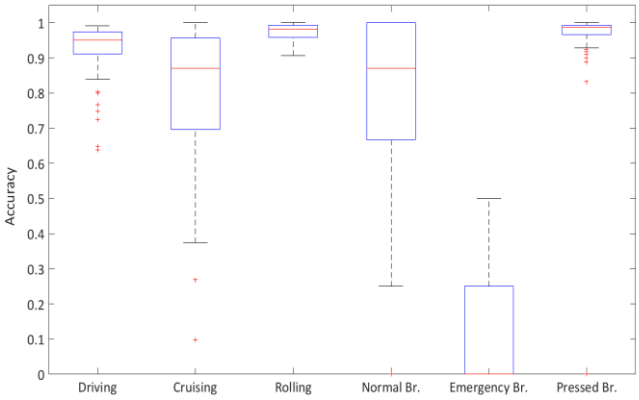

Figure 42: Intention accuracy results with bad labeling

After seeing these results, the experimental data was labeled again taking into consideration the previous results. An automated labeling function was also integrated into the labeling tool to detect the maneuvers that could be automatically detected such as the start of acceleration and start of deceleration with the brake pedal. The validation was then made again and the results are shown in Figure 43. As can be seen, results are much better as well as a drastic increase in the results of the normal braking intention.

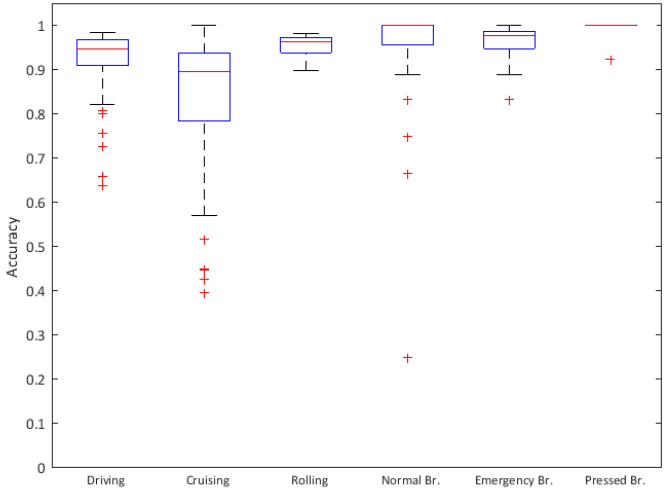

Figure 43: Intention accuracy results with improved labeling

The developed model shows very good accuracy for rolling and braking intentions. However, for acceleration and cruising, the intention isn't that well for the reason described before. Several methods can be used to improve the accuracy and are explained briefly in chapter 4.2.6.

The total accuracy by doing a LOOCV on all experiments and combining the accuracy of all intentions in each experiment gives the following results:

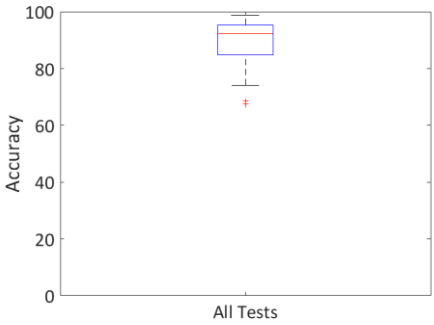

Figure 44: Total accuracy of all experiments

The median of the accuracy is around 92% without any optimization. Optimization will further increase the accuracy.

4.2.6 Optimization

In order to improve the model after testing it for a while and noticing a special intention not working well, new information can be gathered to improve the model and train it again.

However, since batch training is normally used for training, it is necessary to combine the old data with the new data meaning that a record of the old training data has to be kept as shown in Figure 45.

By using an incremental learning process, only the model needs to be saved but not the data that was used to train it. This model can then be upgraded with new training data, without combining it with the old training data as depicted in Figure 46.

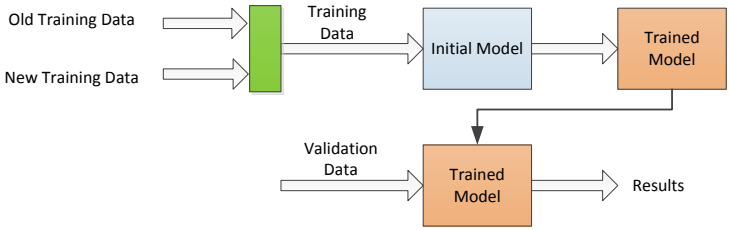

Figure 45: New batch training of parameters

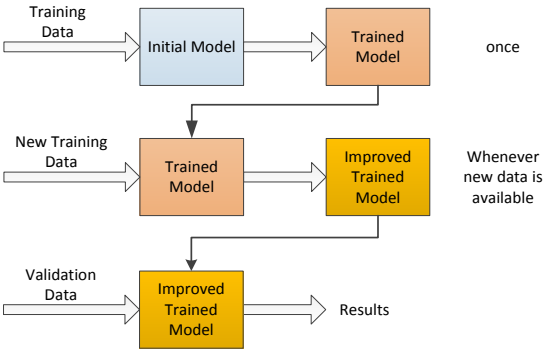

Figure 46: Incremental learning according to [111]

Several methods exist that allow the incremental learning and are described in detail in [111].

Within the scope of this work, [108] investigated this possibility and implemented it to be used in the future to optimize the model. Figure 47 shows how using incremental learning can improve the quality of the model. For testing purposes, each increment used one labeled experiment to re-train the previous model. The x-axis shows the increment number and the y-axis shows the accuracy. However, the model is as good as the available labeled

data and it can be seen that the accuracy can't be increased upon a certain point.

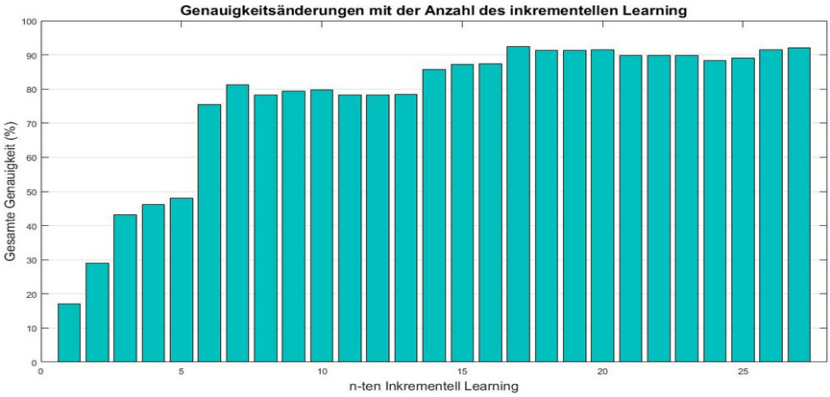

Figure 47: Accuracy improvement with incremental learning [108]

5 Braking Torque Selection

After recognizing the driver type and intention a braking model has to be defined accordingly.

5.1 Braking Torque Selection Boundaries

Selecting a suitable torque for braking is not an easy task. The appropriate torque is limited by a lot of factors as gathered in Figure 48.

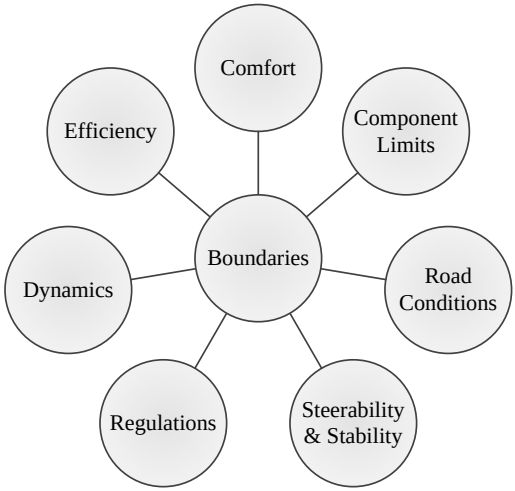

Figure 48: Some of the boundaries affecting the selection of regenerative braking level [7]

By studying the main interactions between the components and their limits it is possible to focus on the most important limitations as seen in Figure 49.

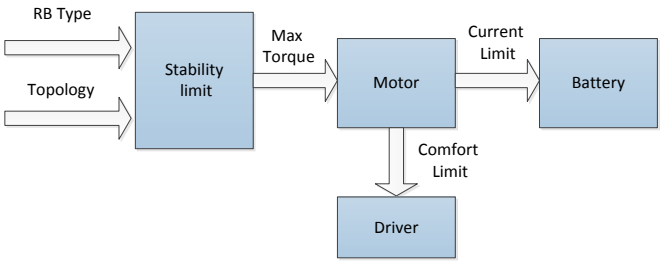

Figure 49: Limits affecting the braking torque selection

It is important to mention that the limits that will be discussed apply to both category A and category B regenerative braking.

5.1.1 Energy Storage

As discussed in 2.1.3 the critical parameters of the electric storage that should be considered during recuperation are SOC and charging current.

The battery manufacturers mainly provide the recommended charging rate, in addition to other charging rates and how long they can be used for (in the case study example, nominal charging is 35 A and max charge rate is 150 A @ 5 sec).

Knowing that the charging current limit can only be used for a certain duration, [56] studied the effect of different regenerative braking strategies with different deceleration limits on the maximum current generated when driving different cycles. However, what was really missing was the link between the maximum allowed charging current, charging time and the state of the SOC.

In [48], Lithium-ion batteries were studied during charging with high currents. It was observed that the lower the starting state of charge is at the

start of a charging session the longer the battery can be charged with the higher currents. This was tested for several charging currents and an almost linear correlation between the state of charge and the charging duration was observed. Taking this into consideration and by using the values of the installed battery in the test vehicle the graphs in Figure 50 were generated:

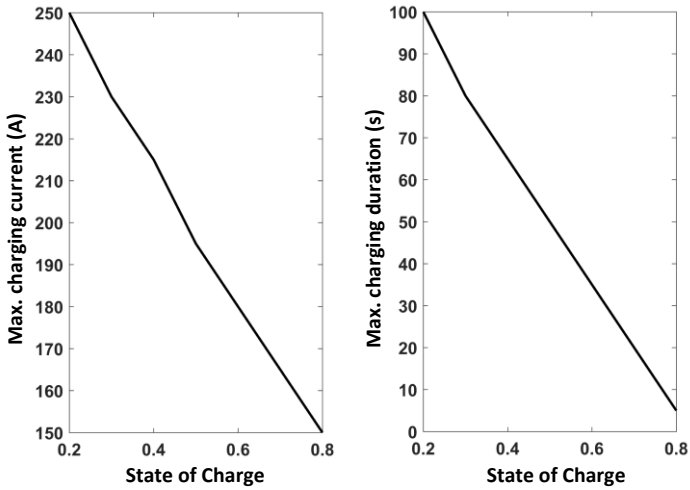

Figure 50: Max. charging current vs. SOC (left). Max. charging duration vs. SOC (right) [89]

These values were then used in the model to set a flag if the charging duration or current exceeded the limit and to check if the current can be used to charge the batteries or used in another form as discussed in chapter 2.1.3.

5.1.2 Electric Motor & Power Electronics

One important limitation for regenerative braking is the torque limitation of the motor since it is dependent on the rotational speed, as well as the current and voltage of the power electronics

First of all, it is interesting to know how big the generated current by the motor at different vehicle speeds and different deceleration rates is and if the battery can cope with these currents.

Using the simulation model, the vehicle was decelerated from 120 km/h to a still stand using only the electric braking by the motor and by setting a constant deceleration rate as the input of the driver controller. The current generated and the required torque at different deceleration rates was recorded and part of the results can be seen in Figure 51.

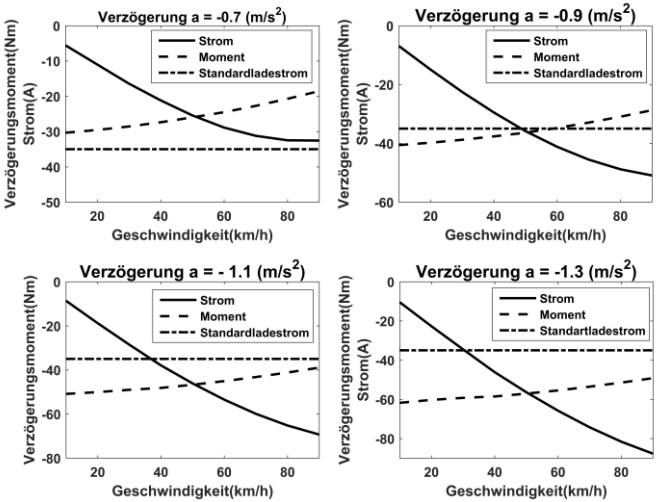

Figure 51: Current and torque at constant deceleration rates [89]

The nominal charging rate of the installed battery (35 A) is also depicted in each of the graphs. It can be seen that at low deceleration rates of -0.7 m/s^2 the generated current never reaches this nominal value at all speeds. However, at higher deceleration rates, the current value exceeds this nominal value (i.e. at a deceleration rate of 0.9 the nominal charging current is reached at the speed of 50 km/h).

Secondly, It is interesting to know if the needed torque for braking is more than the maximum torque that the motor can generate or not.

For that, the previously made measurements (deceleration from 120 km/h to zero using constant deceleration rates) were used. An example is shown in Figure 52:

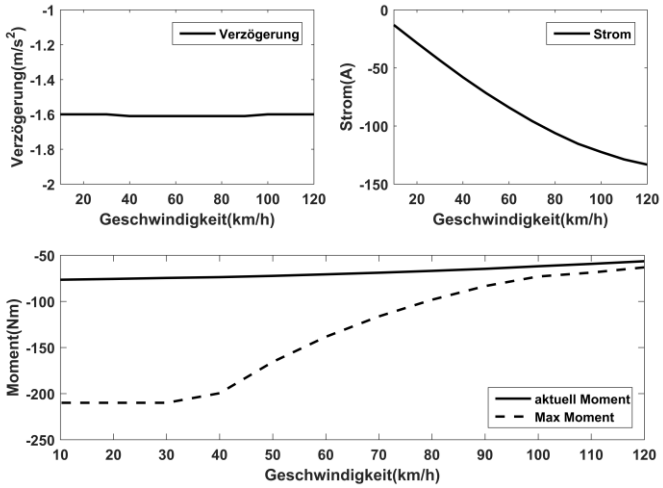

Figure 52: Torque and current at 1.6 m/s^2 deceleration [89]

It can be seen that a constant deceleration rate was achieved at all tested speeds and the torque was also achievable by the motor at all speeds as well.

In [56], the previously mentioned tests were made for deceleration rates from 0 up to 1.7 m/s^2 and it was observed that the torque had a linear relationship with the rotational speed. However, in [89] the tests were redone but with higher deceleration rates. It was found that the relationship wasn't linear anymore because the required torque couldn't be supplied by the motor at all speeds as shown in Figure 53 for a deceleration rate of 2.8 m/s^2.

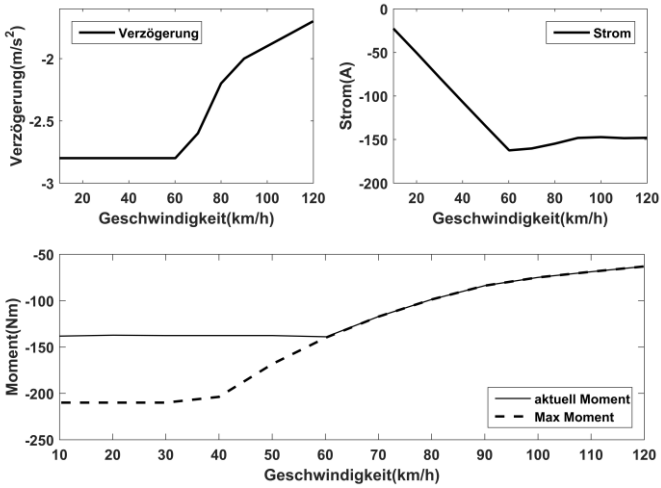

Figure 53: Torque and current at 2.8 m/s2 deceleration [44]

The results of these measurements for the generated current as a relationship with speed and deceleration rate can be seen in Figure 54.

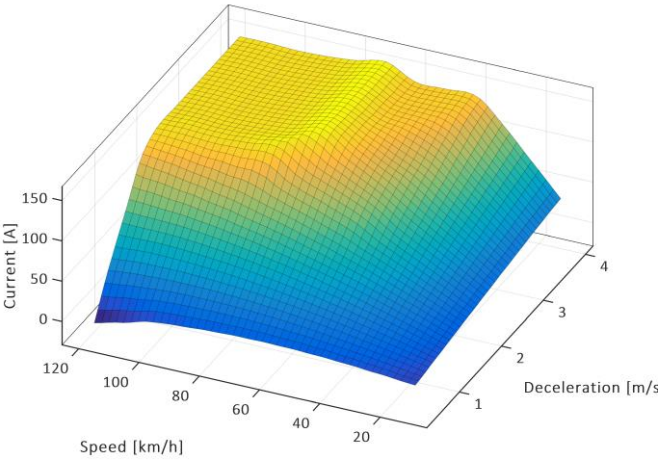

Figure 54: Generated current vs. speed vs. deceleration rate [89]

At low deceleration rates, there is a quadratic relationship between the generated current and speed. At low speeds, the relationship between speed and deceleration rate is almost linear. For example at a deceleration rate of 1 m/s^2, and from 120 to 0 km/h the current never exceeds the 150 A limit. However at higher deceleration rates that current limit is exceeded and it is necessary to prove that it doesn't exceed the time limit when charging at higher current rates.

As a result, it is possible to conclude that at speeds lower than 50km/h a constant deceleration of 4.0 m/s^2 could be covered by the available torque of the motor and the maximum allowed current of the battery isn't exceeded. At higher speeds or at higher deceleration rates that isn't the case.

One of the proposed solutions, in this case, is the combination of a battery and supercapacitors as discussed in [29]. Another solution would be the use

of an electric resistance where the excess power is converted into heat. Another solution would be using a brake-by-wire system as discussed in chapter 2.2.2.3 where the needed braking torque that can't be covered by the electric motor is provided by the hydraulic braking system. Since no changes to the case study vehicle are wanted, the application will be investigated for speeds up to 50 km/h which is already the range that covers urban driving scenarios. It is important to mention that the discussed numbers apply to the specific configuration of the case study and could be different for other vehicle configurations.

In order to implement this in the vehicle and in the simulation model, the relationship between the deceleration value and the required torque and speed of the vehicle should be defined. Using the previously made measurements the required torque vs the deceleration rate and speed of the vehicle can be plotted as seen in Figure 55.

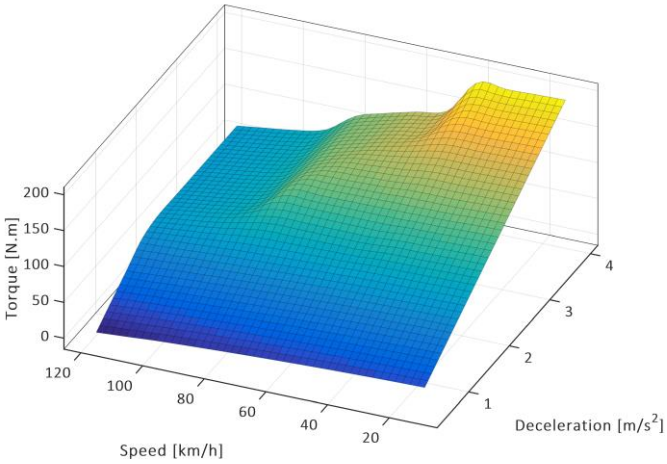

Figure 55: Torque vs. speed vs. deceleration rate

At low speeds up to 50 km/h the required torque has a linear relationship with the deceleration rate with it having a maximum rate of 4 m/s^2. By increasing the speed there isn't enough torque to generate the required deceleration and decelerations up to 1.7 m/s^2 can be only guaranteed for the full speed range. At low constant decelerations, the required torque has a linear relationship with the speed of the vehicle. The mathematical formula was derived in [56] for deceleration rates up to 1.7 m/s^2 and it showed to be a linear function of speed but a quadratic function of deceleration. However, for higher deceleration rates, that formula doesn't work anymore and a newer formula was derived using regression polynomial curve fitting for the whole range in [89] as can be seen in equation ((5.1).

$$T_{dec,max}(a,v) = 7.14 \cdot a^2 + 0.38 \cdot a \cdot v + 0.003 \cdot v^2 - 91.77 \cdot a - 0.68 \cdot v + 45.96 \quad (5.1)$$

with a fitting quality of R-square = 0.9704.

It should also be mentioned that "the braking forces resulting from regenerative braking are not counteracted by the chassis, but by the transmission and engine mounts. This influences the load spectra of these components" [60]. However, this is out of the focus of this work and won't be investigated.

[112] made an investigation for determining of regenerative braking torque based on associated efficiency optimization of electric motor and power battery using genetic algorithms where "the motor and battery can achieve efficient operation in the process of regenerative braking and the recovery of braking energy can be improved".

5.1.3 Stability

Stability is the most important factor that has to be taken into consideration when selecting the braking torque since it can affect the safety of not only the vehicle but also its surroundings.

The impact of regenerative braking on vehicle stability was studied in [113]. The focus of this study was on rear wheel drive vehicles (RWD) since applying the brakes to the rear axle is the most critical in terms of stability. During the regenerative braking phase of any strategy, prior to the introduction of friction braking, the RB is generally used to its maximum extent to increase the recuperated energy. This generally means that the front to rear braking distribution will be less than ideal since it is often only possible to apply a regenerative braking torque to a single axle where the motor is installed (by FWD and RWD vehicles). This can have significant implications for vehicle handling and stability during cornering, particularly if the axle concerned is the rear axle. The authors concluded that on low μ surfaces, "a moderately sized electric motor has the capability to significantly compromise the vehicle stability during cornering". They then considered various solutions and showed that "redistributing the regenerative braking torque using active driveline devices allows vehicle stability to be protected whilst maintaining maximum energy recovery."

From another point of view, the interaction of the regenerative braking system with other stability systems in the vehicle such as Anti-Lock Braking Systems (ABS) and the Electronic Stability Program (ESP) should be taken into consideration.

Standard [1] states that for all systems with regenerative braking capability, the anti-locking braking system (ABS) must have control over regenerative braking torque.

The study [114] investigated the interaction between regenerative braking and anti-lock braking. They state that a limitation for the use of regenerative braking results from “the potentially detrimental interaction between regenerative braking and the Anti-locking Braking System”. A comparison of competing strategies was made. One of the strategies is the abrupt termination of regenerative braking during an ABS event without a blending phase, which is the strategy used in this work. Another strategy is to ramp down the regenerative braking to zero with friction torque blending. The last strategy is to ramp down the regenerative braking to a variable residual level that a certain amount of energy is recovered. However, a vehicle equipped with this strategy is “prone to frequent use of ABS, as part of the braking torque will be out of the range of ABS control”. It was noticed that while the energy recapture was improved, that was at the expense of a longer braking distance.

[115] investigated the potential of using wheel hub motors as actuators for high decelerations. Since electric motors are capable of setting the torque faster than friction brakes, these motors are suitable to take over the ABS functionality. However, energy efficiency isn’t taken into consideration in this case. A strategy for how electric motors can be used during braking without recuperation was shown.

A design for an anti-lock regenerative braking system was proposed in [116].

5.1.4 The Efficiency Aspect

The efficiency of the electric drive components plays an important role in the amount of energy that is able to be recuperated.

The flow of the Kinetic energy from the wheels until it reaches the battery as electric energy during braking goes through several components each having its own efficiency and losses that can be summarized in Figure 56:

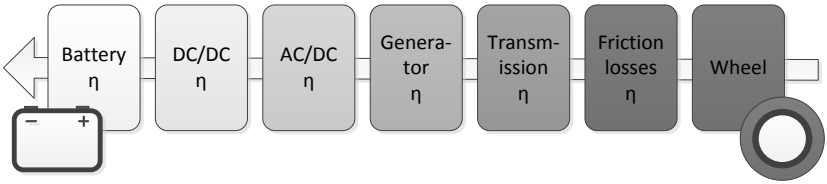

Figure 56: Energy flow during braking and the corresponding losses

The overall efficiency of recuperation is determined by the efficiency of the chain of components of the powertrain from the wheel to the battery.

The effect of all these components was studied in detail in [117].

In the case that no specific braking torque is required from the driver but a deceleration is needed, from an efficiency point of view at a given motor speed, the torque should be selected in a region with high efficiency at that given speed.

Figure 57 shows an example of an efficiency map of the ASM motor/ generator (mathematical model) installed in the case study vehicle.

The electric power generated by the motor can be calculated as a function of this efficiency map and the mechanical power input.

$$P_{electrical} = P_{mechanical} \cdot \eta \qquad (5.2)$$

By using equation ((5.2) the generated power can be plotted in Figure 58.

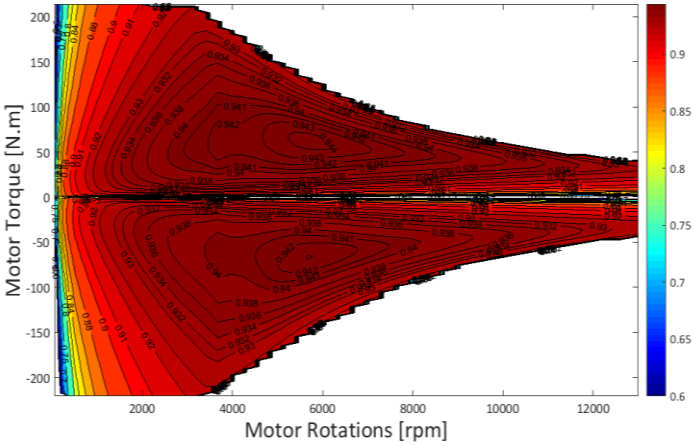

Figure 57: Efficiency map of the ASM electric motor/generator. Data Source [56]

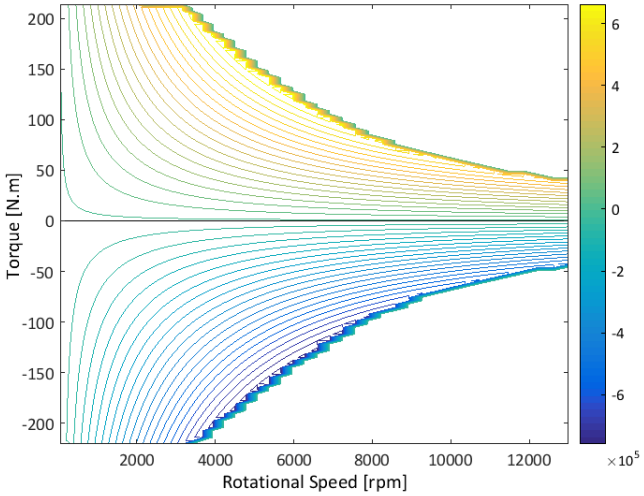

Figure 58: Electric power generated by the generator

By analyzing the maximum efficiency point at each speed a line of maximal efficiency where the generator losses are at a minimum can be extracted. Therefore it would make sense to work in the regions where more power is recuperated during braking. This region is defined by the maximum efficiency line during braking as shown in Figure 59. Even though the efficiency in this region could be less, the overall generated power at any given speed is more.

However, selecting a braking torque in this region does not ensure that the comfort limit of the driver is not exceeded.

5.1.5 The Comfort Aspect

Driving comfort is a subjective experience that depends on several different stimuli on the human body. The stimuli could be acceleration, jerk, vibration, seat comfort, noise, etc. A lot of studies are made to figure out objective measures for the assessment of driving comfort. With the focus on the behavior of the vehicle in the longitudinal direction during braking, It has been proven that acceleration/deceleration and jerk, play a very important role on the driving comfort or in this case braking comfort [118]. According to [118], an acceptable jerk is ±2 m/s^3 and a comfortable jerk is ±1 m/s^3.

Typically, only the acceleration magnitude is taken as a comfort metric. However, [119] considers the acceleration's time-derivative (jerk) to be the best metric to reflect a human comfort.

In [120], a fundamental study of jerk and an evaluation of its influence on ride comfort was conducted supported by experimental data. How the physiological experience of "jerk" corresponded to the actually measured jerk was also explored. The authors classified jerk into transient jerks and durative jerks.

For **transient Jerks**, they concluded that when the magnitude of jerk is lower than 10 m/sec^3, the influence of jerk exerted on the human is almost the same and hard to distinguish. However, when the acceleration and jerk values were high and near this limit, the passengers of the vehicle didn't feel comfortable. Also when the jerk value was low, the passengers felt comfortable even when the comfort limit of acceleration was exceeded.

For **durative jerks**, the passengers felt uncomfortable when the duration of the "exposure to jerk" was long even when the jerk value wasn't high. Another playing factor was the frequency distribution of the jerk. The results of their experiments showed that the rating of the comfort of the passengers was different at different frequency distributions. This factor is still being studied as a research-objective.

To ensure that the jerk values don't exceed the discussed limits, a low pass deceleration filter was designed and built into the controller in [66].

To ensure that the deceleration that is caused by the selected braking torque doesn't exceed the comfort levels of the driver, the relationship between the braking torque and the resulting deceleration must be defined.

By using the equation (5.1) that links the deceleration with the torque, and by using the acceleration limits of different driver types, the limits can be plotted as seen in Figure 59.

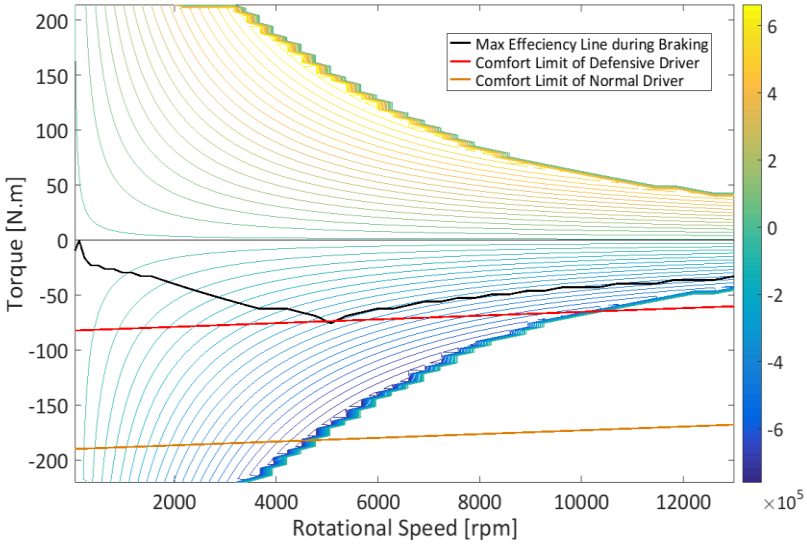

Figure 59: Comfort limits of different drivers

That means, i.e. for a defensive driver, when a deceleration is needed, the optimal region of braking torque that fulfills the efficiency and comfort for the driver is the region between the max efficiency line and the comfort limit of the defensive driver. In this region more power will be generated.

It is important to mention that these values were calculated for the test vehicle of the case study and can be different for different vehicle typologies and characteristics. For instance, it can be seen that this vehicle can't produce enough deceleration that would be uncomfortable for an aggressive driver and that it is not able to achieve high uncomfortable decelerations at high speeds.

Another comfort aspect of category (A) regenerative braking is the reduction of use of the braking pedal and the need to change between pedals.

This was studied by [49] in an urban environment where they showed that a combined pedal solution additionally affected the percentage of time in which hydraulic and electric brakes were used as can be seen in Figure 60, with SPS meaning standard pedal solution and CPS meaning combined pedal solution.

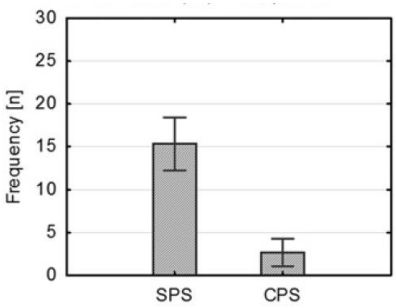

Figure 60: Mean frequency of hydraulic brake usage [49]

5.2 Methods of Torque Selection

Assuming the driver's type and the driver's intention have been recognized, the next step is to define the braking torque applied by the motor.

There are five intentions that correspond to different braking modes:

Table 10: Intentions and their corresponding braking modes

Intention	Braking mode
Cruising	Adaptive Cruising Point (ACP)
Rolling	No braking torque is applied
Normal braking	Regenerative braking is activated when inside the comfort activation distance

	depending on the driver type.
Emergency braking	Max stable RB until the driver brakes with the brake pedal
Brake pedal braking	SBRS or CBRS depending on the vehicle

The Adaptive Cruising Point (ACP) strategy is explained in a scientific publication published within the scope of this work in [7]. In this strategy, when the intention of the driver is to cruise, the motor torque is kept constant at the accelerator's pedal value that corresponded to the cruising intention. If the accelerator were to be pressed, the motor torque request will increase normally. However, if the accelerator is released further, then depending on the new change in intention either a negative torque will be applied causing the vehicle to decelerate or the driving torque will be reduced.

The requirements of the braking strategy in the proposed system are to improve comfort and efficiency and but not to act as an autonomous braking assistant.

Even though this isn't a requirement, it is important to know how near the strategy comes to the safety limits. Whatever the situation, the vehicle should be decelerated in a manner so that at the end of the braking maneuver, a safety distance to the lead vehicle is guaranteed. The comfort limit of the driver shouldn't be exceeded (except in critical cases that can lead to collisions). The kinematics of braking must be also taken into consideration such as the quadratic relationship between braking distance and speed. Several methods that fulfill these criteria will be discussed.

5.2.1 Safety Distance Keeping

According to the road traffic regulations (StVO) in Germany, § 4 states that the distance to a vehicle in front must usually be so large that it can be

stopped behind it even if it is suddenly brakes. Who drives ahead, must also not brake hard without a compelling reason.

In order not to drive into an object that can come to a halt immediately, the safety distance must actually be chosen as large as the entire stopping distance, which is the reaction path plus the braking distance which increases with the square of the speed.

Therefore, the absolute minimum distance must be the personal reaction path. However, adherence to the entire stopping distance is seldom necessary, as the vehicle in the front also has a braking distance, and does not stop immediately. The recommended safety distance thus increases in fact only linearly with the speed.

The reaction time is typically one second inside city limits, t_r = 1s, whereas outside city limits it is two seconds, t_r = 2 s.

In order to combine both to be used as a limit in the system, the following 3 formulas for different situations were described for calculating the safety distance in [66] and are shown in Figure 61:

$$\begin{aligned} d_{safe} &= 1\,\mathrm{s} \cdot v_{ego}\,, \forall \quad 0 \le v_{ego} \le 15\ [m/\mathrm{s}] \\ d_{safe} &= 5\,\mathrm{s} \cdot \left(v_{ego} - 15\right) + 15\,, \forall \quad 15 < v_{ego} < 20\ [m/\mathrm{s}] \\ d_{safe} &= 2\,\mathrm{s} \cdot v_{ego}\,, \forall \quad v_{ego} \ge 20\ [m/\mathrm{s}] \end{aligned} \tag{5.3}$$

5.2.2 Comfort Activation Distance

If the distance at which the accelerator pedal is released is above this activation limit no regenerative braking will be applied. Only when the distance drops below this activation value will regenerative braking be applied depending on the driver's intention.

In [64], several models that fulfill safety constraints and comfort specifications in stop and go scenarios were proposed.

Within the scope of this work, these concepts were analyzed for the proposed system and its requirements, and an empirical formula for calculating the comfort activation distance was derived as follows [66]:

$$d_{comfort} = 0.77 \cdot \frac{v_{ego}^2}{|a_{comfort}|} + d_c \tag{5.4}$$

Whereas d_c is a predefined value for the minimal distance that makes the driver feel safe. The value suggested for d_c is 5 m.

Figure 61 shows the safety and comfort activation distances as a function of speed for different drivers:

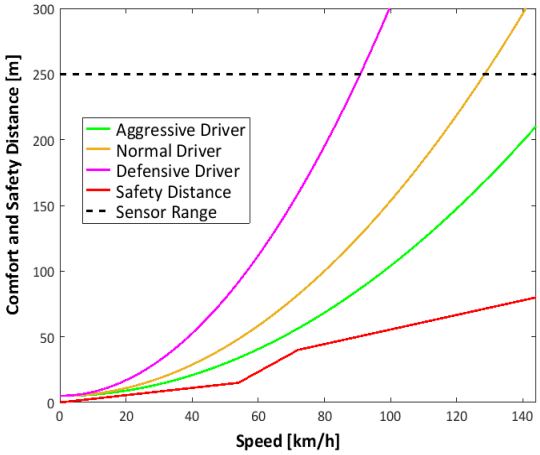

Figure 61: Safety and comfort activation distance

5.2.3 Driver Braking and Following Models

Several models exist that describe the driver during driving in acceleration, following and deceleration phases.

The study [121] studied the deceleration behavior of different vehicle types having a different weight to power ratios and dynamic characteristics that affect their deceleration behavior. A model was developed to describe deceleration behavior over the entire speed range.

The authors of [122] modeled the driver following behavior based on minimum-jerk theory.

In [123], a car following model based on real-time maximum deceleration was developed.

In this chapter, the most relevant models will be explained. The simplest available model is first analyzed and checked to see if it fulfills the goals of the proposed system.

5.2.3.1 Braking Torque Selection according to Gipps' Model (GM)

Gipp's model is used to model both acceleration and deceleration. Sometimes it generates unrealistic acceleration profiles, but this model is the simplest complete and accident-free model that leads to accelerations that are within a realistic range.

According to [124], in the Gipps' model, accidents are prevented by introducing a "safe speed", which depends on the distance to and speed of the leading vehicle. It is based on the following assumptions:

1. Braking maneuvers are always executed with constant deceleration b. There is no distinction between comfortable and (physically possible) maximum deceleration.

2. There is a constant “reaction time” Δt.

3. Even if the leading vehicle suddenly decelerates to a complete stop (worst case scenario), the distance gap to the leading vehicle should not become smaller than a minimum gap $s_{0.}$

Assumption 1 implies that the braking distance that the leading vehicle needs to come to a complete stop is given by:

$$\Delta x_l = \frac{v_l^2}{2 \cdot b_{lead}} \tag{5.5}$$

From assumption 2 it follows that, in order to come to a complete stop, the driver of the considered vehicle needs not only his braking distance, but also an additional reaction distance v.Δt traveled during the reaction time. Consequently, the stopping distance is given by:

$$\Delta x_{ego} = v_{ego} \cdot \Delta t + \frac{v_{ego}^2}{2 \cdot b_{ego}} \tag{5.6}$$

Finally, assumption 3 is satisfied if the gap s exceeds the required minimum final value s_0 by the difference between the stopping distance of the considered vehicle and the braking distance of the leader:

$$s \geq s_0 + v_{ego} \cdot \Delta t + \frac{v_{ego}^2}{2 \cdot b_{ego}} - \frac{v_l^2}{2 \cdot b_{lead}} \tag{5.7}$$

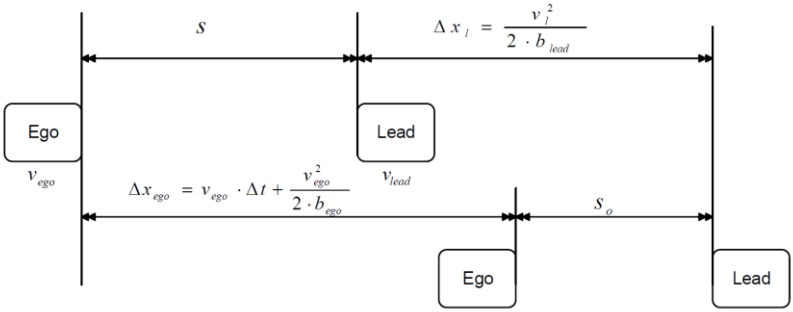

Figure 62: Gipps' Model for braking [89]

Using the past equations, the deceleration of the ego vehicle which is needed in order to avoid collision is:

$$b_{ego} \geq \frac{v_{ego}^2}{2 \cdot \left(s - s_0 - v_{ego} \cdot \Delta t + \frac{v_l^2}{2 \cdot b_{lead}} \right)} \qquad (5.8)$$

Typical values of the parameters in (5.8 on highways and in city traffic can be seen in Table 11.

Table 11: Typical values of the Gipps' Model parameters [124]

Parameter	Highway	City traffic
Reaction time Δt	1.1 s	1.1 s
Deceleration b_{lead}	1.0 m/s^2	1.0 m/s^2
Minimum distance s_0	3 m	2 m

Gipps' model does not differentiate between comfortable and maximum deceleration of the ego vehicle: Assuming that *b* in equation (5.8 denotes the maximum deceleration of the ego vehicle and lead vehicle, the model is accident-free but every braking maneuver is performed uncomfortably with full brakes. On the other hand, if it is desired to use *b* as the comfortable deceleration of the ego vehicle, the model possibly produces accidents if leading vehicles brake harder than $b_{comfort}$ ($b_{lead} > b_{comfort}$).

Modified versions of this model such as the Krauss model are used in several commercial traffic simulators [124].

5.2.3.2 Braking Torque Selection according to the Intelligent Driver Model (IDM)

The problem of Gipps can be solved using the time-continuous Intelligent Driver Model (IDM), which is probably the simplest complete and accident-free model producing realistic acceleration profiles and a plausible behavior in essentially all single-lane traffic situations [124].

Similarly to Gipps' model, the IDM is also based on a number of assumptions according to [125], The most relevant will be highlighted :

- The bumper-to-bumper distance to the leading vehicle is not less than a "safe distance" $s_0 + v \cdot T$, where s_0 is a minimum (bumper-to-bumper) gap, and T the (bumper-to-bumper) time gap to the leading vehicle.

- An intelligent braking strategy controls how slower vehicles (or obstacles or red traffic lights) are approached:

- Under normal conditions, the deceleration increases gradually to a comfortable value b, and decreases smoothly to zero just before arriving at a steady-state car-following situation or coming to a complete stop.

- In a critical situation, the deceleration exceeds the comfortable value until the danger is averted. The remaining braking maneuver (if applicable) will be continued with the regular comfortable deceleration b.

- Transitions between different driving modes (e.g., from the acceleration to the car-following mode) are smooth. In other words, the time derivative of the acceleration function, the jerk J, is finite at all times. Typical values of an acceptable jerk are $|j| \leq 1.5 m/s^3$.

- The parameters should correspond to an intuitive interpretation and assume plausible values.

The acceleration that fulfills all these requirements is a function of comparing the actual speed of the vehicle v to the desired speed v0 which is actually the speed of the lead vehicle and of comparing the current distance s to the desired distance s* and is given in :

$$\dot{v} = a\left[1 - \left(\frac{v}{v_0}\right)^{\delta} - \left(\frac{s^*(v, \Delta v)}{s}\right)^2\right] \tag{5.9}$$

And therefore the desired distance is:

$$s^*(v, \Delta v) = s_0 + v \cdot T + \frac{v \cdot \Delta v}{2 \cdot \sqrt{a \cdot b}} \tag{5.10}$$

This has the safe distance (s0 + vT) term and a dynamic term $v \cdot \Delta v/(2 \cdot \sqrt{(a \cdot b)})$ that implements the “intelligent” braking strategy.

Typical values of the parameters can be seen in Table 12.

Table 12: Typical values of the IDM parameters [124]

Parameter	Highway	City traffic
Minimum gap s0	2 m	2 m

Time gap T	1.0 s	1.0 s
Acceleration exponent δ	4	4
Deceleration b_{lead}	$1.0\ m/s^2$	$1.0\ m/s^2$
Comfortable deceleration b	$1.5\ m/s^2$	$1.5\ m/s^2$

This is where the modification needs to be made as after classifying the driver type it is possible to set the comfortable deceleration to an appropriate value that corresponds to the recognized driver type.

By using the IDM, it is possible to ensure that the strategy dynamically regulates itself against a situation in which the kinematic deceleration corresponds to the comfortable deceleration as discussed in [89].

5.2.3.3 Implementation and Experimental Setup

After calculating the required deceleration, and taking into consideration the classification of the driver type and the corresponding comfort limit, the required braking torque is calculated using the equation (5.1.

The models were then implemented in Simulink and integrated into the control model of the vehicle. It was built in a modular way so that the exchange of different models for comparison is possible.

In order to generally test the two suggested models and compare them a simple test scenario in CarMaker was defined and the vehicle was driven in two scenarios, in the city, and on the highway.

In the city scenario with a typical 50 km/h speed and a lead vehicle driving 30 km/h, the following predefined tests were made:

Table 13: Maneuvers in city scenario

Acc. pedal release distance	Driver type to be recognized	Intention to be recognized
90m	defensive	normal braking
30m	normal	normal braking
20m	aggressive	normal braking
13m (<safety distance)	aggressive	emergency braking

The results of the generated deceleration by using GM and IDM are compared in the following figure:

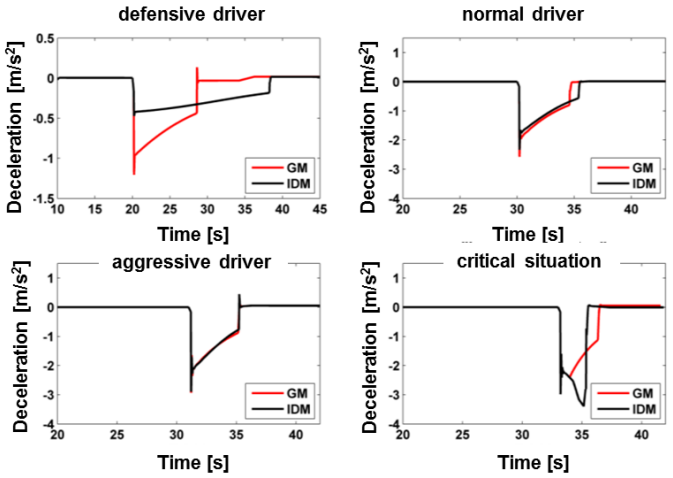

Figure 63: Comparison of GM and IDM in a city scenario [89]

It can be seen that both models worked well with the defensive driver and didn't exceed the comfort limit of 1.5 m/s^2, but the GM caused the vehicle to brake harder and for a shorter period. Since the lead vehicle in this

situation is still far away, it isn't critical and since the IDM generates less deceleration it would be considered more comfortable. With the normal and aggressive driver, there isn't a big difference even though the GM tends to have higher decelerations at the beginning meaning it is less comfortable.

In the critical situation where the distance between the two vehicles was smaller than the safety distance, the IDM excels in terms of safety bringing the vehicle out of the critical situation very fast even though that meant exceeding the comfort limit which is a great advantage of using the IDM.

In the highway scenario with a typical 120 km/h speed and a lead vehicle driving 90 km/h, similar results were seen. The conclusion that the IDM is more appropriate to our system than the GM in terms of both comfort and safety was made.

6 System Testing

In this chapter, the methods used to compare the different strategies are explained. The methods are then used to test the different RB strategies and the results are discussed.

6.1 Driving Range Comparison

In order to measure the advantage of using regenerative braking from an energy efficiency point of view, the drive range of the vehicle without regenerative braking is compared to the drive range of the vehicle with regenerative braking (different strategies), while stating the type of course the vehicle was driven on during the tests which have to be the same in both cases in order for the comparison to be valid. The tests with 'no regenerative braking' will be always used as the reference for comparison. All the results will be given as relative values.

In order to make comparisons, the necessary signals and values to calculate the average energy consumption are logged. The average energy consumption is measured according to:

$$C_{average} = \frac{used\ energy}{driven\ distance} = \frac{\int_{t_{start}}^{t_{end}} U \cdot I \cdot \partial t}{s} \qquad (6.1)$$

The calculation of the percentage increase in driving range is then calculated as the ratio of average energy consumption with the actual RB strategy to the average energy consumption with no RB.

$$\text{Drive range increase} = \frac{C_{average,\ with\ RB}}{C_{average\ ,\ no\ RB}} * 100 \qquad (6.2)$$

6.2 Testing Procedures

Within the scope of this work, a catalog of test procedures was collected and developed in [126]. These tests range from general tests to tests specific for electric vehicles to tests specific to the components and systems of electric vehicles.

The methods discussed in the following chapters will focus on testing the regenerative braking system.

6.2.1 Driving Cycles

To do any energy consumption comparison, the measurements made have to be done under reproducible conditions by using e.g. standardized driving cycles. These cycles are procedures that define the whole setup and conditions of the experiment such as environmental temperature, warm-up phases as well as predefined speed profiles. Appendix 9.3 shows a summary of the characteristics of the considered test cycles.

All considered cycles, except for the NEDC, are based on test drives. The presented cycles cover a wide range of driving situations. Sometimes different profiles are combined in one cycle. In some cases, the cycles are designated urban, interurban or motorway cycles.

It is to notice that these driving cycles are country-specific and are a part of the legal bodies of those countries. For example, In Europe, the New European Driving Cycle (NEDC) is used [127] and in the USA, the Federal Test Procedure FTP-75 is used [128]. Several efforts are being made to normalize these cycles worldwide by replacing the country-specific cycles with the WLTP Cycle which has a different procedure based on a vehicle's power-to-mass (PMR) ratio and its maximum speed. The WLTP cycle is officially ap-

plied to new types of cars from September 2017 and will apply to all new car registrations from September 2018 [129].

The previously mentioned official cycles are mainly used to determine the consumption of vehicles, but several other unofficial cycles exist that can also be used for the assessment of energy consumption, such as the ARTEMIS cycles and the TSECC which was developed specifically for electric vehicles. These cycles were developed to overcome the criticism that the NEDC gets for being unrealistic.

In Europe, the procedures for testing electric vehicles are described in [130]. The vehicle is firstly charged according to a specific procedure and then the NEDC is driven twice. The energy used for the subsequent charging is measured as the consumption.

In order to measure the potential of an RB system, several tests were made with our test vehicle described in Appendix 9.2 on the AARP and in the simulation environment described in Appendix 9.1.

In the course of the simulations, each recuperation strategy discussed in chapter 2.2 was tested in every driving cycle presented. This ensured a broad base of comparable simulation data [117] and the results can be seen in Table 14.

The ARTEMIS highway 130, which is characterized by a very high average speed, shows the lowest range increase. This is due to the fact that a lot of energy has to be applied to overcome the air resistance. In addition, the proportion of recoverable energy is smaller. In this driving cycle, the EBS has a very low range gain, since the engine brake simulation torque is very low at high speeds.

Table 14: Drive range comparison for different cycles. Data source [117]

Driving Cycle	No RB	EBS	SRBS	Combined (SRBS + EBS)	CRBS
ARTEMIS urban	100 %	118,7 %	134,1 %	140,6 %	146,7 %
ARTEMIS rural	100 %	107,1 %	116,5 %	117,5 %	121,2 %
ARTEMIS HWY130	100 %	101,4 %	105,8 %	105,8 %	106,7 %
NEDC	100 %	111,9 %	122,6 %	125,9 %	126,7 %
FTP-75	100 %	108,4 %	116,6 %	116,9 %	116,9 %
WLTP class 3	100 %	108,1 %	115,4 %	116,4 %	116,9 %
TSECC	100 %	103,8 %	109,5 %	110,2 %	110,1 %
Braunschweig	100 %	116,2 %	129,2 %	134,3 %	138,1 %
Average of all	100 %	109,4 %	118,7 %	121,0 %	122,9 %
Relative increase	0%	41 %	82 %	92 %	100 %

The Braunschweig cycle and the ARTEMIS Urban cycle have the highest range increase. These cycles are city cycles at very low speeds, resulting in low energy consumption to overcome air resistance. During these cycles, a large proportion of the drive energy is used to overcome the acceleration resistance. This energy can be recuperated.

The remaining cycles are between the described extremes of range increase.

The SRBS achieves 82% of the technically possible range gains. This illustrates that most of the decelerations in the cycles under consideration are in the range of up to 1 m/s^2. These decelerations are covered with the serial recuperation with a purely electric braking, and high range gains can be achieved.

By combining the SRBS with EBS further range gains can be achieved. As expected, the range gains in the slow city cycles are the greatest. In the cycles with high average speed, the difference to SRBS is lowest.

The cooperative recuperation strategy achieves the maximum, technically possible range gain. This strategy brakes purely electrically until the requested braking torque exceeds the permissible engine torque. This procedure means that the friction brakes are only switched on when the recuperation reaches one of the limits discussed in chapter 5.1.

Figure 64 shows an example of the results of the comparison of the worst and best cycles being the Artemis Highway and Urban driving cycles.

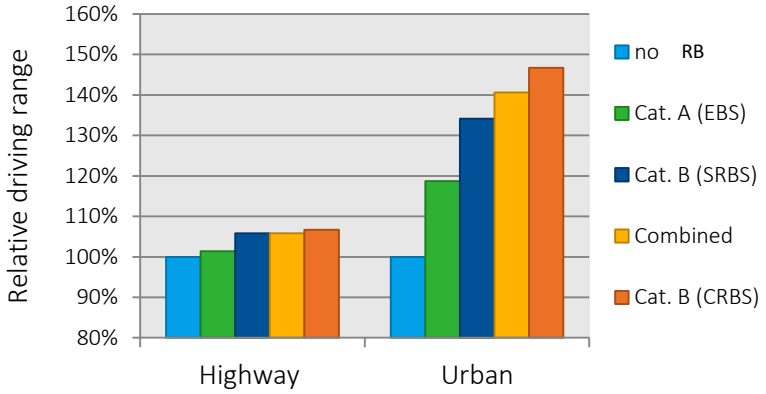

Figure 64: Potential analysis of RB strategies in the Artemis cycles. Data source [117]

In general, one can see the higher potential in urban scenarios, with cooperative braking having the highest potential. However, SRBS also has good potential but without needing to modify the braking system of the vehicle.

These tests were made in the simulation environment where the simulation driver follows the given speed profile exactly. However, all of these cycles have tolerances. The effect of these tolerances on power needs of electric vehicles and on the consumption when doing the tests on the test bench has been investigated in the scope of this work and was published in [131].

It is important to also mention that these tests are not suitable to test the ARB because each cycle has a given speed profile and using it to test different types of drivers is not possible, since they will have to try to stay as accurate as possible to the given speed profile with the given tolerances.

Therefore a method to convert a driving cycle into a maneuver that can be driven by different types of drivers is suggested.

The NEDC as a Maneuver

The NEDC Cycle is mainly criticized for delivering efficiency figures which are not achievable in reality [132]. This is due to the fact that the cycle has low accelerations and long sections of constant speed and many idling events which don't represent real driving situations.

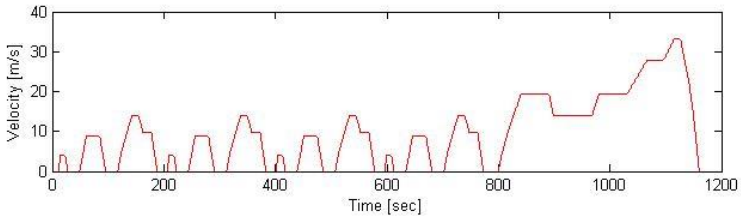

Figure 65: NEDC speed pattern

In this approach, the cycle is converted into a maneuver with stop signs and speed limits that the driver can react to according to his type.

In order to achieve that, the cycle is first converted to depict the speed vs. distance. This is done by simply driving the cycle accurately and measuring the driven distance as seen in Figure 66.

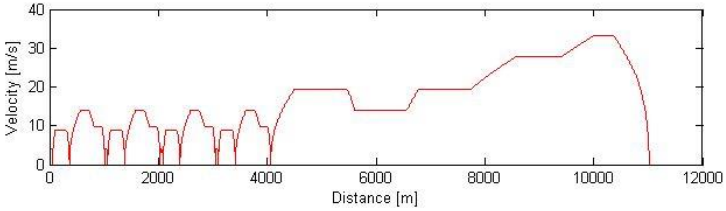

Figure 66: NEDC speed vs distance

After calculating the previous values, a small script was written to extract the stopping points and the speed limits between these stops as well as the points where the speed limits change. This is then used to generate a test run in the simulation environment using the given speed limits and stop signs as markers on the road for the simulation later as shown in Figure 67.

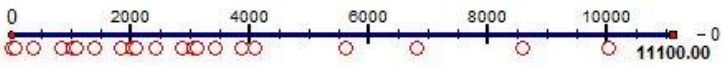

Figure 67: Road marks in simulation environment

In this figure, the circles represent road markers which could be speed limits or stop signs. This is then used as a road in the simulation software and is driven by three different drivers; defensive, normal and aggressive as seen in Figure 68.

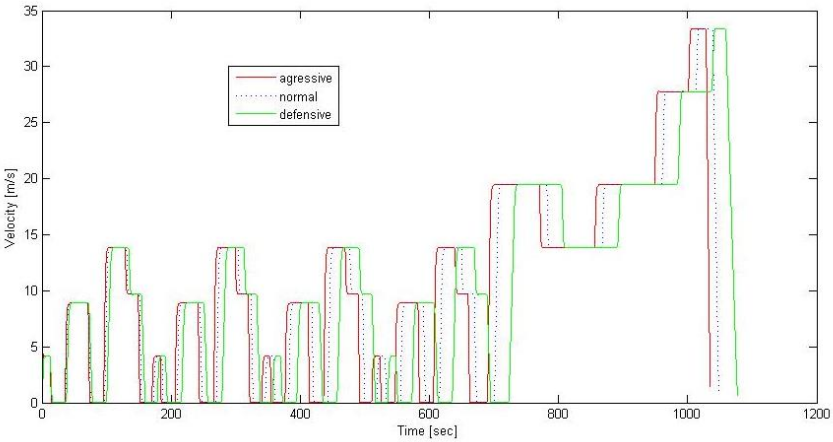

Figure 68: Different drivers driving the NEDC as a maneuver

This maneuver can be used to test the different regenerative braking strategies with different driver types.

6.2.2 Braking Tests with Traffic (Speed Adjustment)

These tests were designed to test the different driver models as discussed in 5.2.3.3. The ego vehicle drives with different speeds and approaches a lead vehicle with different speeds as well. The ego vehicle is decelerated until it reaches the speed of the lead vehicle. Two scenarios were modeled: urban and highway. The values used in these tests are shown in Table 15.

Table 15: Braking tests with traffic

	Urban Scenario	Highway Scenario
Ego vehicle speed	50 km/h	30 km/h
Lead vehicle speed	120 km/h	90 km/h

Driven distance	500 m	1500 m

6.2.3 Test-Bench Testing

To reduce the environmental influences and produce reproducible results, the previously mentioned standardized driving cycles are normally driven on roller dynamometers. An example of such a test bench is the acoustic all-wheel-drive test bench (AARP) [133] available at the Institute of Vehicle Technology as shown in Figure 69.

Figure 69: Vehicle being tested on the AARP

In order to be able to simulate the resistance forces on the test bench; the so-called ABC coefficients that represent the driving resistances should be known.

$$F_w = A + B \cdot v + C.v^2 \qquad (6.1)$$

These coefficients can be determined by doing a coast down test as explained in [127]. They can also be analytically calculated to a very good approximation as was done for this case study in [117].

In order to validate the simulation results achieved in chapter 6.2.1, the NEDC and the WLTP cycle were driven on the chassis dynamometer. The test driver is then provided with a screen that depicts the speed profile he has to drive including the tolerance band that he is allowed to move inside.

The cycles were run with no RB, with SRBS, and with combined SRBS + EBS. The NEDC was chosen because it was the official driving cycle in Europe and because all fuel consumption figures available in the market refer to this cycle. The WLTP cycle has been selected for its future importance as a world consumption cycle and also for having a more realistic speed profile than the NEDC.

The energy flow was measured at the BMS, which allows a simple measurement and ensures a good comparability of experiment and simulation. This approach differs from standard described in [130] which requires the measurement of the energy to be done at the charger. However, charging the batteries is not considered in the simulation. Therefore, in the method used in these experiments, the efficiency of the charger and the cycle efficiency of the batteries are not taken into consideration.

The results of these validation tests are explained in detail in [117].

6.2.4 Traffic Modelling

The possible gains in cruising range of different regenerative braking strategies were estimated by testing the strategies in various driving cycles in a vehicle simulation environment. By using simulation software, it is also possible to model the traffic that the ego vehicle will have to react to.

The available simulation software allows the modeling of the maneuvers of the traffic objects. These maneuvers are simple, such as acceleration, cruising or deceleration. These simple maneuvers could be combined and used to model highly detailed and more sophisticated traffic. However, this process can be time-consuming and the reality of the results depends on the experience of the person modeling these maneuvers.

Within the scope of this work, a tool was developed that allowed the easy modeling of the traffic. The tool allowed the modeling of the traffic according to different traffic classifications and different types of service levels on different types of roads. The tool also allowed the modeling of traffic scenarios on actual roads that were captured via GPS. This enabled testing real-life scenarios that were then converted into maneuvers of traffic objects. These maneuvers are then imported into the simulation environment [134].

6.3 Adaptive Regenerative Braking Results

To compare the advantage of using the ARB, braking tests described in chapter 6.2.2 were made in urban and highway scenarios. The typical RB strategies were compared as well in [89]. Table 16 shows the results comparing different category (A) RB strategies in urban scenarios.

Table 16: Comparison of different category (A) RB strategies in urban scenarios [89]

RB Strategy		Drive Range
	No RB	100 %
	EBS	105 %
Adaptive Regenerative Braking	Defensive GM	122 %
	Defensive IDM	120 %
	Aggressive GM	114 %
	Defensive IDM	116 %

By analyzing these results it can be concluded that compared to other recuperation strategies, more drive range is gained through adaptive recuperation strategy while at the same time keeping the comfort levels of the driver into consideration. The ARB with defensive GM is better in terms of efficiency but not in terms of comfort.

Table 17 shows the results comparing different category (A) RB strategies in highway scenarios.

Table 17: Comparison of different category (A) RB strategies in highway scenarios

RB Strategy		Drive Range
	No RB	100 %
	EBS	98 %
Adaptive Regenerative Braking	Defensive GM	102 %
	Defensive IDM	102 %
	Aggressive GM	106 %
	Defensive IDM	106 %

In comparison to urban scenarios the driving range increase in highway scenarios is generally lower, and no difference between GM and IDM can be seen. The reason for that in this particular case is reaching the limit of the generated current by the motor as discussed in chapter 5.1.2.

It can also be seen that sometimes it is even more efficient to just roll and not apply any regenerative braking. By introducing EBS in these particular scenarios, the driving range was decreased.

The potential shown in Table 16 and Table 17 is for specific maneuver tests described in chapter 6.2.2.

7 Summary and Prospects

7.1 Summary

In summary, the aim of this work was to develop an adaptive regenerative braking strategy for a battery electric vehicle.

At first, the state of the art of electric vehicles and their components was investigated as well as the state of the art of regenerative braking.

The concept of adaptive regenerative braking was then proposed and the requirements to realize such a system were discussed.

For the driver type recognition, a distance-based driver type recognition method has been proposed and developed. The accuracy of the method has been determined by real driving tests on a test track. The comfort limit for different types of drivers was defined based on the results of these experiments.

A model for driver intention recognition was also developed. It was based on an ergodic multi-dimensional hidden markov model. The model and its alphabet were first developed in the simulation environment. It was then trained using measurements and tests also made in the simulation environment to prove the model to be working. In order to optimize and parametrize this model, experiments with the test vehicle and real drivers were made on a closed test track. The data needed to train the model was collected and labeled by a graphical user interface (GUI) developed for this task. Subsequently, the MDHMMs were trained by the labeled data and the accuracy was determined.

For the selection of appropriate braking torque, several limits were taken into consideration.

The safety limits demanded by the regulations are taken into consideration.

The comfort limits of the different types of drivers were investigated and a comfort based triggering distance for each driver type is defined.

A closer look at the battery charge current limit and engine torque limits was made using the simulation model. The batteries manufacturer's specifications were taken into consideration when determining the battery charge current limit for the lithium-ion battery used in the test vehicle. Other experimental investigations were closely considered, and a new battery charge current limit dependent on the state of charge was established.

In the investigation of the engine torque limit, we found out that with the engine used in the research vehicle a maximum deceleration of 4 m/s^2 can be generated in city traffic. However, on the highways and at higher speeds, the maximum deceleration available by the engine is limited. For example, at speeds of 120 km/h, the engine is only able to provide a maximum deceleration of 1.7 m/s^2. These values, however, apply to the test vehicle available and could be different for other vehicle configurations.

Two braking models, respectively Gipps' Model (GM) and the Intelligent Driver Model (IDM) were investigated and implemented in the simulation model. Comfort and safety driving tests were made in the simulation environment for different driver types and the two brake models were compared to each other. The IDM was found to be better than GM in terms of comfort and safety.

However, these models couldn't be tested in the vehicle due to the lack of appropriate sensors and a permit to drive the vehicle on normal roads.

The entire adaptive recuperation strategy along with driver type and intention recognition was compared in the simulation environment in terms of range gain with other recuperation strategies such as Engine Brake Simulation (EBS), Serial Regenerative Braking (SRBS), and combined and Cooperative Regenerative Braking (CRBS).

7.2 Prospect

Due to the lack of a radar sensor and the permits to drive the vehicle on real roads, the tests for the validation of the distance-based driver's type classification method were done with a stationary object. In the future, the system with complete hardware can also be validated for moving objects in real driving tests. So far, the system has been only tested and validated in the simulation environment.

Due to the same reasons, the acceptance of the system by normal drivers couldn't be made on the roads with real traffic. This is also an important point that has to be taken into consideration.

A significant increase in driving range would be possible with the help of a BBW system. With an EHB and an II arrangement of the brake circuits, the braking force of the axles could be controlled individually. In this case, the maximum drive range increase with the highest possible quality grade of braking can be achieved.

The deceleration caused by a regenerative braking system is significant and affects the driving task. This could ultimately impact EV drivers themselves as well as drivers of other vehicles. That is, "others might be surprised when the dynamics of adjacent vehicles differ from what they are normally used to" [135]. This is a topic to be further investigated.

Integrating regenerative braking into a vehicle requires some changes in the driving style which depends on the technical configuration of the system. This takes some time getting used to, but studies have shown that drivers respond positively and try to maximize the energy they can recapture and hereby extend their range [136].

Additionally, the usage of regenerative braking is closely linked to eco-driving. If eco-driving strategies are applied by a large number of drivers, this could have considerable effects on traffic flow. This is also a topic to be researched into.

One interesting research topic is the use of the electric energy recuperated, which can't be taken by the battery. For example, the surplus power can be fed into the heating element in the heating circuit. This measure would reduce the SOC dependency of the deceleration behavior and could simultaneously help to heat the interior of the vehicle, which is a challenge especially for BEVs, as there is only little waste heat.

Another measure would be the use of a pair of energy storage devices in the vehicle. The main unit would be optimized for range (specific energy) and another for power (specific power). The second unit would be recharged from the range unit during stops or less demanding driving.

In some cases, the accuracy of the intention recognition method proposed wasn't optimal. A third layer that includes some logic or that relies on CAR2X data could be added to the intention recognition concept to prevent the intention from changing in unnatural or impossible ways.

Additionally, the proposed method was mainly based on the interaction of the driver to the vehicle in front. By having access to CAR2X data the system can be used to infer the intentions of approaching a traffic light or stop sign as well.

8 References

[1] United Nations Economic Commission For Europe Transport Standards, *Uniform provisions concerning the approval of passenger cars with regard to braking: E/ECE/324/Rev.2.* [Online] Available: https://www.unece.org/fileadmin/DAM/trans/main/wp29/wp29regs/R13hr2e.pdf. Accessed on: 01.08.2017.

[2] D. Sun, F. Lan, Y. Zhou, and J. Chen, "Control algorithm of electric vehicle in coasting mode based on driving feeling," (en), *Chinese Journal of Mechanical Engineering*, vol. 28, no. 3, pp. 479–486, 2015.

[3] S. Oleksowicz, K. Burnham, and A. Gajek, "On the Legal,Safety and control aspects of regenerative braking in hybrid/electric vehicles," (en), *Technical Transactions*, vol. 3, pp. 139–155, 2012.

[4] M. Duval-Destin, T. Kropf, V. Abadie, and M.Fausten, "Auswirkungen eines Elektroantriebs auf das Bremssystem," (de), *ATZ - Automobiltechnische Zeitschrift*, vol. 113, 2011.

[5] P. Cocron *et al.,* "Energy recapture through deceleration - regenerative braking in electric vehicles from a user perspective," (en), *Ergonomics*, vol. 56, no. 8, pp. 1203–1215, 2013.

[6] Volkswagen, *Recuperation in electric vehicles.* [Online] Available: http://www.volkswagen.co.uk/technology/electric-technology/recuperation-in-electric-vehicles. Accessed on: 25.11.2017.

[7] R. Kubaisi, K. Herold, F. Gauterin, and M. Giessler, “Regenerative Braking Systems for Electric Driven Vehicles: Potential Analysis and Concept of an Adaptive System,” (en), *SAE Technical Paper*, no. 2013-01-2065, 2013.

[8] F. Hannig *et al.,* “Stand und Entwicklungspotenzial der Speichertechniken für Elektroenergie-Ableitung von Anforderungen an und Auswirkungen auf die Investitionsgüterindustrie,” BMWi-Auftragsstudie, 2009.

[9] MEET/ WWU Münster, *Elektromobilität – Was uns jetzt und künftig antreibt.* [Online] Available: http://www.bine.info/themen/energiesysteme/stromspeicherung/publikation/elektromobilitaet-was-uns-jetzt-und-kuenftig-antreibt/. Accessed on: 29.10.2017.

[10] International Energy Agency, *Global EV Outlook 2017: Two million and counting.* [Online] Available: https://www.iea.org/publications/freepublications/publication/GlobalEVOutlook2017.pdf. Accessed on: 23.11.2017.

[11] P. Mock and Z. Yang, “Driving electrification: A global comparison of fiscal incentive policy for electric vehicles,” (en), *ICCT White Paper*, 2014.

[12] *Hybrid Electric Vehicle (HEV) and Electric Vehicle (EV) Terminology*, Standard SAE J1715_201410, 2014.

[13] M. Doppelbauer, “Lecture script : Hybridelektrische Fahrzeuge,”Elektrotechnisches Institut (ETI), Karlsruhe Institute of Technology, Winter Semester 17/18.

[14] G. Wu, X. Zhang, and Z. Dong, “Powertrain architectures of electrified vehicles: review, classification and comparison,” (en), *Journal of the Franklin Institute*, vol. 352, no. 2, pp. 425–448, 2015.

[15] J. Larminie and J. Lowry, *Electric Vehicle Technology Explained*. Chichester: Wiley, 2004.

[16] A. Rousseau *et al.,* “Comparison of Energy Consumption and Costs of Different Plug-in Electric Vehicles in European and American Context,” (en), *EVS28 International Electric Vehicle Symposium ,KINTEX, Südkorea*, 2015.

[17] R. Garcia-Valle and J. A. Peças Lopes, Eds., *Electric Vehicle Integration into Modern Power Networks*. New York, NY: Springer New York, 2013.

[18] F. Bühler, P. Cocron, I. Neumann, T. Franke, and J. F. Krems, “Is EV experience related to EV acceptance? Results from a German field study,” (en), *Transportation Research Part F: traffic psychology and behaviour*, vol. 25, pp. 34–49, 2014.

[19] N. Rauh, T. Franke, and J. F. Krems, “Understanding the impact of electric vehicle driving experience on range anxiety,” (en), *Human factors*, vol. 57, no. 1, pp. 177–187, 2015.

[20] H. A. Bonges and A. C. Lusk, “Addressing electric vehicle (EV) sales and range anxiety through parking layout, policy and regulation,” (en), *Transportation Research Part A: Policy and Practice*, vol. 83, pp. 63–73, 2016.

[21] Next Green Car, *EV price vs range comparison.* [Online] Available: http://www.nextgreencar.com/features/7943/ev-price-vs-range-comparison/. Accessed on: 16.11.2017.

[22] Z. Stevic and I. Radovanovic, *Energy Efficiency of Electric Vehicles: New Generation of Electric Vehicles.* [Online] Available: https://www.intechopen.com/books/new-generation-of-electric-vehicles/energy-efficiency-of-electric-vehicles. Accessed on: 26.11.2017.

[23] J. D. Gonder, "Route-Based Control of Hybrid Electric Vehicles," in *SAE World Congress & Exhibition 2008*.

[24] G. A. Hill, M. Neaimeh, P. T. Blythe, and Y. Hübner, "Routing systems to extend the driving range of electric vehicles," (en), *IET Intelligent Transport Systems*, vol. 7, no. 3, pp. 327–336, 2013.

[25] T. van Keulen, B. d. Jager, D. Foster, and M. Steinbuch, "Velocity trajectory optimization in Hybrid Electric trucks," in *Proceedings of the 2010 American Control Conference*, Baltimore, MD, 2010, pp. 5074–5079.

[26] V. Larsson, L. Johannesson Mardh, B. Egardt, and S. Karlsson, "Commuter Route Optimized Energy Management of Hybrid Electric Vehicles," (en), *IEEE Trans. Intell. Transport. Syst.*, vol. 15, no. 3, pp. 1145–1154, 2014.

[27] M. Roth *et al.,* "Porsche InnoDrive–an innovative approach for the future of driving," in *Fahrzeug- und Motorentechnik: 20. Aachener Kolloquium*, Aachen, 2011.

[28] Q. Ren, D. A. Crolla, and A. Morris, "Effect of transmission design on Electric Vehicle (EV) performance," in *2009 IEEE Vehicle Power and Propulsion Conference*, Dearborn, MI, 2009, pp. 1260–1265.

[29] J. Lindenmaier, “Untersuchung eines von Doppelschichtkondensatoren unterstützten Zweispannungsbordnetzes für Mikro-Hybrid-Fahrzeuge,” Dissertation, Universität Ulm, 2010.

[30] S.J. Clegg, “A Review of Regenerative Braking systems: Working Paper,” University of Leeds, Leeds, UK, 1996.

[31] K. Young, C. Wang, L. Y. Wang, and K. Strunz, “Electric Vehicle Battery Technologies,” in *Electric Vehicle Integration into Modern Power Networks*, R. Garcia-Valle and J. A. Peças Lopes, Eds., New York, NY: Springer New York, 2013, pp. 15–56.

[32] D. V. Ragone, “Review of Battery Systems for Electrically Powered Vehicles,” (en), *SAE Technical Paper*, no. 680453, 1968.

[33] M. Gidwani, A. Bhagwani, and N. Rohra, “Supercapacitors: the near Future of Batteries,” (en), *International Journal of Engineering Inventions*, vol. 4, pp. 22–27, 2014.

[34] G. J. Hoolboom and B. Szabados, “Nonpolluting automobiles,” *IEEE Trans. Veh. Technol.*, vol. 43, no. 4, pp. 1136–1144, 1994.

[35] W. Cao, “Novel high energy density lithium-ion capacitors,” Dissertation, The Florida State University, 2013.

[36] A. Hughes and B. Drury, *Electric motors and drives: Fundamentals, types and applications*. Waltham, USA: Elsevier Ltd., 2013.

[37] X. D. Xue, K. W. Cheng, and N. C. Cheung, “Selection of electric motor drives for electric vehicles,” in *Power Engineering Conference*, 2008, pp. 1–6.

[38] M. Ehsani, Y. Gao, and A. Emadi, *Modern electric, hybrid electric, and fuel cell vehicles: Fundamentals, theory, and design,* 2nd ed. Boca Raton: CRC Press, op. 2010.

[39] K. M. Rahman and M. Ehsani, “Performance analysis of electric motor drives for electric and hybrid electric vehicle applications,” in *Power Electronics in Transportation, 1996*, 1996, pp. 49–56.

[40] A. Suchaneck, B. Zhang, and F. P. León, “Regenerative braking in electric vehicles with all-wheel drive,” (en), *IJEHV*, vol. 3, no. 4, p. 340, 2011.

[41] L. de Novellis *et al.,* “Torque vectoring for electric vehicles with individually controlled motors: state-of-the-art and future developments,” in *26th Electric Vehicle Symposium, Los Angeles, California*, 2012.

[42] M. Vaillant, “Design Space Exploration zur multikriteriellen Optimierung elektrischer Sportwagenantriebsstränge,” Disseratation, Institute of Vehicle System Technology, Karlsruhe Institute of Technology, Karlsruhe, Germany, 2015.

[43] K. Reif, *Bremsen und Bremsregelsysteme*. Wiesbaden: Vieweg+Teubner Verlag / GWV Fachverlage, Wiesbaden, 2010.

[44] F. Gauterin, “Automotive Engineering 1: Lecture notes following R.Gnadler,”Institute of Vehicle System Technology (FAST), Karlsruhe Institute of Technology, Winter Semester 17/18.

[45] F. Sangtarash *et al.,* “Effect of different regenerative braking strategies on braking performance and fuel economy in a hybrid electric bus employing CRUISE vehicle simulation,” (en), *SAE International Journal of Fuels and Lubricants*, vol. 1, no. 2008-01-1561, pp. 828–837, 2008.

[46] D. B. Antanaitis, “Effect of Regenerative Braking on Foundation Brake Performance,” (en), *SAE Int. J. Passeng. Cars – Mech. Syst.*, vol. 3, no. 2, pp. 14–30, 2010.

[47] B.J. Varocky, “Benchmarking of Regenerative Braking for a Fully Electric Car,” Internship Report, Department of Mechanical Engineering, Eindhoven University of Technology, Eindhoven, 2011.

[48] Forschungsvereinigung Automobiltechnik., “Energiesparmaßnahmen am Elektroauto: Teil 1: Energieoptimiertes rekuperatives Bremsen; Teil 2: Energieoptimiertes Laden von Traktionsbatterien,” (de), *FAT-Schriftenreihe*, vol. 165, http://worldcatlibraries.org/wcpa/oclc/611752747, 2001.

[49] M. Schmitz, M. Hanig, M. Jagiellowicz, and C. Maag, “Impact of a combined accelerator–brake pedal solution on efficient driving,” (en), *IET Intelligent Transport Systems*, vol. 7, no. 2, pp. 203–209, 2013.

[50] K. Reif, *Kraftfahrzeug-Hybridantriebe: Grundlagen, Komponenten, Systeme, Anwendungen*. Wiesbaden: Vieweg + Teubner, 2012.

[51] T. Zhu and C. Zong, “Research on Electro-Hydraulic Brake System for Vehicle Stability,” in *2009 International Conference on Industrial and Information Systems*, Haikou, China, 2009, pp. 344–347.

[52] B. Bayer *et al.,* “Electro-Mechanical Brake Systems,” in *Handbook of Driver Assistance Systems*, Switzerland: Springer International Publishing Switzerland, 2015, pp. 1–11.

[53] S. R. Cikanek and K. E. Bailey, “Energy recovery comparison between series and parallel braking systems for electric vehicles us-

ing various drive cycles," in *Advanced Automotive Technologies ASME*, New York, 1995, pp. 17–31.

[54] Nissan Motor Corporation, *E-Pedal.* [Online] Available: http://www.nissan-global.com/EN/TECHNOLOGY/OVERVIEW/e_Pedal.html. Accessed on: 16.11.2017.

[55] T. Eberl, R. Sharma, R. Stroph, J. Schumann and A. Pruckner., "Evaluation of interaction concepts for the longitudinal dynamics of electric vehicles," (en), *Advances in Human Factors and Ergonomics 2012- 14 Volume Set: Proceedings of the 4th AHFE Conference*, 2012.

[56] J. Paul, "Aufbau eines Fahrzeugsimulationsmodells für Untersuchungen zum batterieelektrischen Fahrbetrieb," Diploma Thesis, Institute of Vehicle System Technology, Karlsruhe Institute of Technology, Karlsruhe, Germany, 2012.

[57] T. Watanabe, N. Kishimoto, K. Hayafune, K. Yamada, and N. Maede, "Development of an intelligent cruise control system," in *Steps Forward. Intelligent Transport Systems World Congress*, Yokohama, Japan, 1995.

[58] U. Hackenberg and B. Heißing, "Die fahrdynamischen Leistungen des Fahrer-Fahrzeug-Systems im Straßenverkehr," (de), *AUTOMOBILTECH Z*, vol. 84, no. 7/8, 1982.

[59] SAE International, *Heavy brake re-gen feel dominates i3 driving experience.* [Online] Available: http://articles.sae.org/13097/. Accessed on: 16.11.2017.

[60] B. Heißing and M. Ersoy, *Chassis Handbook: Fundamentals, Driving Dynamics, Components, Mechatronics, Perspectives*. Wiesbaden:

Vieweg+Teubner Verlag / Springer Fachmedien Wiesbaden GmbH, Wiesbaden, 2011.

[61] W. Pengyu, W. Qingnian, Wangwei, and Z. Naiwei, “The Affect of Motor Efficiency on Regenerative Braking at Low-Speed Stage,” in *2009 International Conference on Energy and Environment Technology*, Guilin, China, 2009, pp. 388–391.

[62] R. J. Koppa, “State of the art in automotive adaptive equipment,” (eng), *Human factors*, vol. 32, no. 4, pp. 439–455, 1990.

[63] E. Donges, “Aspekte der aktiven Sicherheit bei der Führung von Personenkraftwagen,” (de), *AUTOMOB-IND*, vol. 27, no. 2, 1982.

[64] J.-J. Martinez and C. Canudas-de-Wit, “A Safe Longitudinal Control for Adaptive Cruise Control and Stop-and-Go Scenarios,” (en), *IEEE Transactions on Control Systems Technology*, vol. 15, no. 2, pp. 246–258, 2007.

[65] S. Luh, “Untersuchung des Einflusses des horizontalen Sichtbereichs eines ACC-Sensors auf die Systemperformance,” Dissertation, Technische Universität Darmstadt, Darmstadt, 2007.

[66] H. Li, “Development and Implementation of Comfortable Regenerative Braking Strategy for Electric Vehicle,” Master Thesis, Institute of Vehicle System Technology, Karlsruhe Institute of Technology, Karslruhe, Germany, 2013.

[67] H. Winner, S. Hakuli, F. Lotz, and C. Singer, *Handbuch Fahrerassistenzsysteme: Grundlagen, Komponenten und Systeme für aktive Sicherheit und Komfort,* 3rd ed. Wiesbaden: Springer Vieweg, 2015.

[68] D. H. Hoefs, “Untersuchung des Fahrverhaltens in Fahrzeugkolonnen,” (af), *Strassenbau Und Strassenverkehrstechnik*, no. 140, 1972.

[69] M. W. W. Uhler, “Stop & Go: Systemkonzept und Gesamtfunktionalitat eines erweiterten ACC,” in *Aachener Kolloquium Fahrzeug- und Motorentechnik*, Aachen, 2000.

[70] M. Gießler, A. Fritz, J. Paul, O. Sander, and F. Gauterin, “Converted vehicle for battery electric drive: Aspects on the design of the software-driven vehicle control unit,” in *2nd internat. Energy Efficienct Vehicle Conference (EEVC) 2012*, Dresden, 2012.

[71] A. Albers and T. Düser, “Implementation of a Vehicle-In-The-Loop Development and Validation Platform,” (en), *FISITA World automotive congress, Budapest, Hungary*, no. F2010-C-177, 2010.

[72] T. Bock, M. Maurer, F. van Meel, and T. Müller, “Vehicle in the Loop: Ein innovativer Ansatz zur Kopplung virtueller mit realer Erprobung,” (en), *ATZ - Automobiltechnische Zeitschrift*, vol. 110, no. 1, pp. 10–16, 2008.

[73] R. Schuler, *Situationsadaptive Gangwahl in Nutzfahrzeugen mit automatisiertem Schaltgetriebe*. Renningen: Expert Verlag, 2007.

[74] M.-H. Sigari, M. Fathy, and M. Soryani, “A Driver Face Monitoring System for Fatigue and Distraction Detection,” (da), *International Journal of Vehicular Technology*, vol. 2013, no. 5, pp. 1–11, 2013.

[75] H. Rahman, S. Begum, and M. Ahmed, “Driver Monitoring in the Context of Autonomous Vehicle,” (en), *13th Scandinavian Conference on Artificial Intelligence, Halmstad; Sweden*, pp. 108–117, 2015.

[76] W. König, K.-E. Weiß, and C. Mayser, “S.A.N.T.O.S. - Situations-Angepasste und Nutzer-Typ-zentrierte Optimierung von Systemen zur Fahrerunterstützung: Gemeinsamer Projektabschlussbericht der Robert Bosch GmbH und der BMW Group,” Hannover 19S9826,

2002. [Online] Available: http://edok01.tib.uni-hannover.de/edoks/e01fb02/373006306l.pdf.

[77] E. Assmann, "Untersuchungen über den Einfluss einer Bremsweganzeige auf das Fahrverhalten," Dissertation, Technische Universität München, München, 1985.

[78] C. Lippold, "Weiterentwicklung ausgewählter Entwurfsgrundlagen von Landstraßen," Dissertation, Technische Hochschule Darmstadt, 1997.

[79] D. Ebersbach, "Entwurfstechnische Grundlagen für ein Fahrerassistenzsystem zur Unterstützung des Fahrers bei der Wahl seiner Geschwindigkeit," (de), *Schriftenreihe des Lehrstuhls Gestaltung von Strassenverkehrsanlagen, Technische Universität Dresden*, 2005.

[80] S. Schumacher, "Looking at various methods to identify different driving styles," Bachelor Thesis, Institute of Vehicle System Technology, Karlsruhe Institute of Technology, Karslruhe, Germany, 2013.

[81] B. Deml, J. Freyer, and B. Faerber, "Ein Beitrag zur Prädiktion des Fahrstils," in *Fahrer im 21. Jahrhundert. Human Machine Interface, VDI-Bericht 2015*, Düsseldorf: VDI-Verlag, 2007.

[82] Yi Lu Murphey, Robert Milton, and Leonidas Kiliaris, "Driver's style classification using jerk analysis," in *Computational Intelligence in Vehicles and Vehicular Systems*, 2009, pp. 23–28.

[83] J. Bossdorf-Zimmer, H. Kollmer, R. Henze, and F. Küçükay, "Fingerprint des Fahrers zur Adaption von Assistenzsystemen," (de), *ATZ-Automobiltechnische Zeitschrift*, vol. 113, no. 3, pp. 226–231, 2011.

[84] B. Färber, “Erhöhter Fahrernutzen durch Integration von Fahrerassistenz- und Fahrerinformationssystemen,” in *Fahrerassistenzsysteme mit maschineller Wahrnehmung*, M. Maurer and C. Stiller, Eds., Berlin, Heidelberg: Springer Berlin Heidelberg, 2005, pp. 141–160.

[85] A. Wilde, J. Schneider, and H.-G. Herzog, “Fahrstil-und fahrsituations-abhängige Ladestrategie bei Hybridfahrzeugen,” (de), *ATZ-Automobiltechnische Zeitschrift*, vol. 110, no. 5, pp. 412–421, 2008.

[86] M. Schüler, C. Onnen, and C. Bielaczek, “A Fuzzy-System for a Classification of the Driver Behavior and the Driving Situation,” (en), *IFAC Proceedings Volumes*, vol. 30, no. 8, pp. 693–698, 1997.

[87] C. Kraft, “Gezielte Variation und Analyse des Fahrverhaltens von Kraftfahrzeugen mittels elektrischer Linearaktuatoren im Fahrwerksbereich,” Dissertation, Karlsruhe Institute of Technology, Karlsruhe, Germany, 2010.

[88] H. Kollmer, A. Janßen, and F. Kücükay, “Simulation kundennaher Betriebslasten für Fahrzeugkomponenten,” in *Erprobung und Simulation in der Fahrzeugentwicklung; Mess- und Versuchstechnik*, Düsseldorf, 2007, pp. 197–215.

[89] F. Chen, “Further Development of an adaptive Regenerative Braking Strategy for Electric Vehicle,” Master Thesis, Institute of Vehicle System Technology, Karlsruhe Institute of Technology, Karslruhe, Germany, 2017.

[90] A. Gerdes, “Driving Manoeuvre Recognition,” in *PROCEEDINGS OF THE 13th ITS WORLD CONGRESS*, London, 2006.

[91] F. Schroven and T. Giebel, “Fahrerintentionserkennung für Fahrerassistenzsysteme: Driver Intent Recognition for Advanced

Driver Assistance Systems," (de), *ATZ Extra*, vol. 13, no. 10, pp. 54–59, 2008.

[92] M. Plöchl and J. Edelmann, "Driver models in automobile dynamics application," (af), *Vehicle System Dynamics*, vol. 45, no. 7-8, pp. 699–741, 2007.

[93] T. A. Ranney, "Models of driving behavior: a review of their evolution," (en), *Accident Analysis & Prevention*, vol. 26, no. 6, pp. 733–750, 1994.

[94] A. Doshi and M. M. Trivedi, "Tactical driver behavior prediction and intent inference: A review," in *2011 14th International IEEE Conference on Intelligent Transportation Systems - (ITSC 2011)*, Washington, DC, USA, pp. 1892–1897.

[95] T. Kumagai, Y. Sakaguchi, M. Okuwa, and M. Akamatsu, "Prediction of Driving Behavior through Probabilistic Inference," (en), *Proceedings of the Eighth International Conference on Engineering Applications of Neural Networks (EANN'03), Malaga, SPAIN*, 2003.

[96] Y. Kishimoto and K. Oguri, "A modeling method for predicting driving behavior concerning with driver's past movements," in *2008 IEEE International Conference on Vehicular Electronics and Safety (ICVES 2008)*, Columbus, OH, pp. 132–136.

[97] H. Hou, L. Jin, Q. Niu, Y. Sun, and M. Lu, "Driver Intention Recognition Method Using Continuous Hidden Markov Model," (ca), *International Journal of Computational Intelligence Systems*, vol. 4, no. 3, pp. 386–393, 2011.

[98] H. Mandalia, “Pattern Recognition Techniques to Infer Driver Intentions,” Master Thesis, Department of Computer Science, Drexel University, Philadelphia, 2004.

[99] C. Blaschke, J. Schmitt, and B. Färber, “Überholmanöver-Prädiktion über CAN-Bus-Daten,” (de), *ATZ Automobiltech Z*, vol. 110, no. 11, pp. 1022–1028, 2008.

[100] T. Xianzhi and W. Qingnian, “Driving Intention Intelligent Identification Method for Hybrid Vehicles Based on Fuzzy Logic Inference,” in *2010 3rd International Symposium on Computational Intelligence and Design (ISCID)*, Hangzhou, China, pp. 16–19.

[101] L. Zhang, “Methods for Detection of Driver Intentions in Deceleration Situations,” Master Thesis, Institute of Vehicle System Technology, Karlsruhe Institute of Technology, Karslruhe, Germany, 2014.

[102] H. Berndt, J. Emmert, and K. Dietmayer, “Continuous Driver Intention Recognition with Hidden Markov Models,” in *2008 11th International IEEE Conference on Intelligent Transportation Systems*, Beijing, China, 2008, pp. 1189–1194.

[103] L. R. Rabiner, “A tutorial on hidden Markov models and selected applications in speech recognition,” (en), *Proc. IEEE*, vol. 77, no. 2, pp. 257–286, 1989.

[104] A. Pentland and A. Lin, “Modeling and Prediction of Human Behavior,” (en), *Neural Computation*, vol. 11, pp. 229–242, 1999.

[105] X. Meng, K. K. Lee, and Y. Xu, “Human Driving Behavior Recognition Based on Hidden Markov Models,” in *2006 IEEE International*

Conference on Robotics and Biomimetics, Kunming, China, pp. 274–279.

[106] W. Takano, A. Matsushita, K. Iwao, and Y. Nakamura, "Recognition of human driving behaviors based on stochastic symbolization of time series signal," in *2008 IEEE/RSJ International Conference on Intelligent Robots and Systems*, Nice, 2008, pp. 167–172.

[107] L. He, C.-f. Zong, and C. Wang, "Driving intention recognition and behaviour prediction based on a double-layer hidden Markov model," (ca), *J. Zhejiang Univ. - Sci. C*, vol. 13, no. 3, pp. 208–217, 2012.

[108] L. Xiang, "Parameterisation and further Development of a Method for Driver Intention Recognition," Master Thesis, Institute of Vehicle System Technology, Karlsruhe Institute of Technology, Karslruhe, Germany, 2017.

[109] X. Lu, "Optimization of a method for driver intention recognition," Master Thesis, Institute of Vehicle System Technology, Karlsruhe Institute of Technology, Karslruhe, Germany, 2015.

[110] P. Refaeilzadeh, L. Tang, and H. Liu, "Cross-Validation," in *Encyclopedia of Database Systems*, L. LIU and M. T. ÖZSU, Eds., Boston, MA: Springer US, 2009, pp. 532–538.

[111] W. Khreich, E. Granger, A. Miri, and R. Sabourin, "A survey of techniques for incremental learning of HMM parameters," (en), *Information Sciences*, vol. 197, pp. 105–130, 2012.

[112] L. Chu, F. Zhou, J. Guo, and M. Shang, "Investigation of determining of regenerative braking torque based on associated efficiency optimization of electric motor and power battery using GA," in *Proceedings of 2011 International Conference on Electronic & Mechani-*

cal Engineering and Information Technology, Harbin, Heilongjiang, China, 2011, pp. 3238–3241.

[113] M. Hancock and F. Assadian, "Impact of regenerative braking on vehicle stability," (en), *Hybrid Vehicle Conference, IET The Institution of Engineering and Technology*, pp. 173–184, 2006.

[114] S. A. Oleksowicz *et al.,* "Investigation of regenerative and Anti-lock Braking interaction," (en), *Int.J Automot. Technol.*, vol. 14, no. 4, pp. 641–650, 2013.

[115] R. de Castro, R. E. Araújo, M. Tanelli, S. M. Savaresi, and D. Freitas, "Torque blending and wheel slip control in EVs with in-wheel motors," (en), *Vehicle System Dynamics*, vol. 50, no. sup1, pp. 71–94, 2012.

[116] M. M. Tehrani, M. R. Hairi -Yazdi, B. Haghpanah-Jahromi, V. Esfahanian, M. Amiri and A. R. Jafari, "Design of an Anti-Lock Regenerative Braking System for a Series Hybrid Electric Vehicle," (en), *International Journal of Automotive Engineering*, vol. 1, no. 2, pp. 14–27, 2011.

[117] K. Herold, "Design and implementation of a regenerative braking strategy for a front-wheel driven electric vehicle," Diploma Thesis, Institute of Vehicle System Technology, Karlsruhe Institute of Technology, Karlsruhe, Germany, 2013.

[118] X. Wei and G. Rizzoni, "Objective Metrics of Fuel Economy, Performance and Driveability - A Review," (en), *SAE Technical Paper*, no. 2004-01-1338, 2004.

[119] L. L. Hoberock, “A survey of longitudinal acceleration comfort studies in ground transportation vehicles,” (af), *Journal of Dynamic Systems, Measurement, and Control*, vol. 99, no. 2, pp. 76–84, 1977.

[120] Q. Huang and H. Wang, “Fundamental Study of Jerk: Evaluation of Shift Quality and Ride Comfort,” (en), *SAE Technical Paper*, no. 2004-01-2065, 2004.

[121] A. K. Maurya and P. S. Bokare, “Study of different deceleration behaviour of different vehicle types,” (af), *IJTTE*, vol. 2, no. 3, pp. 253–270, 2012.

[122] T. Hiraoka, T. Kunimatsu, O. Nishihara, and H. Kumamoto, “Modeling of driver following behavior based on minimum-jerk theory,” in *Proceedings of the 12th World Congress ITS*, San Francisco, California, 2005.

[123] L. Yang, X. Zhang, J. Gong, and J. Liu, “The research of car-following model based on real-time maximum deceleration,” (en), *Mathematical Problems in Engineering*, vol. 2015, 2015.

[124] M. Treiber and A. Kesting, “Car-Following Models Based on Driving Strategies,” in *Traffic Flow Dynamics*, M. Treiber and A. Kesting, Eds., Berlin, Heidelberg: Springer, 2013, pp. 181–204.

[125] M. Treiber and A. Kesting, Eds., *Traffic Flow Dynamics*. Berlin, Heidelberg: Springer, 2013.

[126] P. Lehr, “Analysis of an operating strategy in selected test cases,” Bachelor Thesis, Institute of Vehicle System Technology, Karlsruhe Institute of Technology, Karslruhe, Germany, 2015.

[127] *Richtlinie des Rates vom 20. März 1970 zur Angleichung der Rechtsvorschriften der Mitgliedstaaten über Maßnahmen gegen die*

Verunreinigung der Luft durch Emissionen von Kraftfahrzeugen, (70/220/EWG), 1970.

[128] *EPA Federal Test Procedure (FTP).* [Online] Available: https://www.epa.gov/emission-standards-reference-guide/epa-federal-test-procedure-ftp. Accessed on: 03.10.2017.

[129] www.WLTPfacts.eu, *When Will The WLTP Changes Take Place?* [Online] Available: http://wltpfacts.eu/when-will-wltp-changes-take-place/. Accessed on: 20.01.2018.

[130] United Nations Economic Commission For Europe Transport Standards, *Uniform provisions concerning the approval of passenger cars powered by an internal combustion engine only, or powered by a Hybrid Electric Power train with regard to the measurement of the emission of carbon dioxide and fuel consumption and/or the measurement of electric energy consumption and electric range, andof categories M1 and N1 vehicles powered by an electric power train only with regard to the measurement of electric energy consumption and electric range.: E/ECE/324 ECE R101.* [Online] Available: https://www.unece.org/fileadmin/DAM/trans/main/wp29/wp29regs/r101r2e.pdf. Accessed on: 02.04.2013.

[131] R. Kubaisi, F. Gauterin, and M. Giessler, "A method to analyze driver influence on the energy consumption and power needs of electric vehicles," in *2014 IEEE International Electric Vehicle Conference (IEVC)*, Florence, Italy, 2014, pp. 1–4.

[132] P. Kageson, *Cycle Beating and the EU Test Cycle for Cars.* [Online] Available:

https://www.transportenvironment.org/sites/te/files/media/T&E%2098-3_0.pdf. Accessed on: 02.11.2017.

[133] T. Dreher, M. Frey, F. Gauterin, and M. Geimer, "Akustik-Allradrollenprüfstand für mobile Maschinen," (de), *ATZ offhighway Sonderausgabe ATZ*, vol. November 2011, no. 09, 2011.

[134] C. Arndt, "Modelling of different traffic situations in the simulation environment CarMaker," Bachelor Thesis, Institute of Vehicle System Technology, Karlsruhe Institute of Technology, Karslruhe, Germany, 2013.

[135] P. Cocron *et al.,* "Methods of evaluating electric vehicles from a user's perspective – the MINI E field trial in Berlin," (en), *IET Intell. Transp. Syst.*, vol. 5, no. 2, p. 127, 2011.

[136] H. Strömberg *et al.,* "Driver interfaces for electric vehicles," in *Proceedings of the 3rd International Conference on Automotive User Interfaces and Interactive Vehicular Applications*, Salzburg, Austria, 2011.

[137] M. Alhanouti, M. Gießler, T. Blank, and F. Gauterin, "New Electro-Thermal Battery Pack Model of an Electric Vehicle," (en), *Energies*, vol. 9, no. 7, p. 563, 2016.

[138] M.-M. Tosic, "Parameter optimization of the electric components of an electric vehicle simulation," Bachelor Thesis, Hybrid electric vehicles HEV, Karlsruhe Institute of Technology, Karlsruhe, Germany, October/2015.

9 Appendix

9.1 Simulation Model

The simulation model used in the scope of this work is a simulation model developed in a co-simulation environment using Matlab/Simulink and IPG CarMaker

CarMaker is a software program for doing vehicle dynamic simulations, and can also be used to make energy consumption analysis.

Figure 70 shows a graphical presentation of the modeled vehicle in this software. The green, blue and red beams at the wheels quantitatively represent the driving and braking forces, the cornering and the normal forces respectively that affect each wheel.

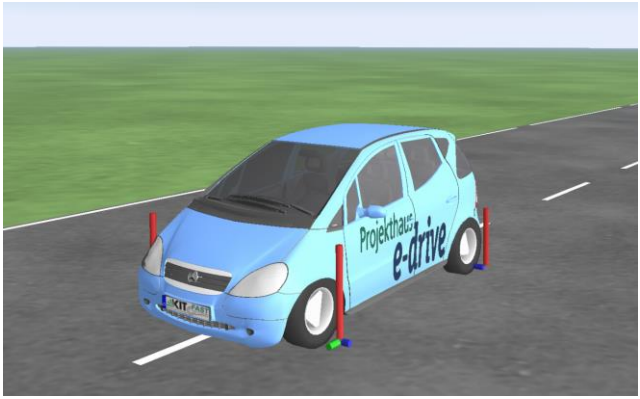

Figure 70: Vehicle in simulation software CarMaker (IPG Movie)

By using Carmaker for Simulink, the conventional powertrain model can be overwritten and modeled into an electric powertrain. The focus of the modeling process was the electric powertrain and its parameterization, whereas the task of calculating the driving dynamics is handled by CarMaker.

In [56] the main components of the drive-train were modeled which include the MCU, power electronics, the electric motor, the powertrain, the high voltage battery as well as the low volt battery and utilities such as the servo steering system as seen in Figure 71. This basic model was afterward extended and upgraded to support other functions and concepts that were developed and tested in the scope of this work.

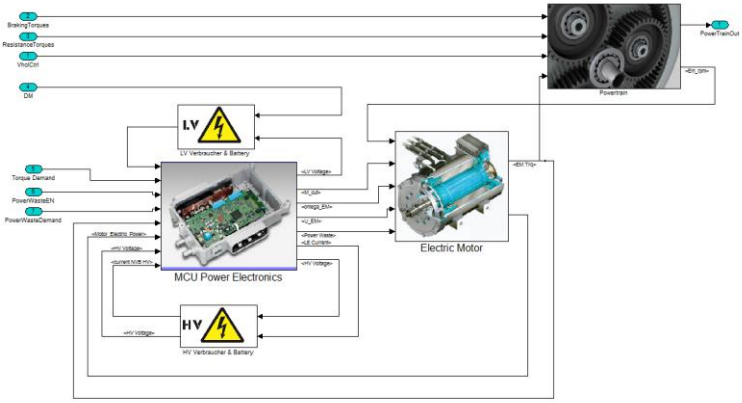

Figure 71: Electric Drive-Train Components

In [117], the regenerative braking functionality of this model was extended to allow for different kinds of regenerative braking configurations (as discussed in 2.2.1).

This functionality was introduced in a dedicated longitudinal control block.

In this block, the allowed recuperation level is determined at first according to the limits discussed in (4.2.4). Afterwards, the maximum allowed braking torque, resulting from motor and battery limits is determined

Both category A and category B regenerative braking were implemented which allowed us to do the experiments in chapter 6.2.1

One of the great advantages of using Simulink and Carmaker was the ability to add a CAN bus Mask that can be switched between simulated CAN bus inputs and real CAN Bus signals from the vehicle. The reason for that is that Simulink was used to build the logical control of the VCU which is also used to model the test vehicle's rapid prototyping hardware. This allowed us to run the same Vehicle Control Unit (VCU) on the simulation model and on the test vehicle which in turn allowed for the validation of the simulation model afterward.

As discussed in chapter 4, a driver type recognition block and a driver's intention block were developed and integrated into the model.

The battery limits and the motor limits that were analyzed in detail to ensure that the batteries and motor aren't damaged during operation as discussed in chapter 5.1 were implemented in the model as well.

A new battery temperature model [137] was developed based on simulated battery module temperature evolution curves and tests on the individual battery cells used in the test vehicle, and a thermal torque de-rating method was included [138].

9.2 Test Vehicle

At the Institute of Vehicle Technology, a Battery Electric Vehicle was developed for research and teaching purposes in the Projekthaus e-drive[4] at KIT as shown in Figure 72.

Figure 72: Test BEV

The vehicle is based on a fuel-cell (FCEV) Mercedes-Benz W168 which was converted into a BEV [70] by installing high voltage battery modules as well as a battery management system from the company Valence.

The battery used is a Valence UEV-18XP and its properties can be seen in Figure 4. It has triple the specific energy of the Ni-MH battery built in the Toyota Prius II [56].

The control software for the vehicle was made with Matlab / Simulink and was then compiled to run on the rapid software prototyping hardware

[4] http://www.projekthaus-e-drive.kit.edu/

installed in the vehicle which is a dSpace Autobox. The components of the vehicle communicate using the CAN Bus. The Motor Control Unit (MCU) receives a torque request signal from the Vehicle Control Unit (VCU) and the power electronics determines the permissible torque and sends it back to the VCU.

The front axle of the vehicle is propelled by an induction motor that is connected to a planetary gearbox and a differential both with a constant gear ratio.

Based on the estimation for the gains in range in chapter 6.2.1 and an estimation of the effort required for implementation, a serial regenerative braking strategy with a switchable combined regenerative braking strategy was chosen for implementation because very little changes had to be made to the vehicle to realize it. The only additional change made to realize this work was by designing and installing a measuring jig for the brake pedal position [117].

The control software was developed and tested using a software-in-the-loop environment CarMaker and then later exported into the VCU (Vehicle Control Unit) which is a dSpace Autobox.

The braking system installed is a hydraulic braking system with two circuits in an x configuration and an electrical pump for generating the vacuum for the braking force booster.

The braking force distribution was measured and is 84:16 between the front and rear axle respectively [117]. This value was taken into consideration when discussing stability.

The safety functions of ABS and ESP are implemented and if any one of them is activated the regenerative braking is automatically turned off in order not to interfere as the system was not designed originally for that.

The gear-selector's "+/-" button was used to select the different RB strategies for testing or to simply activate and deactivate the EBS.

Since the proposed system depends on a radar to determine the actual situation and intention and because the vehicle does not have a permit to drive on normal roads and interact with another vehicle a 'peiseler wheel' or what is called a 'fifth wheel' was used to determine the covered distance when driving and this value, in turn, can be used to determine the distance to a stop sign or traffic light with a known position as was used for the experiments in chapter 4.1.2.1 and also the distance change rate needed for the intention recognition.

Figure 73: Peiseler wheel attached to the test vehicle

Rolling tests were performed in [117] for the parameterization and validation of the simulation model on the dynamometer (AARP) of the Institute of Vehicle System Technology at the Karlsruhe Institute of Technology (KIT) [133].

The schematics of the electrical drive train of the vehicle can be seen in Figure 74.

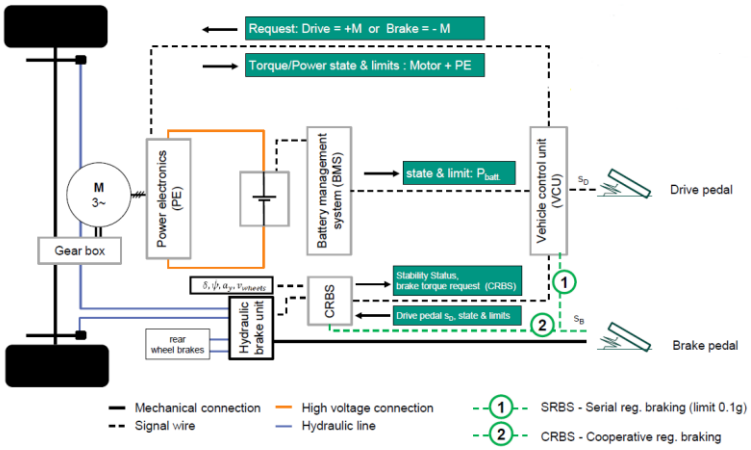

Figure 74: Schematics of the electrical drive-train of the test vehicle [70]

9.3 Driving Cycles Characteristics

These are listed in Table 18. The average speed of the cycles includes the downtime. The average deceleration takes into account only the duration when the vehicle was decelerated. Acceleration and constant driving phases are not included in the calculation. The last column shows the percentile part of the deceleration phases during which the deceleration was below 1 m/s^2.

Table 18: Cycles taken into consideration. data source [117]

Driving Cycle	Distance	duration	Average speed	Average dec.	Dec. < $1m/s^2$
ARTEMIS urban	4,86 km	993 s	17,7 km/h	0,732 m/s^2	74%
ARTEMIS rural	17,3 km	1082 s	57,5 km/h	0,494 m/s^2	90%
ARTEMIS hwy130	28,7 km	1068 s	96,9 km/h	0,408 m/s^2	92%
NEDC	10,9 km	1180 s	33,4 km/h	0,541 m/s^2	94%
FTP-75	17,8 km	1874 s	34,1 km/h	0,511 m/s^2	82%
WLTP class 3	23,3 km	1800 s	46,5 km/h	0,422 m/s^2	90%
TSECC	60 km	3600 s	60,0 km/h	0,328 m/s^2	92%
Braunschweig	10,9 km	1740 s	22,5 km/h	0,540 m/s^2	85%

9.4 CarMaker IPG Driver

Several built-in types already exist: defensive, normal and aggressive. Figure 75 shows the most important parameters that can be used to describe the behavior of the driver.

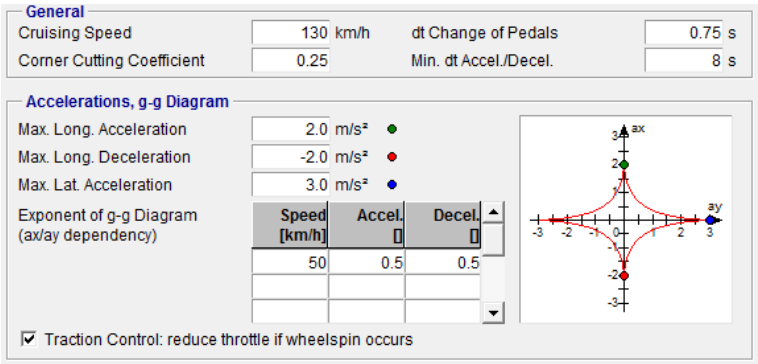

Figure 75: IPG Driver panel

The parameters of the three different drivers are summarized in the following table:

Table 19: IPG CarMaker default driver parameters

Parameter	Defensive	Normal	Aggressive
Cruising speed [km/h]	130	150	250
Corner cutting coeff.	0.25	0.5	0.8
Δt change of pedals [s]	0.75	0.5	0.25
Δt between acc./dec. [s]	8	4	0.25
Max. long. acc. [m/s^2]	2.0	3	4
Max. long. dec. [m/s^2]	-2.0	-4.0	-6.0
Max. lat. acc. [m/s^2]	3.0	4.0	5

9.5 Labeling Tool

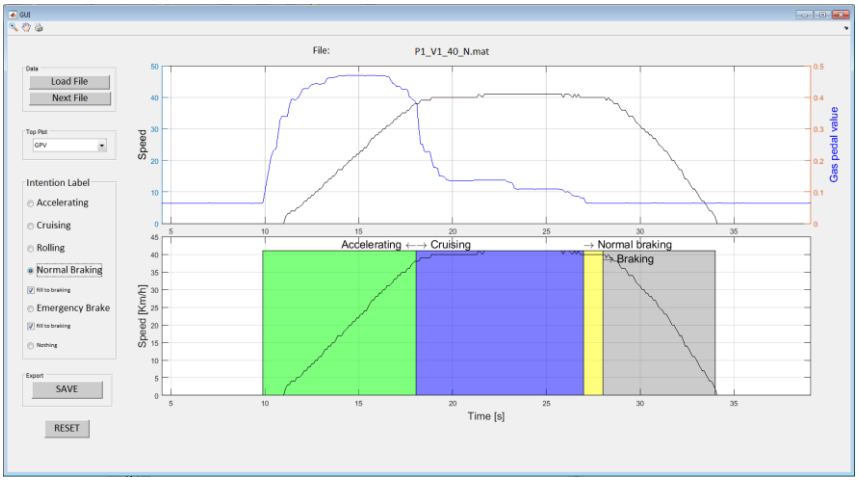

Figure 76: Screenshot of the labeling GUI

The upper graph portion of the GUI is used to show specific acquired values that help the labeler determine where the intention changed or started. Some points can be also automatically detected such as the starting point of acceleration and the starting point of the actuation of the braking pedal. However, labeling is not an easy task since it is not 100 % clear where the driver's intention changed. This may lead to inaccuracies especially at the transition phases between intentions.

In the lower graph, the intentions are labeled where there are 6 predefined labels to select from which were listed in Table 9.